supervising scientist report 132

Application of a catchment evolution model to the prediction of long-term erosion on the spoil heap at Ranger uranium mine

Initial analysis

G Willgoose & SR Riley

Environment Australia
Department of the Environment

supervising scientist

Garry Willgoose – Department of Civil, Surveying and Environmental Engineering,
The University of Newcastle, Callaghan, NSW 2308, Australia

Steven Riley – Environmental Research Institute of the Supervising Scientist,
Locked Bag 2, Jabiru NT 0886 Australia. Present address: Faculty of Engineering,
University of Western Sydney, PO Box 10, Kingswood, NSW 2747, Australia

This report should be cited as follows:

Willgoose G & Riley SR 1998. *Application of a catchment evolution model to the prediction of long-term erosion on the spoil heap at Ranger uranium mine: Initial analysis*. Supervising Scientist Report 132, Supervising Scientist, Canberra.

The Supervising Scientist is part of Environment Australia, the environmental program of the Commonwealth Department of the Environment and Heritage.

Supervising Scientist
Environment Australia
GPO Box 787, Canberra ACT 2601 Australia

ISSN 1325-1554

ISBN 0 642 24335 2

Printed in Darwin by NTUniprint.

Contents

Figures

Tables

Acknowledgments

The field data used here was supplied by workers of the Geomorphology Group of the Environmental Research Institute of the Supervising Scientist, Jabiru. Their assistance is appreciated. Computational work was carried out using resources of the School of Engineering, The University of Newcastle, NSW.

Variables

$\boldsymbol{a}$	=	channel initiation function
$\boldsymbol{A}$	=	area per unit width
β_1, m_1, n_1	=	sediment transport coefficient and discharge and slope exponents respectively
β_3, m_3, n_3	=	runoff coefficient, and discharge and slope exponents respectively
β_5, m_5, n_5	=	channel initiation threshold coefficient, and discharge and slope exponents respectively
c_0	=	tectonic uplift
D	=	diffusivity
$f(\boldsymbol{Y})$	=	a sediment transport coefficient dependent on the pattern of channelisation
$\boldsymbol{G}$	=	a function dependent of the runoff process modelled
O_t	=	ratio of hillslope to channel erosion rate
$\boldsymbol{q}$	=	discharge per unit width
$\boldsymbol{Q}$	=	discharge in the channel
$\boldsymbol{q_s}$	=	sediment transport per unit width (mass/time)
ρ_{sb}	=	bulk density of the sediment
$\boldsymbol{S}$	=	slope in the steepest downstream direction
t	=	time
τ	=	the bottom shear stress for the flow and
τ_c	=	a shear stress threshold
x,y	=	horizontal distance
$\boldsymbol{Y}$	=	channel indicator variable (0 = hillslope, 1 = channel)
$\boldsymbol{z}$	=	elevation

Abstract

There is a need to assess the long-term stability of engineered landforms associated with the rehabilitation of Ranger Uranium Mine, Northern Territory, Australia, as it is a requirement that mill tailings must be contained for periods in excess of 1000 years. The geomorphic model, SIBERIA, is calibrated on hydrology and erosion data collected by a combination of monitoring and rainfall simulation experiments on the waste rock dumps of Ranger. Preliminary analysis of Ranger's preferred above-grade and below-grade rehabilitation options suggests that erosion of the order of 7–8 m will occur on the structure in a period of 1000 years. This depth of erosion may be sufficient to compromise the integrity of the containment. It is shown that SIBERIA has significant advantages over steady-state erosion models. Suggestions are made for the design that will enhance the stability of the structure and extend the structural life of the containment.

1 Introduction

1.1 Overview

It is necessary to determine whether the rehabilitated landforms of Ranger Uranium Mine, Northern Territory, Australia, will meet their design specifications, specifically, the containment of uranium mill tailings for several hundred years. Computer modelling of geomorphic processes, and particularly of the degradation of the engineered landforms, is a crucial aspect of the assessment program. As a first stage in the development of assessment procedures, the computer model developed by Willgoose et al (1989, 1990, 1991a,b,c,d), which can simulate the evolution of landscapes over time (SIBERIA), is calibrated to existing hydrogeomorphic data. This report presents details of the calibration of the model and predictions made by it of the likely development of engineered landforms of a rehabilitated Ranger uranium mine.

Details of the research strategy and background to the problem of geomorphic modelling of Ranger are given in Riley (in prep). The following is a brief discussion, details are given in Riley (in prep). It is assumed in the following sections that the reader has access to the background report.

Ranger uranium mine is located in the seasonally wet tropics, has an average annual rainfall of 1500 mm, and is an area of low relief and extremely low rates of denudation (<20 mMa^{-1}). The mine is located in the World Heritage Listed Area of Kakadu National Park, adjacent to Magela Creek, along which are important wetlands and cultural heritage sites.

The rehabilitation of the mine will involve shaping waste rock dumps, consisting of more than 100 million tonnes of waste rock and low grade ore, and containing the mill tailings. The mill tailings may be rehabilitated either above- or below-grade and must be contained in structures with 'structural lives' in excess of 1000 years. Ranger Mines Pty Ltd (RUM) prefers the above-grade option. However, the Environmental Requirements for the mine specify tailings disposal options as follows: 'that by dealing with tailings... the environment will be no less well protected than by transferring the tailings to the mine pits...'. Engineered landforms will be constructed from waste rock—a chlorite rich schist that weathers rapidly to gravels and clay fractions. Geomorphic processes will largely determine the long-term stability of the structures.

Supervisory and regulatory authorities need a means of determining whether designs will perform in accordance with design guidelines. A geomorphic model is needed to assess the long-term stability. The model needs to predict the long-term changes in landforms and the likely water and sediment discharge from the site over time. The research program for developing and testing this model has involved detailed studies of erosion and hydrologic processes on waste rock and natural sites, as well as assessment of risk of dispersal of potential contaminants. Monitoring and simulation were used to collect hydrogeomorphic data for examining the critical processes and providing a data set for calibration of hydrogeomorphic models.

A review of available models suggested that the geomorphic model, SIBERIA, was suitable for the assessment. Hence, it was calibrated on the hydrogeomorphic data and predictions made of landform stability. A series of objectives were set as part of this evaluation.

1.2 Objectives

The objective of this project is to assess the long-term erosional stability of engineered landforms at the Ranger uranium mine using the Willgoose Catchment Evolution Model (SIBERIA).

Specific objectives of this project are:

1 To calibrate the Willgoose Catchment Evolution model (SIBERIA) using data supplied by the Geomorphology Group at ***eriss***.

2 To test the erosional stability of the 'above- and below-grade' options for engineered landforms as currently proposed by RUM.

3 To identify sections of SIBERIA that may need modification and outline the research needed to undertake these modifications.

4 To identify geomorphic research needed to further develop SIBERIA for use at RUM.

5 To present the model in a form that will enable different design options for the engineering of rehabilitation landforms to be tested, within the constraints of the model.

6 To predict particulate discharge in the form of sedigraphs.

The work to achieve these aims is divided into two stages. This report discusses the first stage of the project and addresses objectives 1–4. The second stage report addresses objectives 5 and 6.

1.3 SIBERIA – long-term landscape evolution model

SIBERIA is a computer model for studying the erosional development of catchments and their channel networks. A crucial component of this model is that it explicitly incorporates the interaction between the hillslopes and the growing channel or gully network based on physically observable mechanisms. The elevations within the catchment—both hillslope and channel—are simulated by a mass transport continuity equation applied over geologic time. Mass transport processes considered include fluvial sediment transport, such as modelled by the Einstein-Brown equation, and mass movement mechanisms such as creep, rainsplash or landslide. An explicit differentiation between the processes that act on the hillslopes and in the channels is made. The growth of the channel network is governed by a physically based threshold mechanism, where if a function (called the channel initiation function) is greater than some predetermined threshold then channel head advance occurs. The channel initiation function is primarily dependent on the discharge and slope at that point, and the channel initiation threshold is dependent on the resistance of the catchment to channelisation. Channel growth is thus governed by the hillslope form and processes that occur upstream of the channel head, but in a way that that can be independent of channel growth stability arguments (Smith & Bretherton 1972). The elevations on the hillslopes and the growing channel interact through the different transport processes in each regime and the preferred drainage to the channels that results. The interaction of these processes produces the long-term form of the catchment. The preferential erosion in the channels results in the familiar pattern of hills and valleys with hillslope flow being towards the channel network in the bottoms of the valleys.

The model has two main components. The first component is a model of elevation variation; the second component is a model of where the channels are formed in the catchment. The channels develop in response to changes in the elevation, and in turn, the elevations change in response to the channels.

The first component of the model, the variation of elevation within the catchment, is simulated by a mass transport continuity equation applied over geologic time. If more material enters a region than leaves it, then the elevation rises and vice versa. The mass transport processes in SIBERIA include both fluvial sediment transport and a conceptualisation of diffusive mass movement mechanisms such as creep, rainsplash and landslide. The model averages these processes in time so that the elevations (and the channel network) are indicative of the average, with time, of the full range of erosion events; the elevations simulated are average elevations with time. The model explicitly differentiates between the transport processes that act on the hillslope and in the channel.

The model's second component, the channel network, is simulated by an equation that initiates the advance of the channel heads into the surrounding hillslopes. Catchments start with an initial pattern of channelisation, or no channelisation at all, and channel head advance occurs when a channel initiation function, nonlinearly dependent on the local slope and discharge, exceeds a threshold, characteristic of the landscape. Conceptually this threshold can represent overland flow velocity or shear stress, subsurface flow criteria or criteria based on local landsliding at the channel head.

The first component of the model, the governing equation of the elevations in the catchment model, is expressed as:

$$\frac{\partial z}{\partial t} = c_0 + \frac{\nabla.\boldsymbol{q_s}}{\rho_{sb}} + D\left(\frac{\partial^2 z}{\partial x^2} + \frac{\partial^2 z}{\partial y^2}\right) \qquad 1.3.1$$

where

where	x,y	horizontal directions
	z	elevation
	t	time
	c_0	tectonic uplift
	$\boldsymbol{q_s}$	sediment transport per unit width (mass/time)
	ρ_{sb}	bulk density of the sediment
	D	diffusivity

Variables whose variation in space and time is dependent on the form of the catchment, and thus change as the simulated catchment evolves in time, are highlighted here in bold. All other parameters, though they may vary in space and time, are considered independent of the evolving form of the catchment. The detailed behaviour of these equations will not be discussed in detail here as it has been dealt with adequately elsewhere (Willgoose et al 1991a,b,c,d).

The differential equation for elevation (equation 1.3.1) is a continuity equation in space for sediment transport. It is an average equation that models the average sediment transport over many erosion events to give the average elevations with time. The first term in the elevation equation is the rate of tectonic uplift (positive upwards). This term may be time varying. The third term in the elevation equation represents diffusive mechanisms occurring in certain mass transport processes, such as creep, rainsplash and landsliding (Culling 1963, Dunne 1980, Andrews & Bucknam 1987). The rate of these processes is governed by the diffusivity D. Both the diffusivity and tectonic uplift may vary over the catchment but are not dependent on the form of the catchment. In principle, it is possible to use more sophisticated diffusive processes in models of hillslope evolution but at this time data do not appear to be available to define them accurately. These enhancements (eg viscous and plastic flow) are typically spatially variable and dependent on soil depth. At this time SIBERIA does not model the chemical and physical processes associated with weathering and soil formation. Accordingly, it cannot model those processes that depend on soil depth.

The sediment transport process, $\boldsymbol{q_s}$, modelled by the second term in equation 1.3.1, can be parameterised in any way that is believed to reflect the processes occurring in the catchment. Willgoose et al (1989) and others (eg Kirkby 1971) suggest that a realistic formulation is of the form

$$\boldsymbol{q_s} = f(\boldsymbol{Y})\, \boldsymbol{G}\, \boldsymbol{q}^{m_1} \boldsymbol{S}^{n_1} \qquad 1.3.2$$

where	$\boldsymbol{q_s}$	sediment transport per unit width (mass/time)
	$\boldsymbol{q}$	discharge per unit width
	$\boldsymbol{S}$	slope in the steepest downstream direction
	f($\boldsymbol{Y}$)	a sediment transport coefficient dependent on the pattern of channelisation, discussed below
	$\boldsymbol{G}$	a function dependent of the runoff process modelled, discussed below
	m_1, n_1	sediment transport coefficients

This fluvial sediment transport term is one that has been commonly used by geomorphologists (Kirkby 1971, Smith & Bretherton 1972, Moore & Burch 1986) to represent a transport-limited process. It can be directly related to generally accepted instantaneous sediment transport physics, such as Einstein-Brown, by averaging over the range of flood events. Briefly, when modelling the instantaneous sediment transport rate the appropriate discharge to use is the instantaneous discharge at that time. However, here the equation is used to model the mean sediment transport, so that the appropriate discharge to use is the mean peak discharge derived from a frequency analysis of runoff events (Willgoose et al 1989). This averaging of the sediment transport is carried out in section 4.3. Note that we describe as fluvial erosion any sediment transport processes that result from surface runoff, whether they be on the hillslope, as sheet or rill flow, or in the channels.

The function $\boldsymbol{G}$ indicates what *proportion of storms* saturate that point and thus generate surface runoff. It is only during those storms when surface runoff is generated that fluvial erosion occurs. The calculation of this parameter is discussed in further detail in Willgoose et al (1991e). Suffice to say that for Hortonian runoff it might be assumed that $\boldsymbol{G}$=1. For subsurface saturation generated runoff, smaller storms saturate a smaller proportion of the catchment than do larger storms. Thus for subsurface saturation runoff, $\boldsymbol{G}$ is less than 1 and largest in those parts of the catchment saturated most frequently.

The slope in the fluvial sediment transport equation is determined directly from the catchment elevations and the direction of steepest downhill drainage. The discharge relationship, dependent on area and slope, can be formulated to reflect the processes that occur in the field. However, it is important to note that if the sediment transport equation is to model the *long term average* sediment transport equation then the discharge per unit width, $\boldsymbol{q}$, should be interpreted as the mean annual peak discharge, analogous to the idea of a dominant discharge (Willgoose et al 1989), so that

$$\boldsymbol{Q} = \beta_3\, \boldsymbol{A}^{m_3}\, \boldsymbol{S}^{n_3} \qquad 1.3.3$$

where $\boldsymbol{Q}$ discharge in the channel

β_3 runoff rate constant

$\boldsymbol{S}$ slope in the steepest downstream direction

$\boldsymbol{A}$ area per unit width

m_3, n_3 exponents

This relationship is calibrated in section 4.2 of this report. This empirical relationship accounts for runoff routing effects within the catchment and the spatial correlation of rainfall (Leopold et al 1964, Pilgrim 1987).

A crucial feature of this model is its ability to explicitly model the extension of the channel network and to allow for different sediment transport processes in the channels and on the hillslopes. A variable is defined, $\boldsymbol{Y}$, that identifies where channels exist ($\boldsymbol{Y}\approx 1$) versus where the catchment is hillslope ($\boldsymbol{Y}\approx 0$). Initially a catchment can either have no channels or it can have a predefined channel network and drainage pattern. The extension of the network occurs when a function, nonlinearly dependent on contributing area slope, called the channel initiation function $\boldsymbol{a}$, exceeds a threshold value called the channel initiation threshold a_t. The exact means by which the transformation from hillslope to channel occurs appears to be unimportant, though Willgoose and co-workers have extensively used one that results in channels being permanently formed at a point once the threshold has been exceeded at that point. More important is the functional dependence of the channel initiation function on discharge and slope which Willgoose and co-workers have formulated as

$$\boldsymbol{a} = \beta_5\, \boldsymbol{q}^{m_5}\, \boldsymbol{S}^{n_5} \qquad 1.3.4$$

where $\boldsymbol{a}$ channel initiation function

β_5, m_5, n_5 coefficients

Again, within the conceptual framework of the model, the form of the channel initiation function can be formulated as seen fit in light of physical processes observed in the field. The formulation above results from consideration of surface flow driven channel formation processes where it has been postulated that channel formation occurs when a critical velocity or tractive force is exceeded by overland flow or where the head gradient in the groundwater exceeds a specified piping threshold (Willgoose et al 1989). It is consistent with field data collected by other workers (Montgomery & Dietrich 1988, Patton & Schumm 1975). This relationship will be calibrated in section 4.4 of this report using preliminary data from Tin Camp Creek.

The channel network calculated by the model is used to determine the rate at which fluvial sediment transport occurs as

$$f(\boldsymbol{Y}) = \begin{cases} \beta_1 O_t & \boldsymbol{Y} = 0 \text{ (hillslope)} \\ \beta_1 & \boldsymbol{Y} = 1 \text{ (channel)} \end{cases} \qquad 1.3.5$$

where $\boldsymbol{Y}$ channel indicator variable

β_1 erosion rate constant

O_t ratio of hillslope to channel erosion rate

The transport rate β_1 can be spatially variable in any predefined way; structural controls due to the differential erodibility of strata can be easily modelled. However, the sediment transport rate β_1 is not varied as a result of the evolving catchment's hills and valleys so that differential sediment transport rates in valleys and interfluves cannot be modelled other than with a crude area or slope dependence. Very little data are available to calibrate such a dependence. The parameter O_t is generally assumed to be somewhat less than 1 and this reflects the increased velocities, and thus transport rates, in channels over that occurring on the hillslopes. Diffusive transport is assumed to occur at the same rate on both hillslopes and channels.

Note that the sole use of the channel network *within the model* is in determining the differential rates of erosion that occur in the channel and on the hillslopes. No field interpretation is made regarding whether a channel head is an abrupt or gradual transition, only that the fluvial transport rate changes abruptly. Willgoose and co-workers have normally assumed that the actual channel network observed in the field and the channel network postulated in the model are synonymous.

In summary, the important feature of the presented model—the one that distinguishes the networks it generates from other stochastic network generation models (Leopold & Langbein 1962, Howard 1971)—is that the network extension process is governed by physical conditions: the drainage pattern on the hillslopes and the local slopes in the hillslopes around the channel head. That channels can be assumed to erode faster than the hillslopes facilitates the natural tendency towards convergence of flow on the hillslopes around the channel heads. The pattern of pre-existing channels governs the valley erosion, which in turn governs the drainage pattern of the hillslopes and their slopes, and thus, the spatial pattern of the channel initiation function. This complicated interaction of flow and sediment transport in both the channels and hillslopes over long time scales is central to the channel network extension process and it gives catchments their form.

1.4 Hydrology model

Runoff is the most important determinant of soil erosion. Thus it is important to simulate runoff as accurately as possible to provide a reliable erosion assessment. To do this a digital terrain based rainfall-runoff model will be calibrated to the field data collected at experimental sites on the spoil. This model will then be used to calibrate the runoff required by SIBERIA. The model will also be used to simulate the long-term runoff series that will be used to determine the relationship between the short-term erosion rate measured during runoff events and the long-term erosion over the historical range of runoff events.

The hydrology model used to fit to the rainfall simulator and natural rainfall plots is based on the 1-D kinematic wave flood routing model described by Field and Williams (1987) called the Generalized Kinematic Catchment Model (GKCM). This model is a conceptual rainfall-runoff model (fig 1.1) that breaks the catchment up into a number of subcatchments connected together with a channel network (fig 1.2) draining to a single catchment outlet. More specifically it includes:

1 Nonlinear storage of water on the hillslope surface

2 Philip infiltration from the surface storage to a linear groundwater store

3 Discharge from the surface storage to the channel

4 Discharge from the groundwater storage to the channel

5 Routing of the runoff down the channel by use of the kinematic wave

This form of the model has been tested on a number of catchments and has been shown to give satisfactory results. As conceptualised by the developers this model is a Hortonian runoff model.

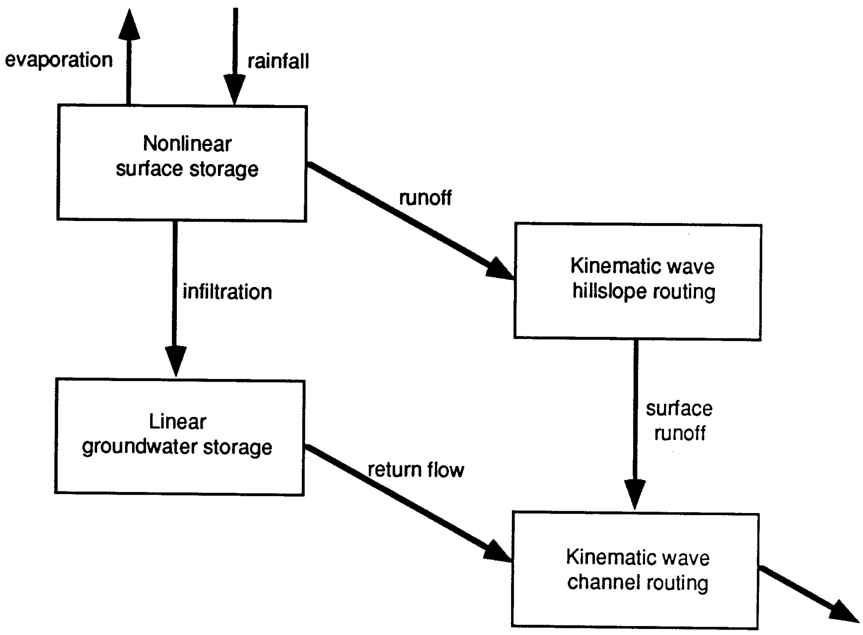

Figure 1.1 Conceptual arrangement of the Field-Williams rainfall-runoff model as extended by Willgoose (DISTFW)

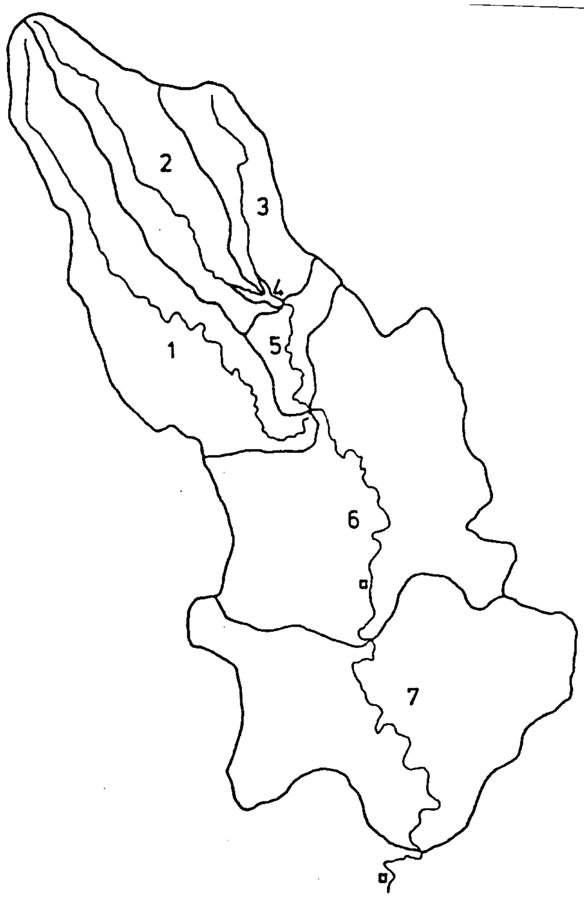

Figure 1.2 Typical division of catchment into subcatchments (from Field & Williams 1987)

This model has been extended to use digital terrain elevation data on a square grid; hereafter this new extended model will be called the Distributed Field-Williams Model (DISTFW). Each grid point is considered to be a subcatchment and drainage from node to node and through nodes occurs by a kinematic wave on the overland flow. For the purposes of this project the modifications to the model include:

1 The drainage pattern from node to node is determined on the basis of the steepest slope direction using the same algorithm used in SIBERIA.

2 The groundwater component on the model has been disabled. Infiltration is assumed to drain to a very deep aquifer which does not discharge to the surface within the study site. This is believed to be a good representation of the waste rock dump.

3 The area associated with each subcatchment (node) is equal and equal to the square of the grid spacing. The DTMs provided for the waste rock dump are on a 30 m grid so that the area of each node is 900 m^2.

This extended model maintains the conceptualisation of Hortonian runoff but by using the digital terrain extensions it is possible to model subsurface saturation runoff using the methodology of Moore and Grayson (1991). The subsurface saturation runoff mechanism is not considered important on the waste rock dump because of the lack of a well developed soil profile exhibiting decreasing hydraulic conductivity with depth and underlying impermeable bedrock layer.

1.5 Erosion model

The overland flow erosion model used to fit the erosion data is one commonly used by geomorphologists and soil scientists. It is of the general form

$$\boldsymbol{q_s} = \beta_1 \, \boldsymbol{q}^{m_1} \, \boldsymbol{S}^{n_1} \left(\tau - \tau_c\right) \tag{1.5.1}$$

where $\boldsymbol{q_s}$ sediment discharge/unit width

$\boldsymbol{q}$ discharge/unit width

$\boldsymbol{S}$ local slope

τ bottom shear stress for the flow

τ_c shear stress threshold

The parameters β_1, m_1 and n_1 are fixed by the flow geometry and erosion physics. This equation parameterises the total load; ie the sum of both the suspended and bed loads. For instance, for a constant width channel with sediment transport according to the Einstein-Brown equation m_1 = 1.8 and n_1 = 2.1. For flow in rills the parameters are approximately $m_1 \approx 1.3$ and $n_1 \approx 2.2$ (Moore & Burch 1986, Willgoose et al 1989). Exact values for these parameters depend on the rill geometry. The parameter β_1 gives the rate of sediment transport and is primarily a function of sediment grain size.

Riley (1992) attempted to identify a shear stress threshold as in equation 1.5.1 for the material from the waste rock dump using a small flume and concluded that the value was very small, and that he was unable to reliably estimate it. On this basis the shear stress threshold in all the work that follows will be assumed to be zero.

We also note that bottom shear stress, τ, can be described by a function of discharge and slope (ie Willgoose et al 1989) so that the sediment transport model that is used here has the form

$$\boldsymbol{q_s} = \beta_1 \, \boldsymbol{q}^{m_1} \boldsymbol{S}^{n_1} \tag{1.5.2}$$

This model does not incorporate hysteric effects in the sediment rating curve that may result from sediment storage. However, since there is no data for the region that indicates the possible importance of this effect over areas of the size of the waste rock dump this effect has been ignored. It is not possible at the current time to predict the magnitude of this effect without extensive field data for large catchments.

For smaller areas the overland erosion is dominated by rainsplash, or rain-flow, erosion. Rainsplash is generally modelled by an additive Fickian diffusion term where the diffusivity, D, is a function of the applied rainfall energy (in turn a function of the energy of the individual raindrops and the rainfall rate) so that $D = D'R$ where R is the rainfall rate. The total erosion rate is then given by the expression

$$q_s = \beta_1 q^{m_1} S^{n_1} + DS = \beta_1 q^{m_1} S^{n_1} + D'RS \tag{1.5.3}$$

For calibration, this result is more conveniently expressed in terms of the concentration

$$c = \beta_1 q^{m_1 - 1} S^{n_1} + \frac{DS}{q} = \beta_1 q^{m_1 - 1} S^{n_1} + \frac{D'RS}{q} \tag{1.5.4}$$

These equations indicate that as the discharge decreases, or the area of the plot decreases, then the second, diffusive term will begin to dominate the expression for concentration. For large areas the diffusive term becomes relatively less important. That the diffusive term is additive implies that the processes that cause diffusive transport and those that cause fluvial transport do not interact. Thus a higher or lower level of diffusive transport does not of itself change the rate of fluvial transport.

In using SIBERIA it is necessary to clearly distinguish between the instantaneous sediment transport rate and the long-term sediment transport rate. The instantaneous transport rate is that which is measured at some instant in time, for instance, within a runoff event by a grab sample. This is the quantity that is measured during field trials. The long-term sediment transport is the average rate of transport of sediment per year; the average of all the erosion events during the year. As well as being a function of the short-term rate, this quantity is a function of the average runoff properties and climate of the catchment. Willgoose et al (1989) showed that it if the sediment transport rate was described by equation 1.5.2, then the long-term average could also be expressed in that form. The interpretation of β_1 and q are modified (β_1 is a frequency factor and q is the mean peak discharge) and the runoff modelling of this report is aimed at simulating this runoff data for the waste rock dump.

The model of equation 1.5.1 is primarily used for ‘transport limited’ sediment transport. That is, it is assumed that there is always sufficient material on the surface to satisfy the transport demands of the flow. This is not the case when sediment starvation or source limitation occurs and it is not established that equation 1.5.1 is necessarily complete for this case. There does appear to be some evidence to suggest that sediment starvation can occur at Ranger (Riley, in prep). Riley (1992) showed that for a constant discharge the concentration of sediment decreased over a period of 1 hour but the effect appeared to be small. Moreover, some of the concentration data for the natural rainfall events exhibited clockwise rating curves with discharge. However, if the sediment transport model is calibrated to the natural data rather than simulated runoff data, this effect will be accounted for, on average, in the calibration. For natural runoff events, the recorded data will be for the naturally sediment starved flow; the calibrated β_1 will be lower, reflecting the sediment starvation. If, however, the sediment transport model is calibrated with the rainfall simulator trials then sediment starvation has to be accounted for explicitly. This study uses the natural data wherever possible to circumvent this problem. In any event, the small differences between the simulated rainfall and natural rainfall concentration data appear to have negligible effect on the relationship between discharge and concentration.

2 Hydrology model calibration

2.1 Overview

2.1.1 Data

Natural rainfall runoff events for the caprock and batter sites were supplied by staff of the Geomorphology Branch at ***eriss***. Tables 2.1 and 2.2 summarise the runoff and rainfall data that have been used in this study. Maps of the field sites are provided in appendix A and the data are tabulated in appendix B. Catchment characteristics are summarised in table 2.3.

Some of the rainfall and runoff data were checked by double mass curves. A very good correlation was found for most storms (see fig 2.1 & 2.2) as would be expected by their closeness. For the 16/2/91 event, the batter gauge appears to have missed the first peak of a two-peaked storm.

The plot characteristics (eg area, slope) were determined from the contour maps in appendix A.

Table 2.1 Runoff data supplied for caprock and batter sites[c]

	Caprock sites[a]					Batter sites		
Storm	WT1	WT2	WT3	RT1	OUT	RT2	WT1	WT2
25/12/90								
28/12/90								
7/1/91 (20:50)[b]	?				✓[d]			
7/1/91 (14:55)[b]		✓		✓	✓[d]			
8/1/91					✓[d]			
10/1/91 (7:55)[b]	✓	✓		✓	✓[d]			
10/1/91 (14:00)[b]					✓[d]			
11/1/91					✓[d]			
21/1/91	✓	✓						
27/1/91								
28/1/91					✓[d]			
30/1/91								✓
4/2/91		✓					✓	
6/2/91			✓			✓	✓	✓
13/2/91						✓		
16/2/91	✓		✓			✓	✓	✓
22/2/91						✓	✓	

(a) Site notation as per Neave (1991); (b) Two events supplied for this day, approximate beginning time in 24 hour clock;
(c) Notation is ✓ = data appears to be accurate; × = data appears to be inaccurate; ? = data conflicts with other data;
(d) Data is truncated above discharge 15 L/s.

Table 2.2 Supplied rainfall data[(b)]

Storm	Site CAP	Site BAT	Storm	Site CAP	Site BAT
25/12/90	✓		27/1/91	✓	
28/12/90	✓		28/1/91		✓
7/1/91 (20:50)[(a)]	✓		30/1/91	✓	✓
7/1/91 (14:55)[(a)]	✓		4/2/91	✓	✓
8/1/91	✓		6/2/91	✓	✓
10/1/91 (7:55)[(a)]	✓		13/2/91		✓
10/1/91 (14:00)[(a)]	✓		16/2/91	✓	×
11/1/91	✓		22/2/91		✓
21/1/91	✓	✓			

[(a)] Two events supplied for this day, approximate beginning time in 24 hour clock; [(b)] Notation is ✓ = data appears to be accurate, × = data appears to be inaccurate, ? = data conflicts with other data.

Table 2.3 Catchment characteristics

	Area (m^2)	Mean slope	Mean width (m)	Length (m)
COUT	2182	0.03	(b)	(b)
CRT1	461	0.029	(b)	(b)
CRT2	330	0.039	(b)	(b)
CRT3	731	0.034	(b)	(b)
CWT1	149 [(a)]	0.04	4.57	32.6
CWT2	102	0.035	1.87	54.4
CWT3	91	0.036	1.63	55.6

[(a)] see text; [(b)] variable width and length

2.1.2 Calibration

The primary data used for calibration of the rainfall-runoff model were the natural rainfall events. Reliable events were selected for several sites and the model parameters adjusted by trial and error to give a good fit. The broad range of hydrographs available in the provided data (single peaked versus double peaked hydrographs for a variety of closely spaced sites) exercised all components of the model. The rainfall simulator trials had less variation in discharge and did not exercise all the components of the model, making it difficult to reliably estimate their parameters. They provide useful verification data and if the natural event data were poor or unavailable would have been a crucial data source.

As far as possible parameters were determined from, or checked against, other independent data. For instance, Manning *n* values for the kinematic wave routing have been checked against measures of surface roughness.

Where extra runoff event data were available verification of the selected model parameters was carried out. This verification is an important part of the process of ensuring that the selected model and parameters are satisfactory. If the parameters are satisfactory then the predictions of the model for an independent site and runoff event should provide a satisfactory fit without adjustment of model parameters. The goodness of fit for the verification sites and events is not normally as good as for the calibration runs, for obvious reasons, but they should at least exhibit a correspondence in volume, peak discharge and its timing, and an overall shape of the hydrograph.

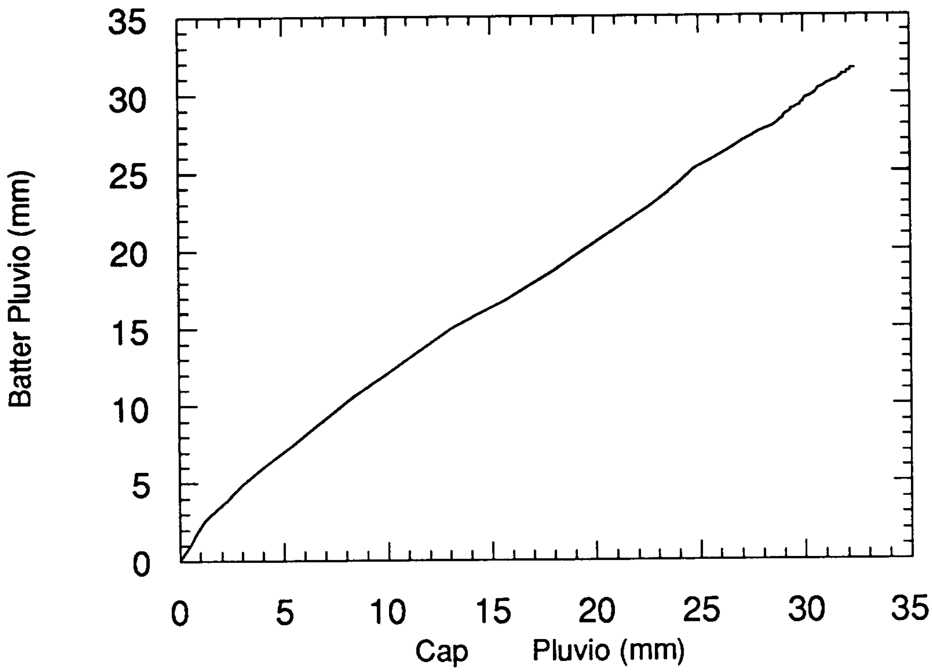

Figure 2.1 Double mass curve for the batter and caprock pluviographs used to measure the natural rainfall events

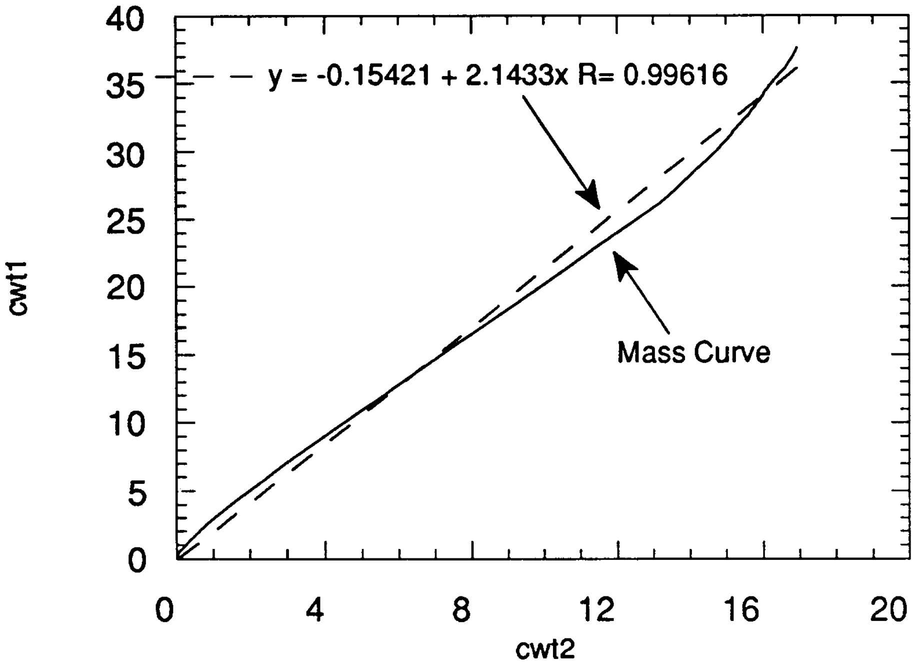

Figure 2.2 Double mass curve for catchment CWT1 and CWT2 for the event of 10/1/91

2.2 Caprock sites calibration

2.2.1 Natural rainfall data

The first of the plots to be calibrated was CWT2. Three reliable storms were chosen and parameters fitted by trial and error. The only difference for the parameters for the three storms were initial soil wetness conditions, parameterised by the initial sorptivity. The parameters adopted are given in table 2.4 (see section 2.4). The simulations of runoff for the three storms are given in figures 2.3, 2.4, and 2.5. The chosen parameters fit all aspects of the hydrographs well. There appears to be a slight problem with the data for the second peak of the hydrograph for the 7/1/91 storm but there were insufficient data to check these observed data against other data by use of double mass curves. In all cases the timing of peaks is satisfactory indicating that the conveyance parameters (ie Mannings *n*) are satisfactory. The widths of the hydrographs are satisfactory indicating that the surface storage parameters are satisfactory. Finally the volume and the distribution of this volume within the hydrographs are well matched indicating that the infiltration parameters are satisfactory.

The next plot to be calibrated was CWT3. The first attempt at calibration used the parameters as derived from CWT2. The conveyance was modified by the width of the plot given the values in CWT2. Since these plots were only about 70 m apart it was believed that the parameters of the two plots would have similar characteristics. However this gave a hydrograph that had too much volume, though the peak was satisfactory. It was possible to identify high infiltration zones within the catchment near the bottoms and the tops of the catchment. These zones had a long-term infiltration rate of about 40 mm/hr, much higher than 6.5 mm/hr found in CWT2. The two events examined, 6/2/91 and 16/2/91, are illustrated in figures 2.6 and 2.7. The predicted hydrographs are given for the adjusted CWT2 parameters and using the high infiltration zone parameters. This high infiltration rate may result from a number of causes including cracks in the surface or zones of lower compaction in the surface layer. That the infiltration rate is higher in CWT3 than elsewhere is supported by a double mass curve analysis for storm 16/2/91 using CWT1 and CWT3 (fig 2.8). This double mass curve suggests that the runoff in CWT1 is approximately four times that CWT3 even though their areas are very similar.

The parameters derived for plots CWT2 and CWT3 were then used to calibrate/verify the runoff events for plot COUT. This is believed to be one of the better data sets, however, all data have been truncated above about 15 L/s so that only lower flow values can be compared. However, the timing of the rises can be used to assess the value of the conveyance, and thus the Mannings *n*, and the lower peaks in the storms can be used to provide some support for the infiltration values for this site. It is expected that the parameters of CWT2 should be indicative of the parameters for COUT because CWT2 is a subcatchment of COUT. Indeed this was the case. Plots of estimated storms are provided in figures 2.9 and 2.10. For these storms the initial sorptivity was estimated; all other parameters are as calibrated for CWT1 (table 2.4).

Finally site CWT1 was examined. This site has a number of rainfall events that are common with the calibration events described above. To validate the model it was decided to use the parameters fitted above and the initial conditions identified above to fit the events on CWT1. This section is then a true validation test because no parameters are fitted. If the model parameters are incorrect then the predictions would be poor; otherwise they should be good. The two events used were 10/1/91 and 21/1/91. The observed and predicted runoffs are given in figures 2.11 and 2.12. An initial peak in the event of 21/1/91 has been estimated in the simulation. This appears to be an error in the observed runoff record for this site since an initial peak is indicated by both pluviograph records. The fit of the simulation data to the runoff data for these two events appears to be satisfactory.

A further verification of the model was carried out with the data for CRT1. The event of 7/1/91 was fitted for COUT. These parameters, and catchment properties from the maps were used to predict the response of CRT1. The results are shown in figure 2.13. The initial conditions on the sorptivity were those fitted for that event at COUT. The overall verification is very satisfactory with both peaks and volumes being well fitted.

2.2.2 Comparison of fitted hydrologic parameters with other data

Samples of the surface lag material were taken and their grading analysed by workers at ***eriss***. This grading data can be used to estimate a value of Mannings n for comparison with the value calibrated in the runoff-routing. There were 4 sites on the caprock surface C1F3S1, C1F3S2, C1F3S3, and C1F3S3 where samples were taken. Henderson (1966) gives an expression relating the size below which 75% of the material falls and Mannings n of

$$n = 0.031\ d_{75}^{\ 1/6} \qquad 2.2.1$$

The d_{75} of the four sites were 6, 2, 2.4 and 2 mm respectively yielding values of Mannings n of 0.018, 0.015, 0.015, and 0.015 respectively. These values reflect only the roughness of the surface due to the grain roughness and the actual measured Mannings n will be somewhat higher. They do not account for form drag on the surface (due to lumps and undulations in the surface), rapid changes in the cross section of the flow, and tortuosity of the flow paths. Chow (1959) outlines a method of allowing for these effects (table 5.5, p 109). Allowing for these effects (minor irregularity, occasional cross-section changes and appreciable meandering) suggests an increase in n of about 0.01–0.015 so that the Mannings n of the surface should be about 0.03. This value is in good agreement with the calibrated value (see table 2.4).

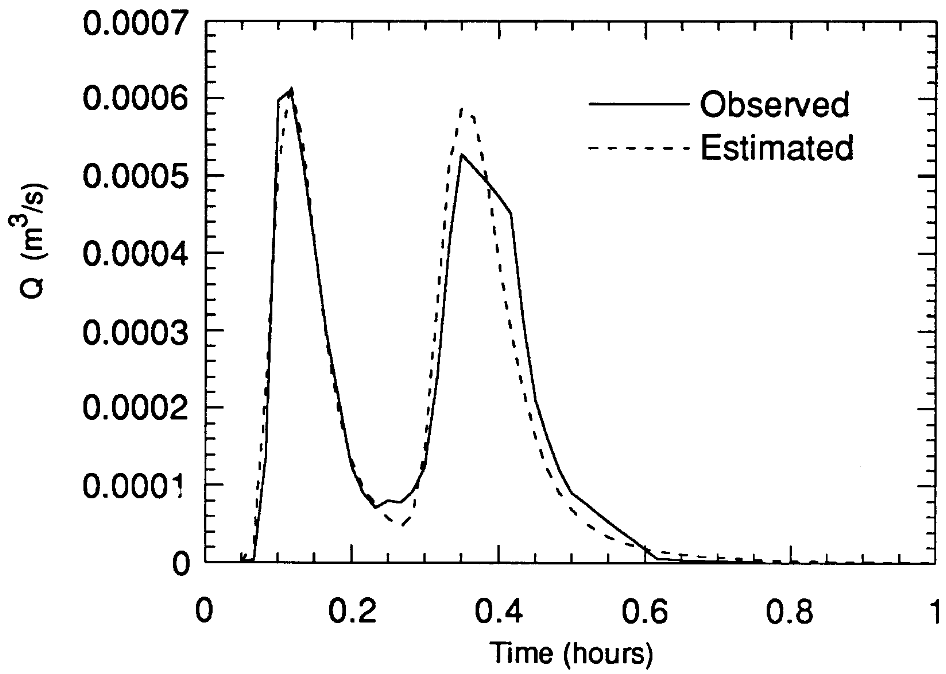

Figure 2.3 Calibration for CWT2 on 7/1/91

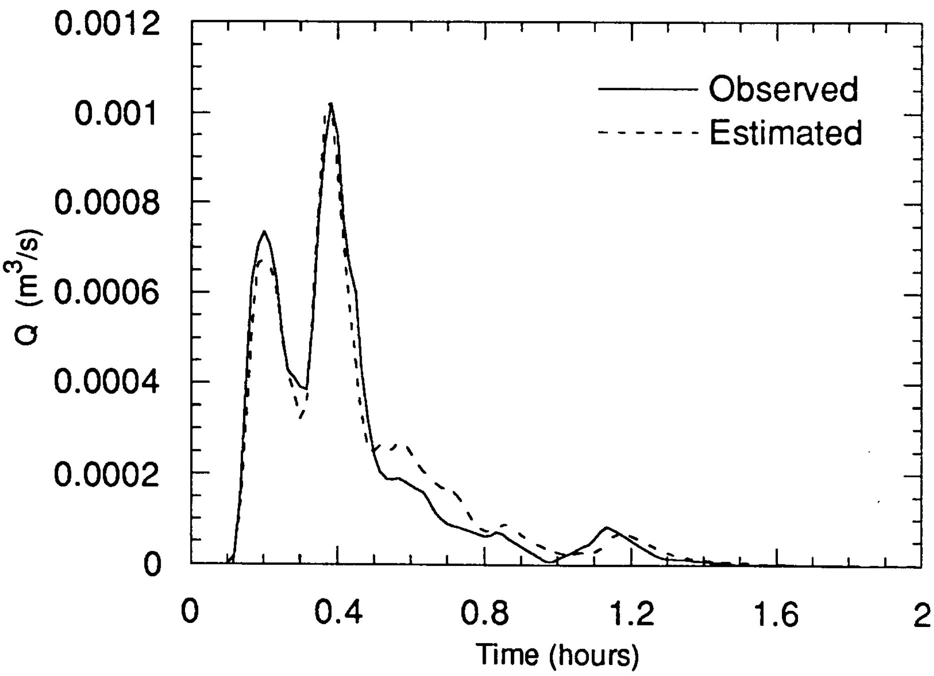

Figure 2.4 Calibration for CWT2 on 10/1/91

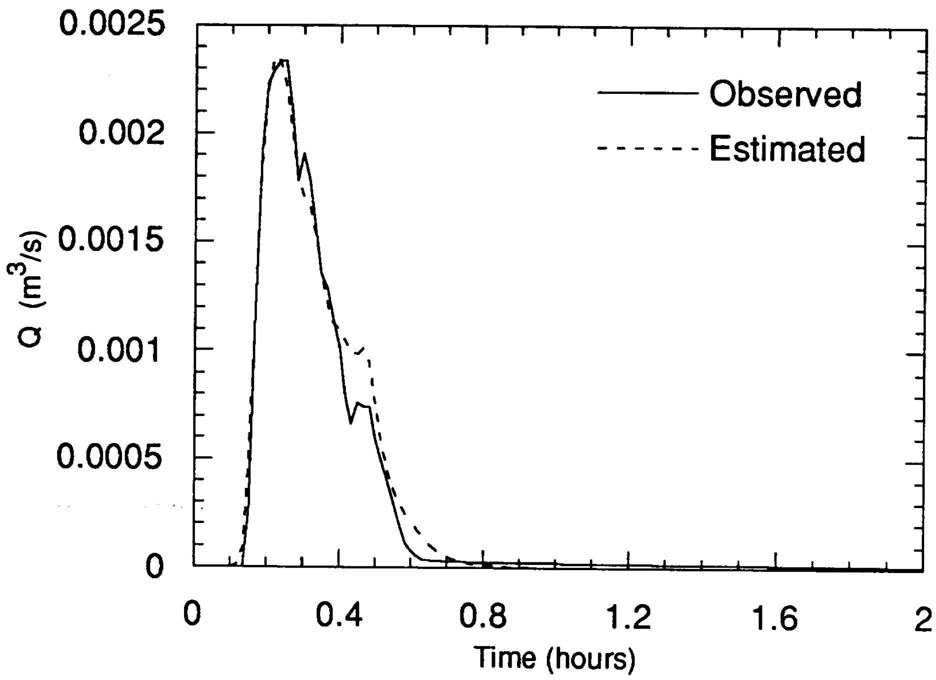

Figure 2.5 Calibration for CWT2 on 21/1/91

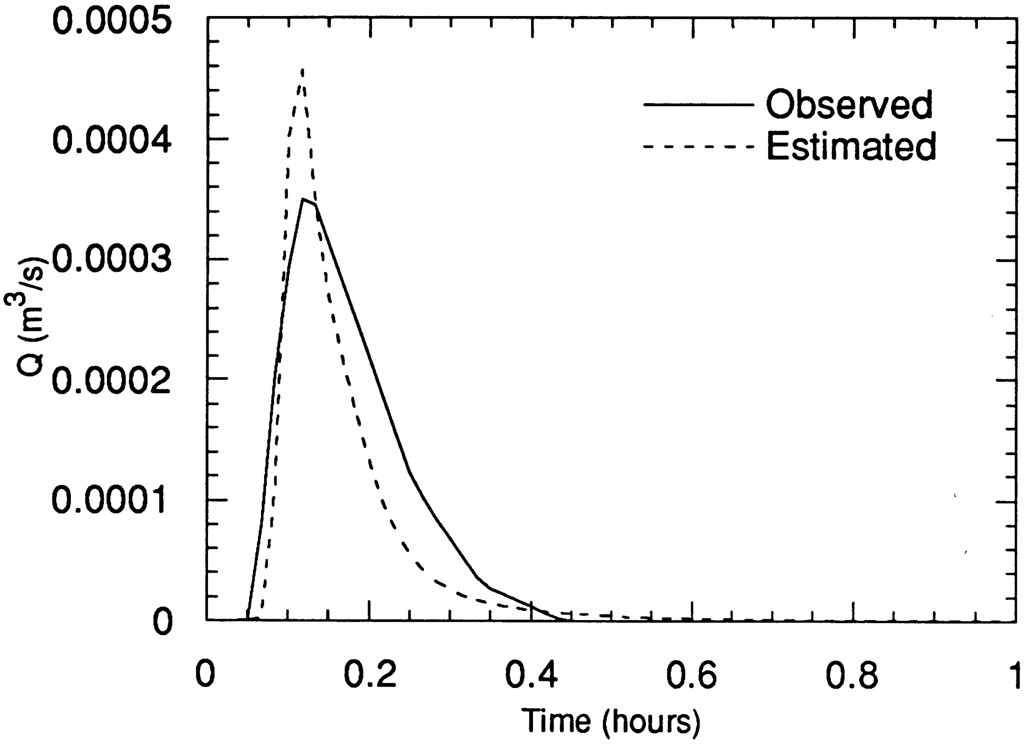

Figure 2.6 Calibration for CWT3 on 6/2/91

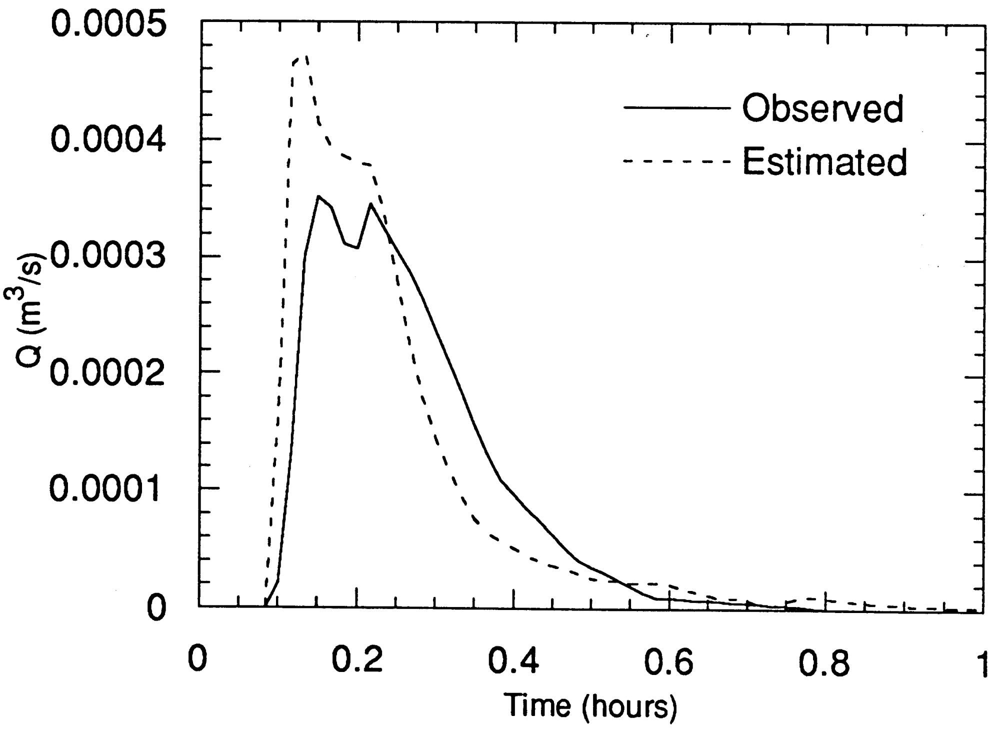

Figure 2.7 Calibration for CWT3 on 16/2/91

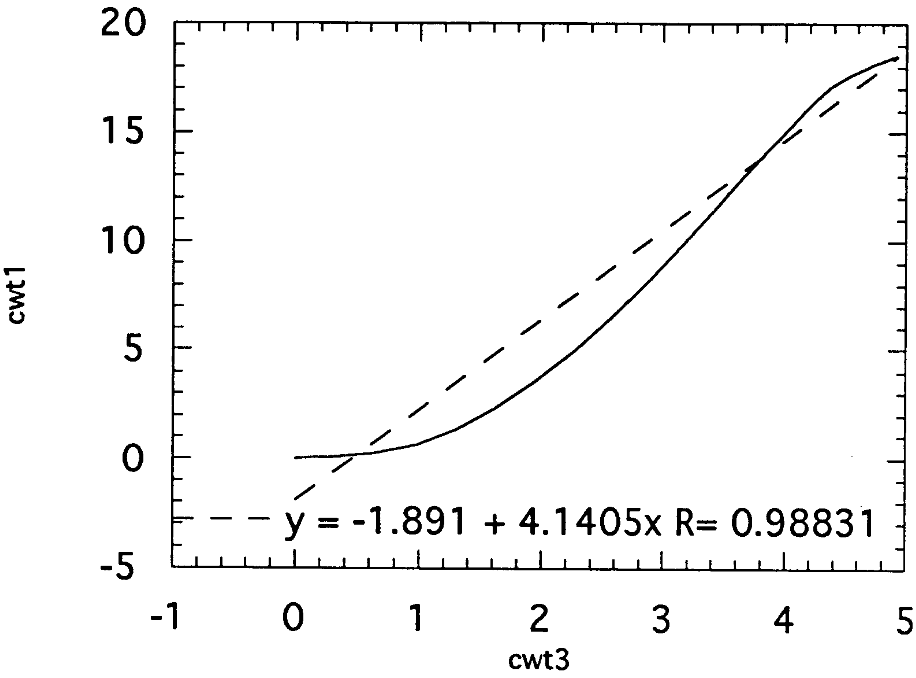

Figure 2.8 Double mass curve for CWT1 and CWT3 for event 16/2/91

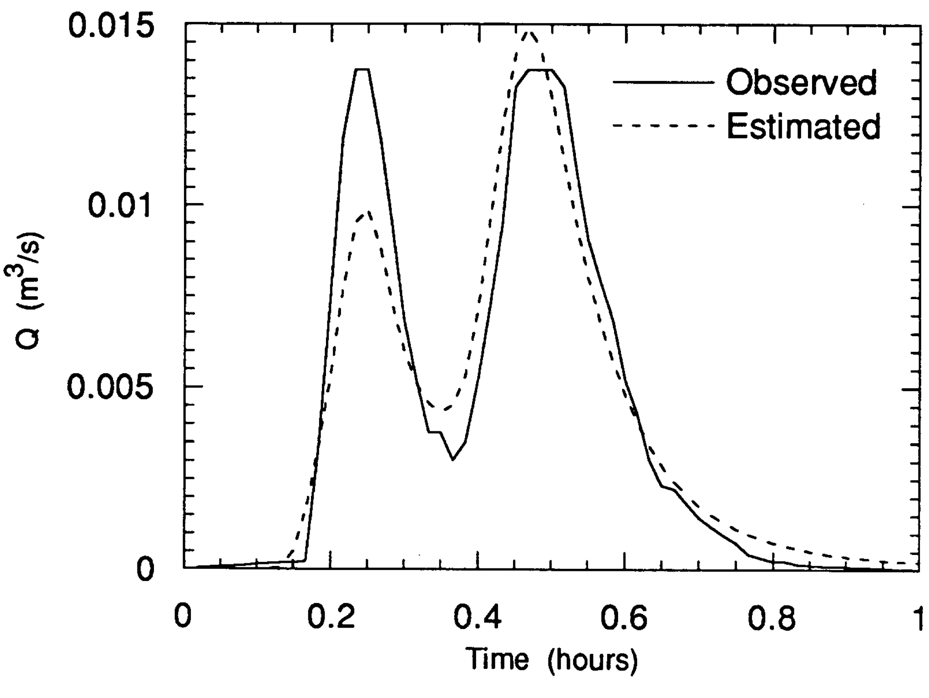

Figure 2.9 Calibration for COUT on 7/1/91

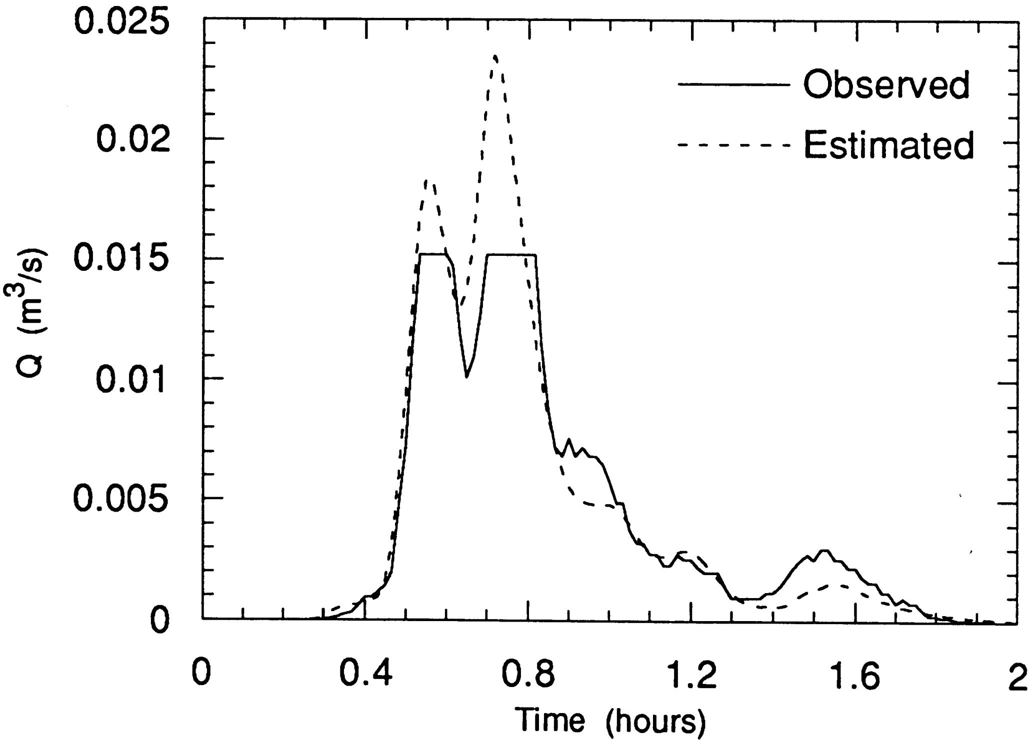

Figure 2.10 Calibration for COUT on 10/1/91

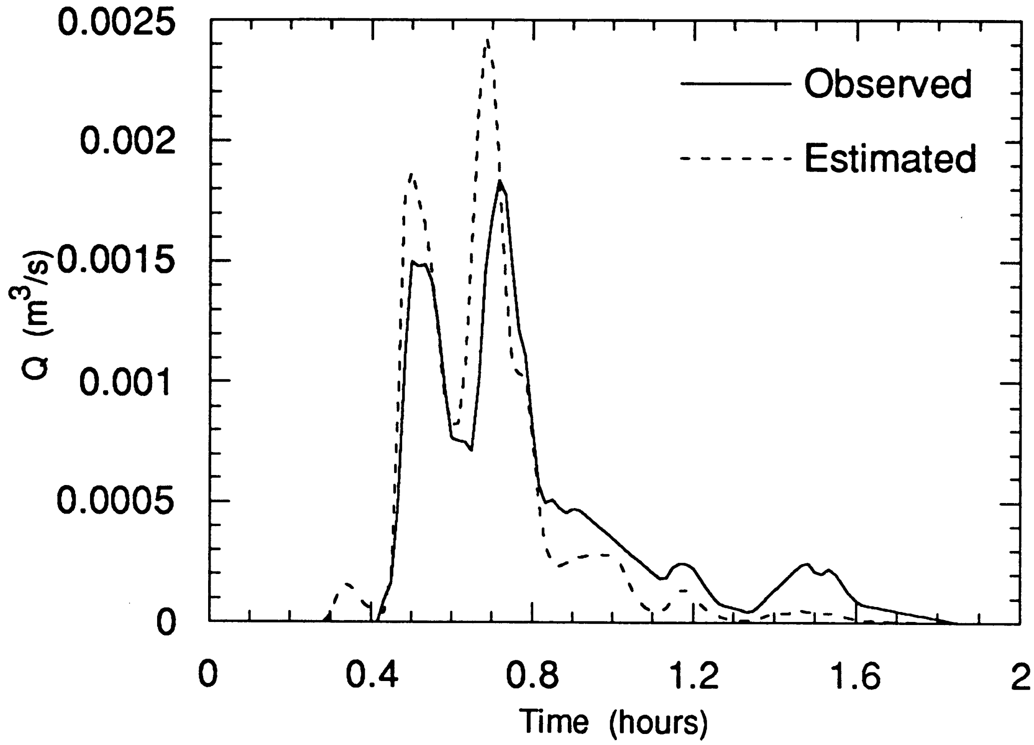

Figure 2.11 Verification for CWT1 on 10/1/91

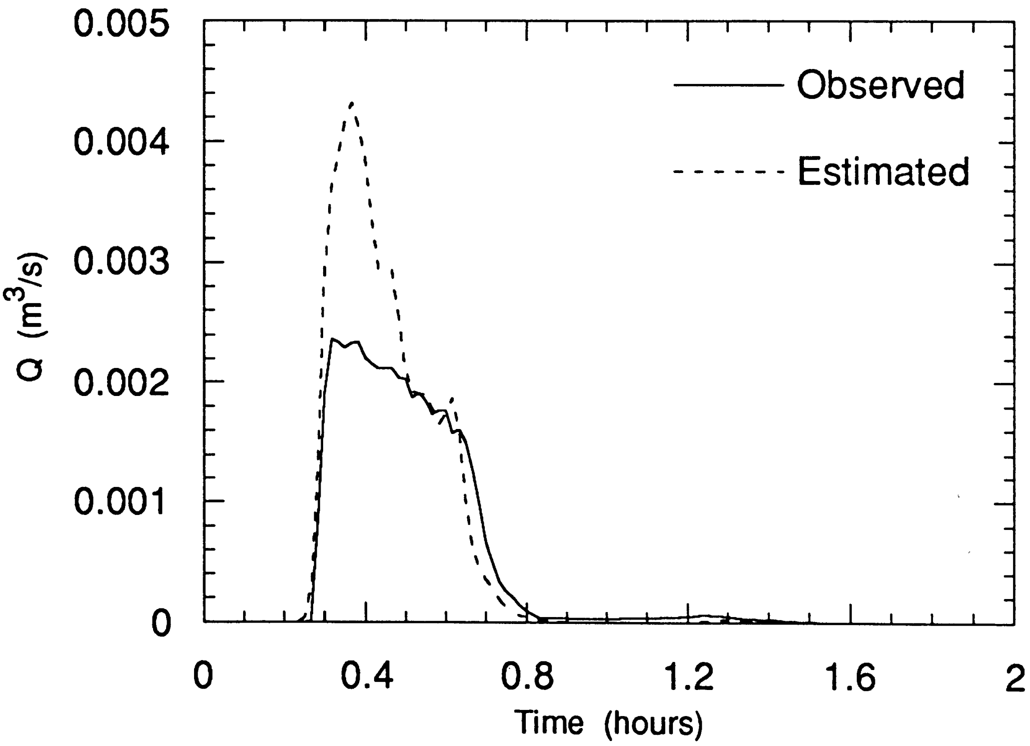

Figure 2.12 Verification for CWT1 on 21/1/91

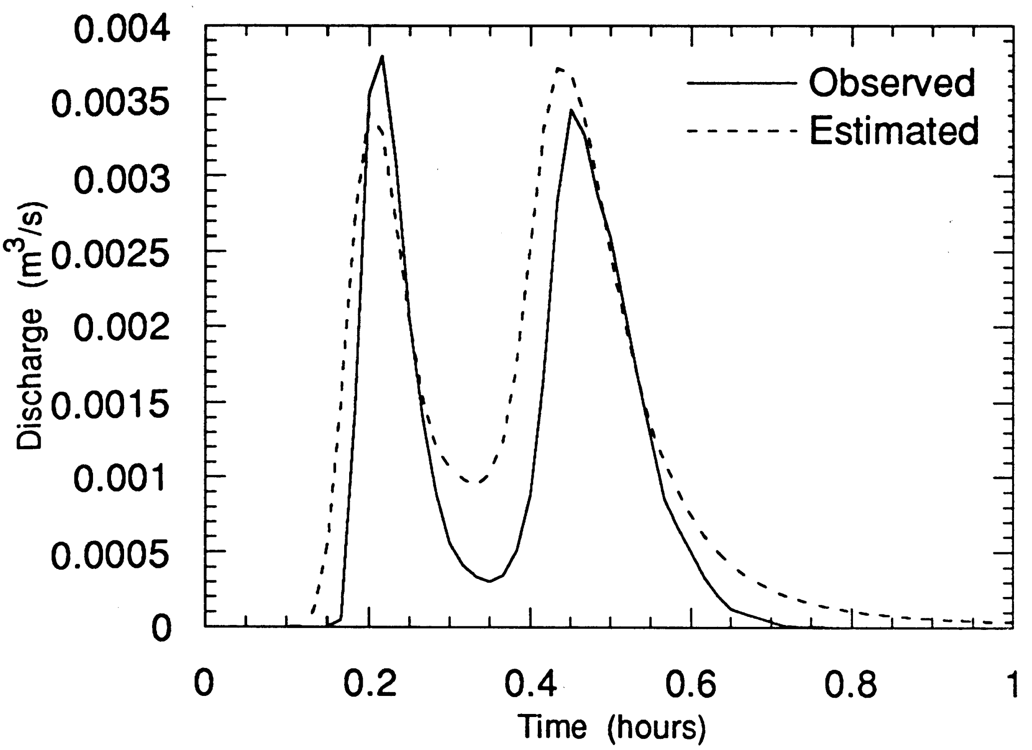

Figure 2.13 Verification for CRT1 on 7/1/91

2.3 Batter sites calibration

2.3.1 Natural rainfall data

The parameters fitted in the previous section for the caprock sites were used as the starting point for the calibration of the batter sites. Only three sites had reliable data for calibration of the hydrology. Of these two plots (BWT2 and BWT3) were discarded as being too short to be able to check the routing behaviour of the plots; the lags between peak rainfall and peak discharge were judged to be too small. The remaining site, BRT2, had 4 rainfall events of which three were considered reliable. The fourth had fluctuations in the rainfall that were not exhibited in the runoff. Two of the events, those on 6/2/91 and 22/2/91, were used for the verification of the parameters. These were a small flood (max 1.5 L/s) and a large flood (max 5 L/s) respectively, allowing the hydrology model to be verified over a range of discharges.

The fits for the 6/2/91 and 22/2/91 sites are illustrated in figures 2.14 and 2.15. The runoff volumes appear too small, particularly for the event of 22/2/91. Overall, however, the parameters as fitted for the caprock appear to be satisfactory for prediction of runoffs from the batter.

The Manning *n* used for predicting the runoff from the batters in figure 2.14 and 2.15 was the same as that for the caprock. The rising limb of the 6/2/91 event appears to be leading slightly, suggesting a higher value of Mannings *n* may be appropriate (of about 0.003), however, the rising limb for 22/2/91 appears to be satisfactory suggesting no change. The grading of the surface material on the batter appears to be similar to that on the caprock suggesting that the value of Mannings *n* should be the same as that measured/calibrated for the caprock sites. On balance, given the good overall fits, no case could be made for significant changes in Mannings *n* from the caprock to the batter.

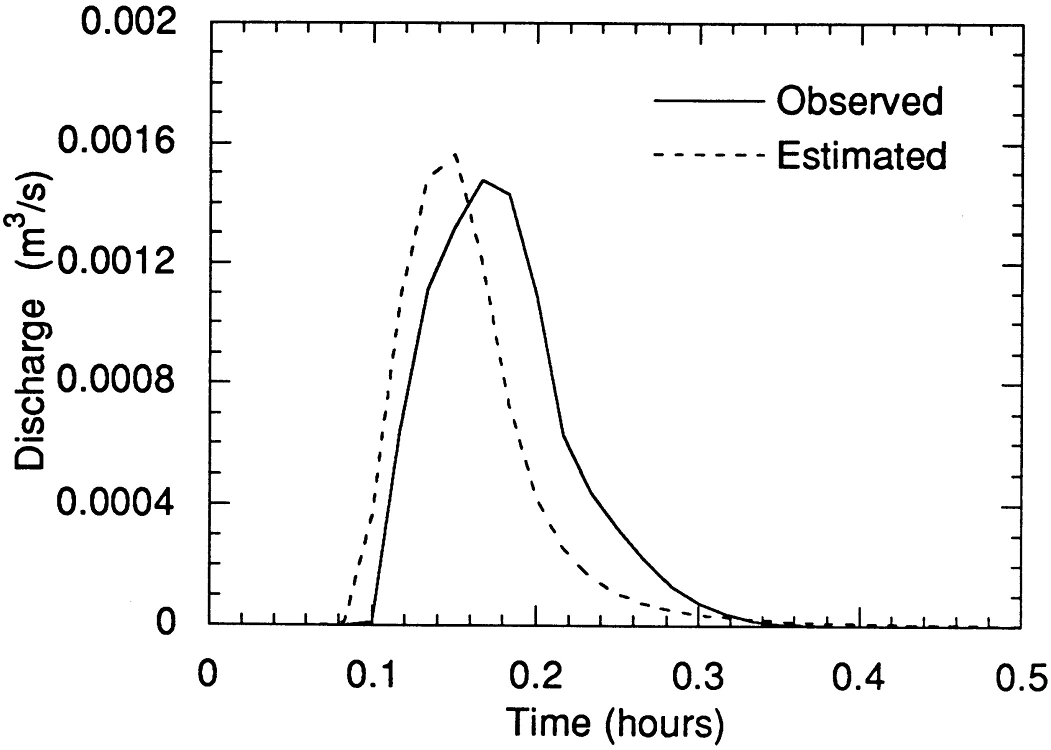

Figure 2.14 Verification of BRT2 event 6/2/91

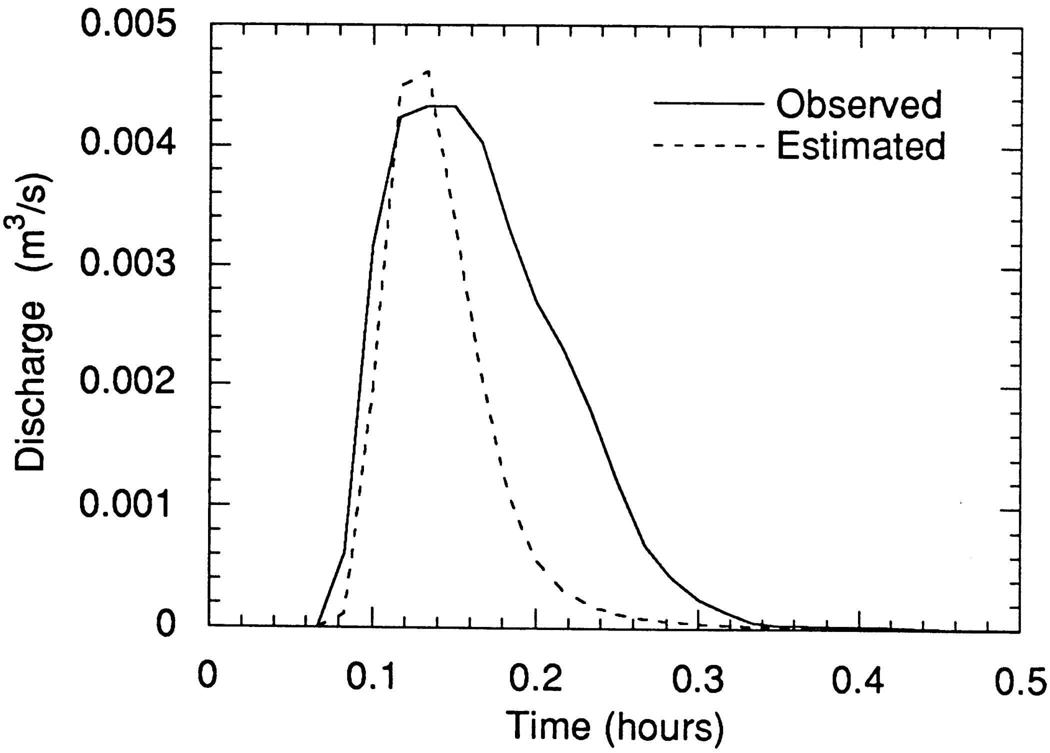

Figure 2.15 Verification of BRT2 event 22/2/91

2.3.2 Rainfall simulator data

There were a small amount of batter data available for validation of the parameters determined above. Not all the data were examined but one simulation experiment for the largest of the plots was selected. This simulation is referred to as Plot 4 Run 2 in the computer data file B1RF2QSS (see appendix B). An area of 67.8 m^2 has been adopted as the catchment area for this plot. The rainfall applied to this plot was measured by two pluviographs, both situated within the plot; the average of these two pluviographs has been adopted as the applied rainfall. Timing discrepancies in the observed runoffs and rainfalls were apparent and the data were adjusted accordingly. Figure 2.16 show the result of a simulation using the adopted parameters in table 2.4 for these data (ϕ=6.5 mm/hr). The considerable scatter of the simulated data around the observed data is due to the highly responsive plot responding to fluctuations in the applied rainfall, presumably due to random effects of wind during the simulator trials. What we need to consider is the mean trend of the simulated data averaging out these fluctuations.

The volume of this hydrograph for ϕ=6.5 mm/hr is too high by about 20%. The long-term infiltration rate, ϕ, was adjusted to 35 mm/hr and the simulation run again. This yielded a hydrograph that is marginally too low in volume by about 5%. This raises the question of what is the appropriate ϕ to adopt for this study. A value of ϕ=35 mm/hr is too high for two reasons. Firstly, the simulation data suggest it is. Secondly, a value of ϕ greater than 20 mm/hr results in no runoff occurring in the many natural storms that have been measured for both the caprock and batter. Thus it appears that the simulation data are in conflict with the data collected for the natural rainfall events. Whether this conflict is real or simply an artefact of the calibration procedure would require a statistical study of the parameter estimates from the natural and simulate rainfall experiments (eg Kuczera 1983). Until more definitive data are available, it is recommended that the value of 6.5 mm/hr fitted to the natural runoff events be adopted for the batter sites. This value is conservative and is consistent with the natural rainfall-runoff data.

No other parameters can be verified for the batters because the plot response is too quick to allow accurate calibration-verification of the plot response parameters (eg Mannings *n*). However, it is apparent in figure 2.16 that the rising and falling limb of the simulations for the observed and simulated data have similar slopes and timings, so that the parameters adopted in the simulations appear to be consistent with those observed in the field.

2.4 Conclusion

The distributed Field-Williams rainfall-runoff model (DISTFW) has been shown to provide a satisfactory fit to the data collected on the caprock and batter sites. Scatter in the infiltration parameters was observed from site to site, possibly suggesting localised porous zones in the fill. The sorptivity also exhibited small fluctuations depending on whether a rainfall event had occurred previously that day. This variation in the sorptivity appears to be important but its variation with antecedent wetness conditions could only be estimated roughly in this study because of the lack of detailed data testing specifically for this parameter. The adopted parameters are listed in table 2.4.

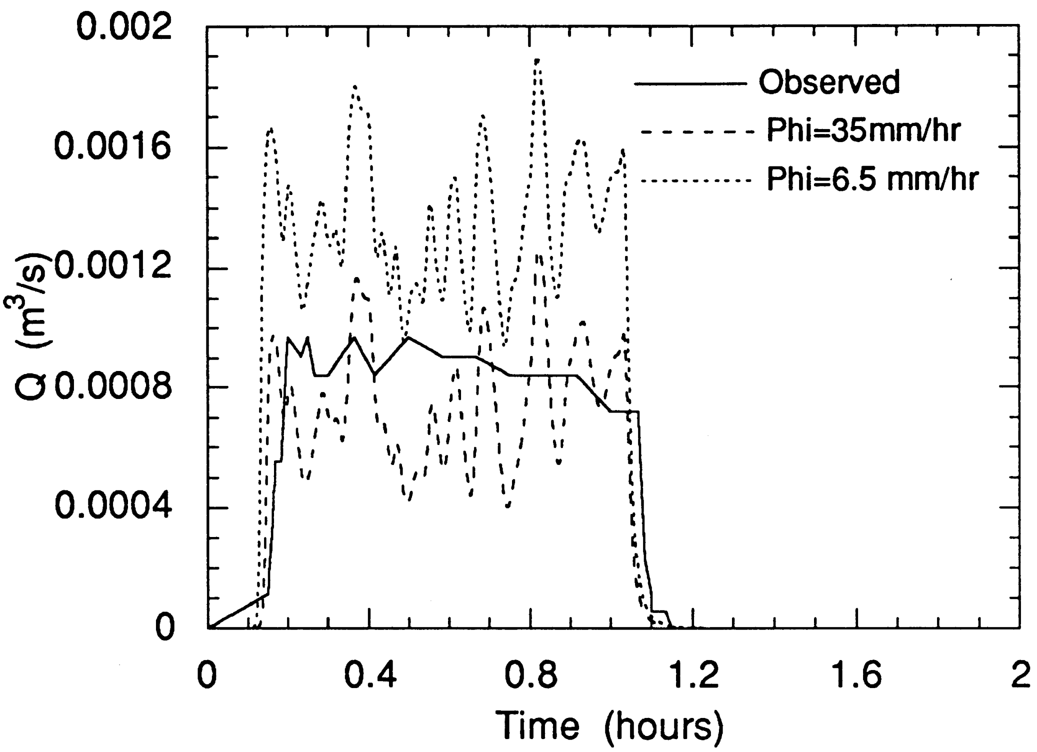

Figure 2.16 Batter Plot 4 Run 2 rainfall simulation experiment

Table 2.4 Adopted parameters for the Distributed Field-Williams Model

Parameter		Value	(Range)
S_{ϕ}	Sorptivity, initial infiltration	3.85 mm/hr$^{1.2}$	(0–3.85)
ϕ	Long-term infiltration rate	6.5 mm/hr	(6.5–40)
n	Mannings coefficient	0.03	(0.025–0.035)
C_r	Conveyance coefficient for 30 m wide sheetflow	7.0	(6–8.5)
e_m	Conveyance exponent	1.66	
c_s	Surface storage coefficient	0.03	
γ	Surface storage exponent	0.375	

3 Erosion model calibration

3.1 Overview

Natural rainfall runoff events for the caprock and batter sites were supplied by staff of the Geomorphology Branch at ***eriss***. Table 3.1 summarises the sediment yield data used in this study. Maps of the field sites are provided in appendix A and the data used in the study are tabulated in appendix C.

Data for a range of rainfall simulation data were provided in report and computer readable form. The computer data are summarised in table 3.2. These simulator rainfall-concentration data have been checked for consistency and appear to be accurate, with no obvious signs of error.

Table 3.1 Sediment yield data supplied for caprock and batter sites[c]

	Caprock sites[a]						Batter sites		
Storm	WT1	WT2	WT3	RT1	RT2	OUT	RT2	WT1	WT2
7/1/91 (20:50) [b]	✓	×		×	×	?			
7/1/91 (14:55) [b]	×	✓		✓	×	?			
8/1/91						?			
10/1/91 (7:55) [b]						?			
10/1/91 (14:00) [b]	×	×		×		?			
11/1/91				×		?			
21/1/91	✓	✓					×		
28/1/91							×		
30/1/91							×	×	
4/2/91		✓				×	×	✓	
6/2/91			✓				✓	✓	✓
13/2/91							✓	✓	
16/2/91	✓		✓				✓	✓	✓
22/2/91							✓	✓	

(a) Site notation as per Neave (1991);

(b) Two events supplied for this day, approximate beginning time in 24 hour clock;

(c) Notation is ✓ = data appears to have reliable matching discharge data, × = no matching reliable discharge data; ? = part or whole of the matching discharge hydrograph is questionable.

Table 3.2 Computer readable rainfall simulator data supplied

Datafile	Run	Date	Area (m^2)	Slope
Batter: B1RF1QSS	plot1 (runs 1–5), uncovered	5–7/10/90	1.2	0.152
	plot2 (runs 1–5), covered	5–7/10/90	0.99	0.185
Batter: B1RF2QSS	plot1 (runs 1–3)	17–18/10/91	1.2	0.152
	plot2 (runs 1–3)	17–18/10/91	10.2	0.187
	plot3 (run 1)	17/10/91	0.99	0.99
	plot4 (runs 2–3)	18/10/91	107.7[b]	0.19
Cap: C1RT2SS	plot1 (runs 2–4)	23–25/4/90	113.5	0.021
	plot2 (runs 2–4)	23–25/9/90	116.5	0.025
Cap: MESO	plot1 (runs 1–5)[a]	22–25/4/90	7.8	
	plot2 (runs 1–5)[a]	22–25/4/90	4.5	

[a] the suspended solids data for plot1 run5 and plot2 run 4 were not available;
[b] area possibly erroneous (see section 2.3.2)

The intention of this section is to calibrate the instantaneous sediment transport model described by equation 1.5.2. This will be converted to the long-term erosion rate in section 4.3. There are thus 3 parameters that require determination: β_1, m_1 and n_1, the transport rate, and the exponents on the discharge and slope respectively. The process adopted will be to use multiple regression on the available data, over a range of discharges, catchment areas and slopes, to estimate these parameters.

3.2 Natural rainfall data

The range of sediment transport events from natural rainfall events were examined and the data used to calibrate a sediment transport relationship of the form of equation 1.5.2. A number of events were discarded because either the sediment data or the discharge data were suspect. For instance, many of the storm event data were only for the falling limb of the hydrograph.

A common characteristic of the data was that if the rising limb at the start of the storm had been observed the first datum point at the start had an anomalously high concentration. This behaviour is not uncommon and is commonly believed to result from rainfall detachment of particles at the start of the event, while depressions are being filled, and before runoff has begun. This hyper-concentrated water is then flushed in the first minutes of the storm after which concentrations fall back to normal levels (Loch, pers comm). The total mass of sediment in that first flush is not a significant proportion of the total mass of the event and because these data bias the multiple regression procedure they were deleted from those events where they were observed.

The result of the multiple regression analysis with the remaining reliable data yield a relationship of the form

$$c = 0.27\, q^{0.22}\, S^{0.01} \;\; ; \;\; r^2 = 0.29 \qquad 3.2.1$$

The overall fit of this expression to the data is quite poor as indicated by the correlation coefficient. Figures 3.1 and 3.2 show the concentration data against the slope and discharge. Partial regression tests indicate that the exponent on discharge is significantly different from 0, as is the multiplicative constant at the 5% level, while that for slope is not. Finally, there was no significant difference between the sediment concentrations for the wash traps and the rill traps.

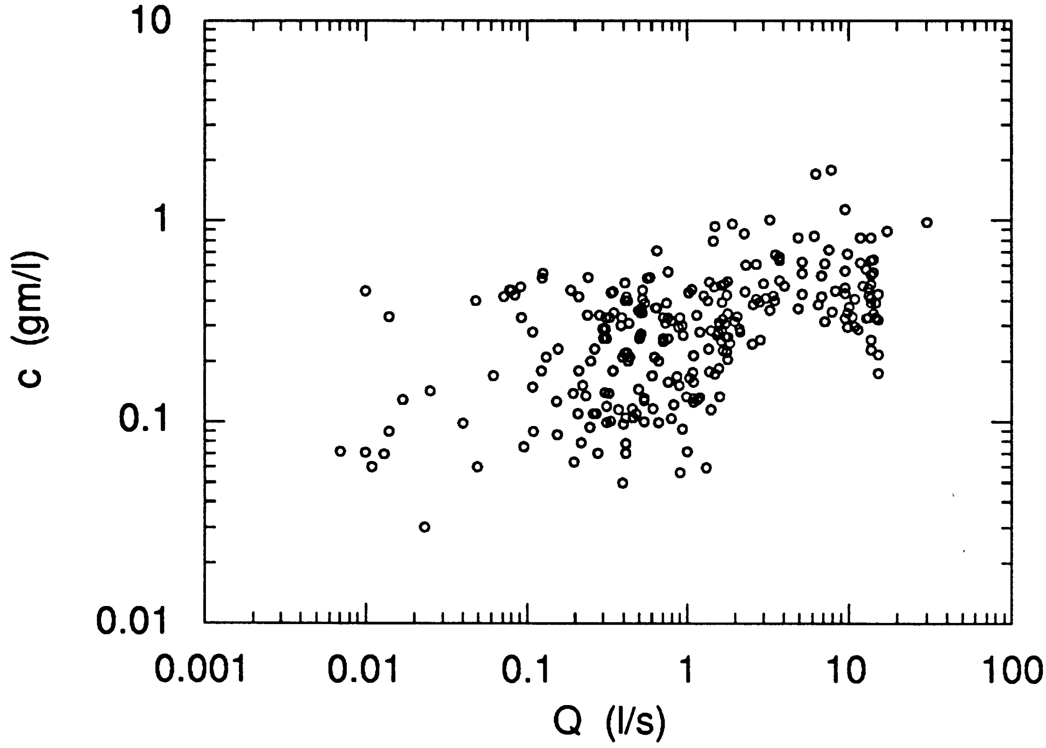

Figure 3.1 Concentration versus discharge for the natural rainfall events on both the batter and the caprock sites

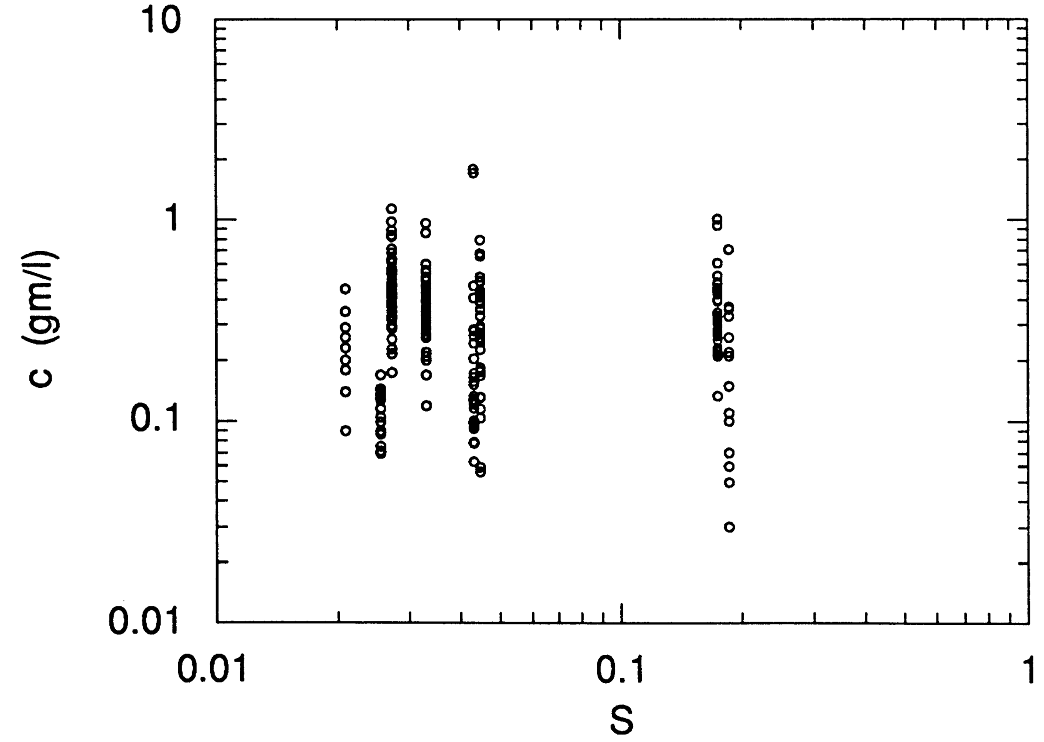

Figure 3.2 Concentration versus slope for the natural rainfall events on both the batter and the caprock sites

The independence of the concentration from slope is surprising and disturbing but a close examination of the results in figure 3.2 suggest a reason. The concentrations for the batter sites (slope ≈ 0.2) are notably lower than those of the caprock sites (slope ≈ 0.02–0.04). In the initial culling of the data it was not possible to remove all the data that came from events where only the falling limb of the data was sampled otherwise very little data would have been left. The rating curves with discharge indicated that clockwise loop ratings were common, though not universal. This type of rating is indicative of sediment concentrations peaking before the hydrograph (Williams 1989) but may also be a result of sediment starvation. If only the falling limb of the hydrograph is sampled then the concentrations will be lower than the mean values. Examination of the data suggest that the higher slope sites on the batter seemed to have sampled the falling limbs of the hydrograph more often than the caprock sites so that the concentrations on the batter slopes were biased downwards. This effect clearly reduces the reliability of the slope estimate for concentration.

3.3 Rainfall simulator data

The larger simulator catchments from the batter and cap plot 4 from B1RF2QSS and C1RF2QSS (see table 3.1) were used to calibrate the fluvial sediment transport equation of equation 1.5.2 on the presumption that they would be least dominated by rainsplash. That way multiple regression could be used to directly fit the parameters on discharge and slope.

Figures 3.3 and 3.4 show the variation of the concentration with the discharge and slope for these large plots. The result of the multiple regression was

$$c = 3.55 \ Q^{0.42} S^{0.66} \ ; \ r^2 = 0.620 \qquad 3.3.1$$

The correlation coefficient indicates that the fit of this equation is better than that obtained with the natural rainfall data. The exponent on discharge is consistent with fluvial transport according to Einstein-Brown sediment transport on a rilled surface (about 0.3–0.5, Willgoose et al 1989) and other field data (Loughran 1977, Moore & Burch 1986). The variation of concentration with discharge for one rainfall simulation experiment is illustrated on figure 3.5. Note that the apparent decline in concentration with time is strongly associated with the period of initially increasing discharge and that this apparent starvation effect appears to be complete within about 20 minutes. Thereafter, concentration decreases with decreasing discharge as expected in the non starved case.

The exponent on the slope in equation 3.3.1, however, is considerably less than that expected for a rilled surface (about 1.5–2). One possible explanation for this deviation is that the batter (hence higher slope) plots may have had a coarser lag layer (compared with the caprock plots) so reducing the transport rate on the higher slope surfaces. The exponent of 1.5–2 is derived using the assumption that the material grading properties do not change with discharge or slope. Grading of samples taken from the caprock and batter regions suggest that there are minor differences in the lag layer, but not of the magnitude needed to explain the deviations from theory observed.

To calibrate the diffusive transport, the data were fitted using multiple regression with trial and error estimates for the diffusive transport by using the transformation

$$c - \frac{DS}{q} = \beta_1 \ q^{m_1 - 1} \ S^{n_1} \qquad 3.3.2$$

The best estimate that was obtained by this process was

$$c = 3.59 \ q^{0.68} \ S^{0.69} + \frac{0.178 RS}{q} \ ; \ r^2 = 0.638 \qquad 3.3.3$$

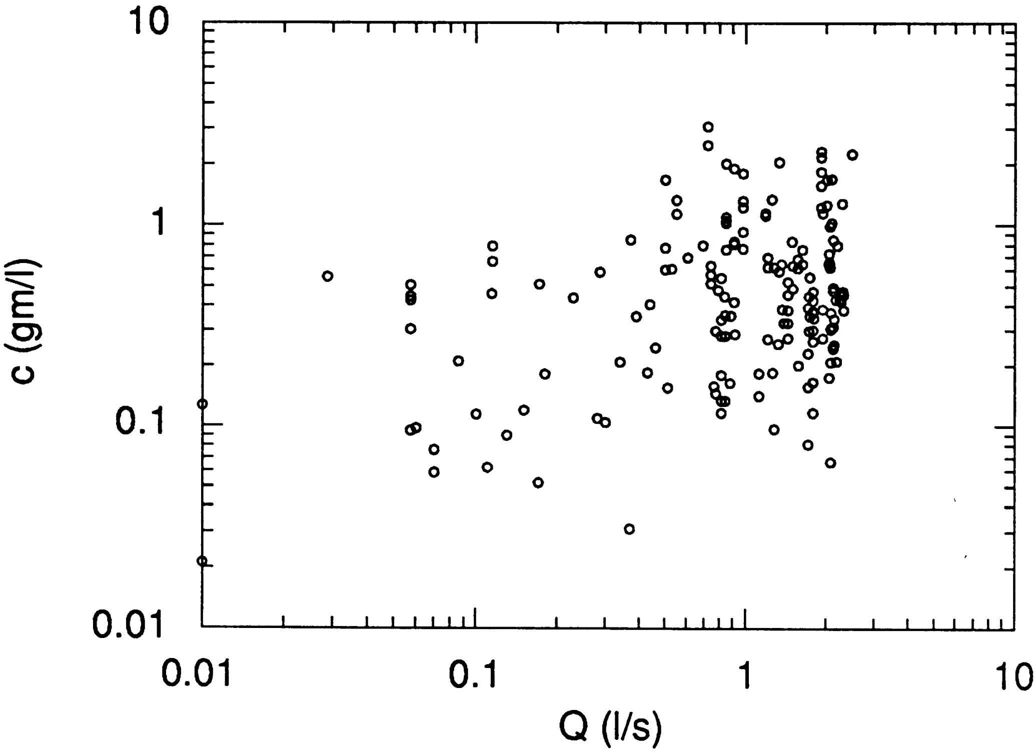

Figure 3.3 Concentration versus discharge for the large plots

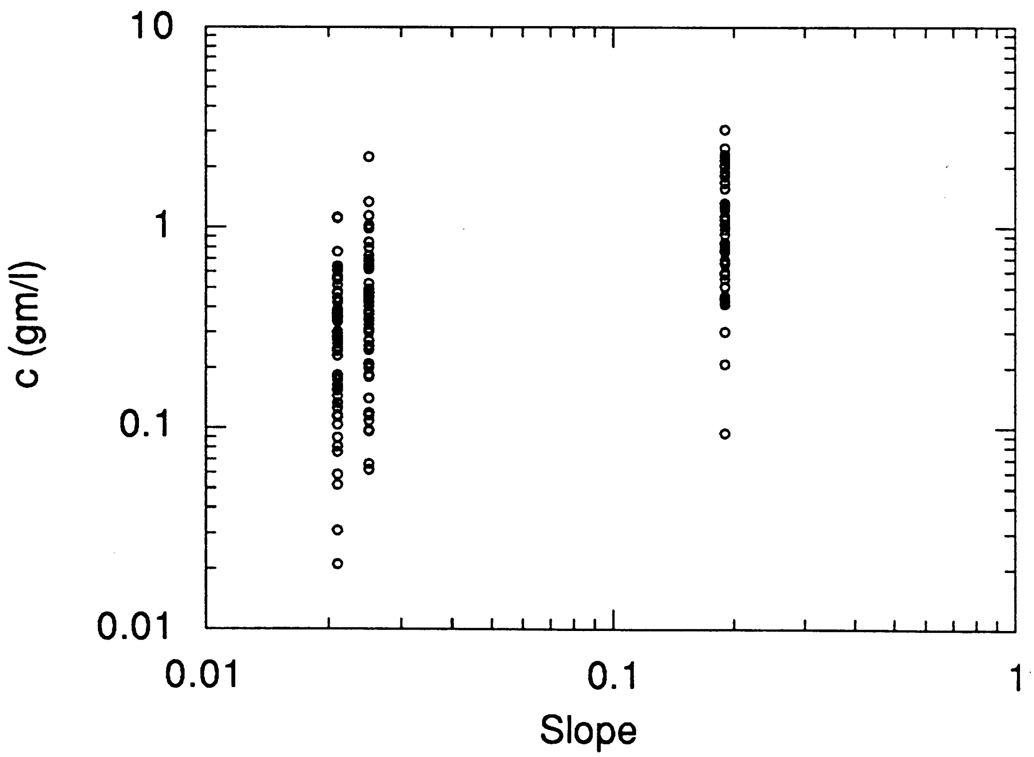

Figure 3.4 Concentration versus slope for the large plots

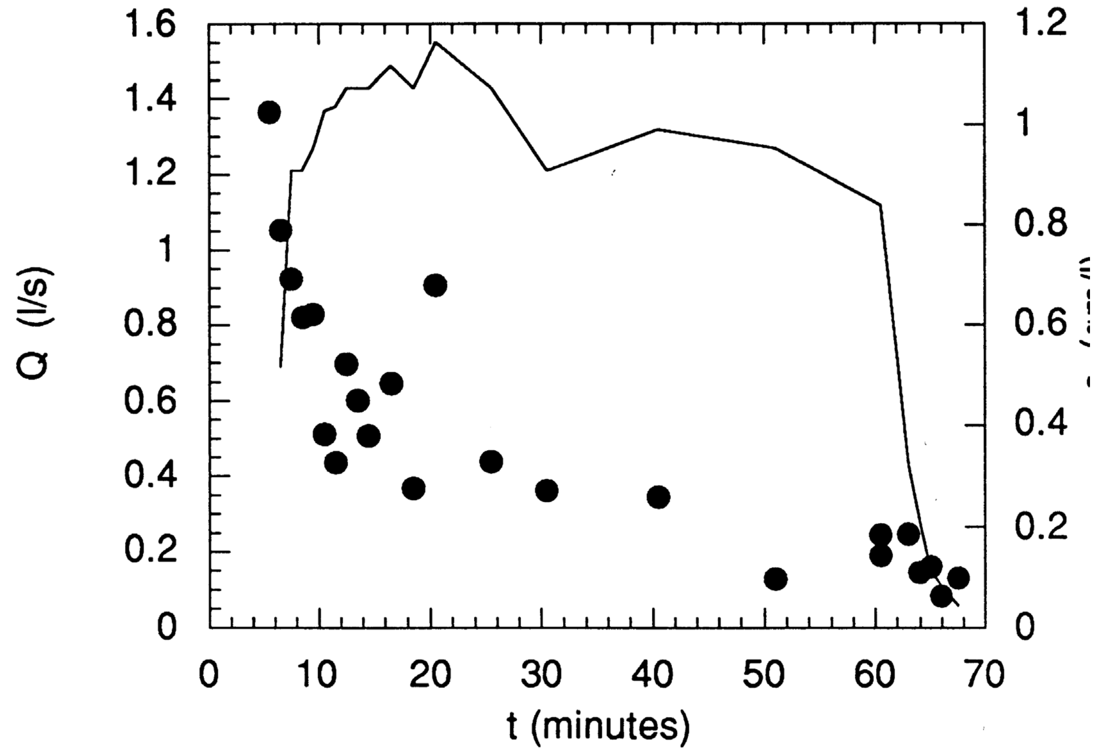

Figure 3.5 Sample hydrograph and sediment samples for caprock, large plot rainfall simulation

The estimated parameters are only slightly different from those determined from the case ignoring diffusive transport in equation 3.3.1 and there was a small, though significant, improvement in the correlation coefficient for this case. The exponent on the discharge was significantly increased, though the value is still in the range to be expected for rill flow. The exponent on slope was not significantly changed.

The diffusivity obtained for the small plot data for the batter (plots 1 and 2 from B1RF1QSS) were used to independently check the diffusivity calculated above. These plots have comparable area and slope and vary only in that one was covered and one was not. The purpose of the covering was to break the fall of the raindrops and thus dissipate the rainsplash energy. On the small area of 1 m^2 rainsplash is expected to dominate overland erosion. The difference in the transport of the two plots could thus be expected to be a good indicator of the magnitude of the rainsplash transport and thus the diffusivity.

The concentration versus discharge for the two plots is illustrated in figure 3.6. This change in concentration for the two plots can be expressed as

$$\Delta c = \beta_1 q^{m_1 - 1} S^{n_1} - \left(\beta_1 q^{m_1 - 1} S^{n_1} + \frac{DS}{q} \right) = \frac{DS}{q} \qquad 3.3.4$$

This calculation gave a value of D = 0.26. This value is in good agreement with the value calculated from the large area plots of D = 0.178. It is worthwhile to note that the plots' behaviour was consistent with the Fickian diffusion mechanism with transport being independent of discharge, validating its use for the modelling small scale sediment transport behaviour.

Finally the MESO rainfall simulator plots were examined. The areas of these plots (5–8 m^2) were mid-range area between the small plot (1 m^2) and the large plots (100 m^2) so that they would be expected to exhibit behaviour midway between that of the small and large plots. This was the case. For the lower rainfall rates (and thus lower discharges) rainsplash (diffusive) transport was dominant. For higher rainfall rates the behaviour appeared more like the fluvial transport mechanism (figs 3.7 & 3.8). However, of note was that if all the MESO data was plotted together there is a clear downward trend with increasing discharge (fig 3.9).

This appears to be due to sediment starvation, as the MESO experiments were performed over 4 days with increasing rainfall rates (yielding large discharges) being applied in each day. It is believed that each day's erosion was starved because of the depletion of the sediment store that had occurred with the previous days experiments. It is important, however, to observe that during each high rainfall rate experiments there was a positive correlation with discharge, consistent with all the results for the other plots discussed above. It is asserted here that the parameters m_1, n_1 and D fitted above are adequate for describing sediment transport during any event, but that the parameter β_1 may vary from event to event reflecting the amount of sediment removed from storage by previous days' runoff events.

3.4 Conclusion

The data for the natural rainfall data and the simulator rainfall data have a significantly different functional dependence on slope though similar relationship with discharge. The problem remains as to which are the most reliable data. To this end the two sets of data were aggregated and examined as a whole. These data are plotted against discharge and slope in figures 3.10 and 3.11.

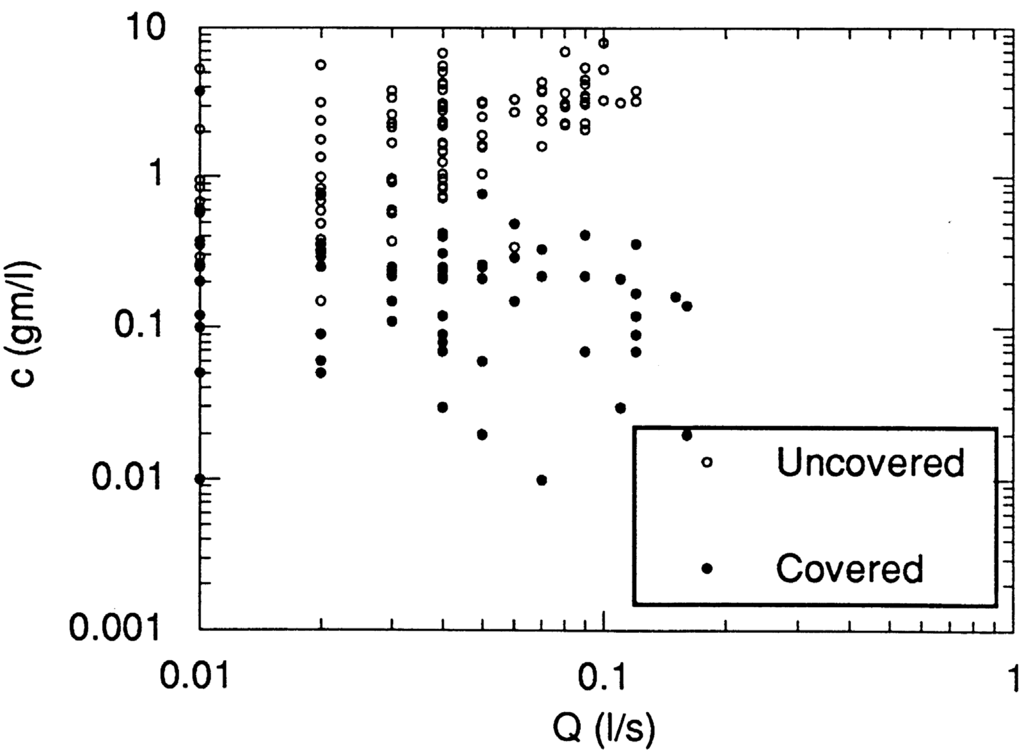

Figure 3.6 Concentration versus discharge for the covered and uncovered plots

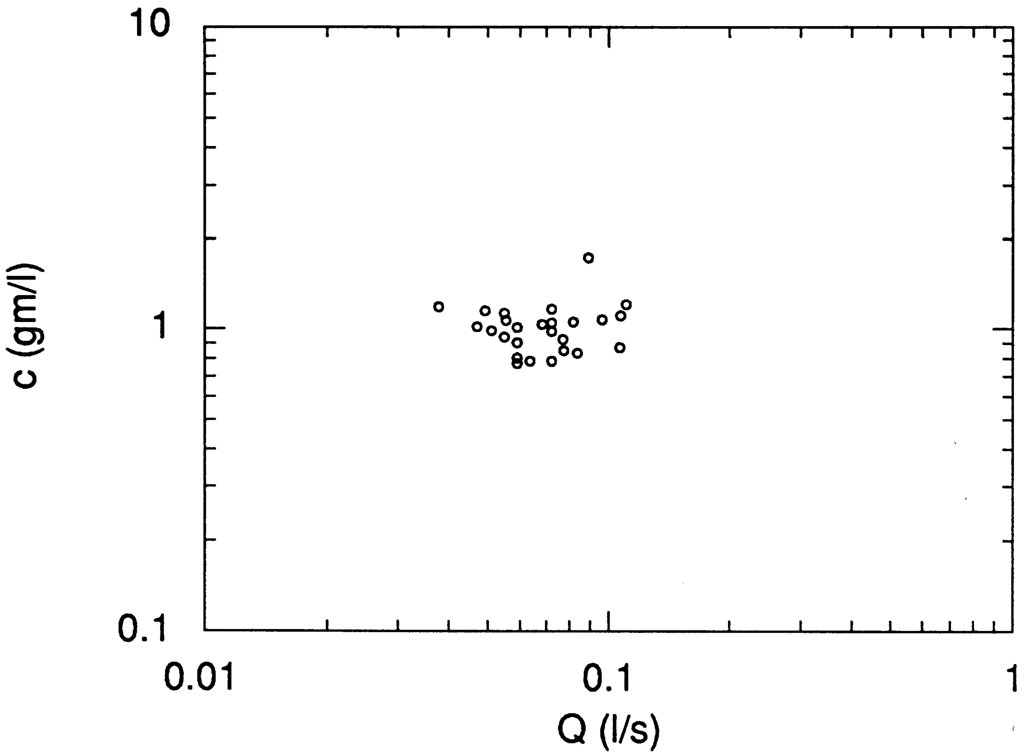

Figure 3.7 MESO plot (area 7.8 m^2) for low discharge. Note the lack of any trend with discharge

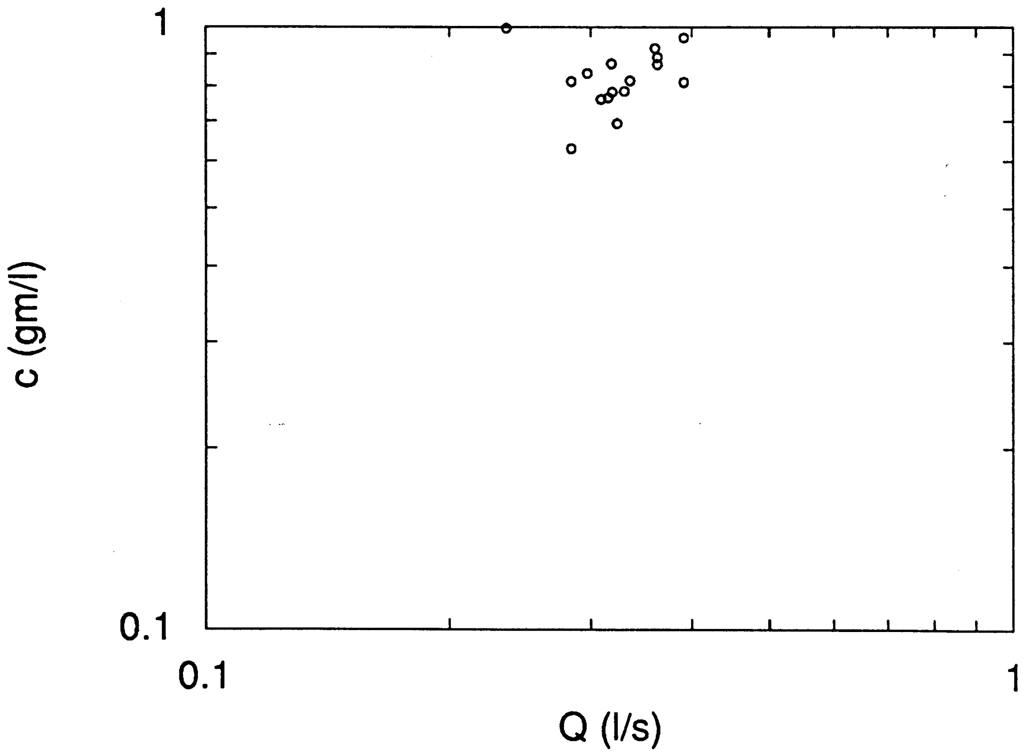

Figure 3.8 MESO plot (area 7.8 m^2) for high discharge. Note the positive trend with discharge

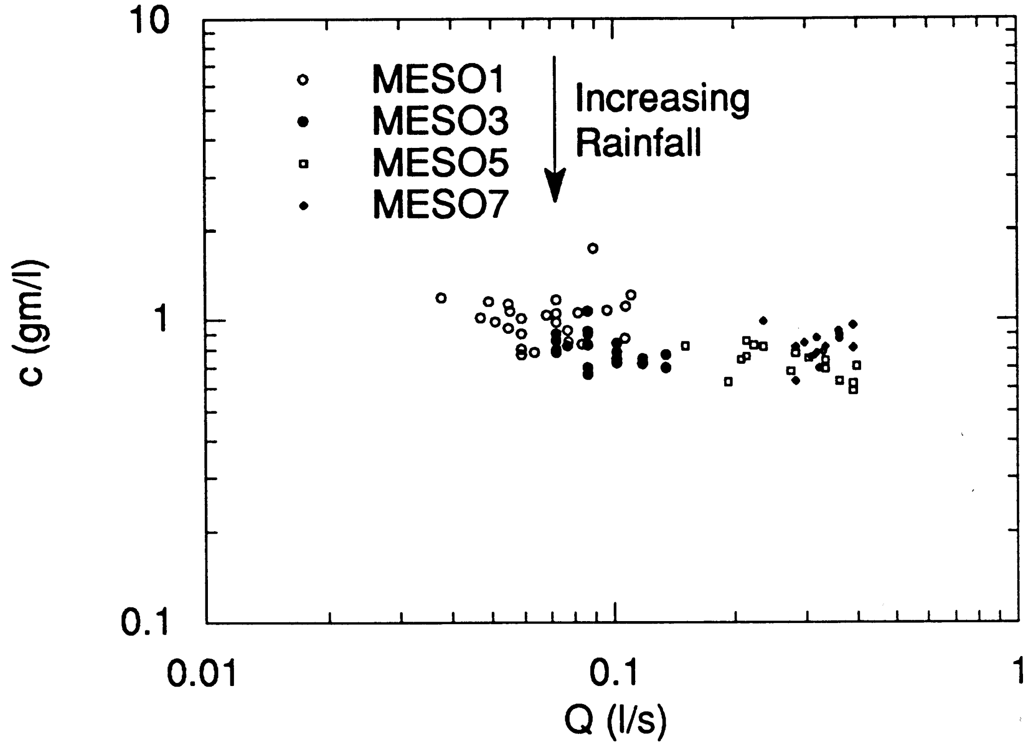

Figure 3.9 All available concentration-discharge data for the MESO plot of area 7.8 m^2

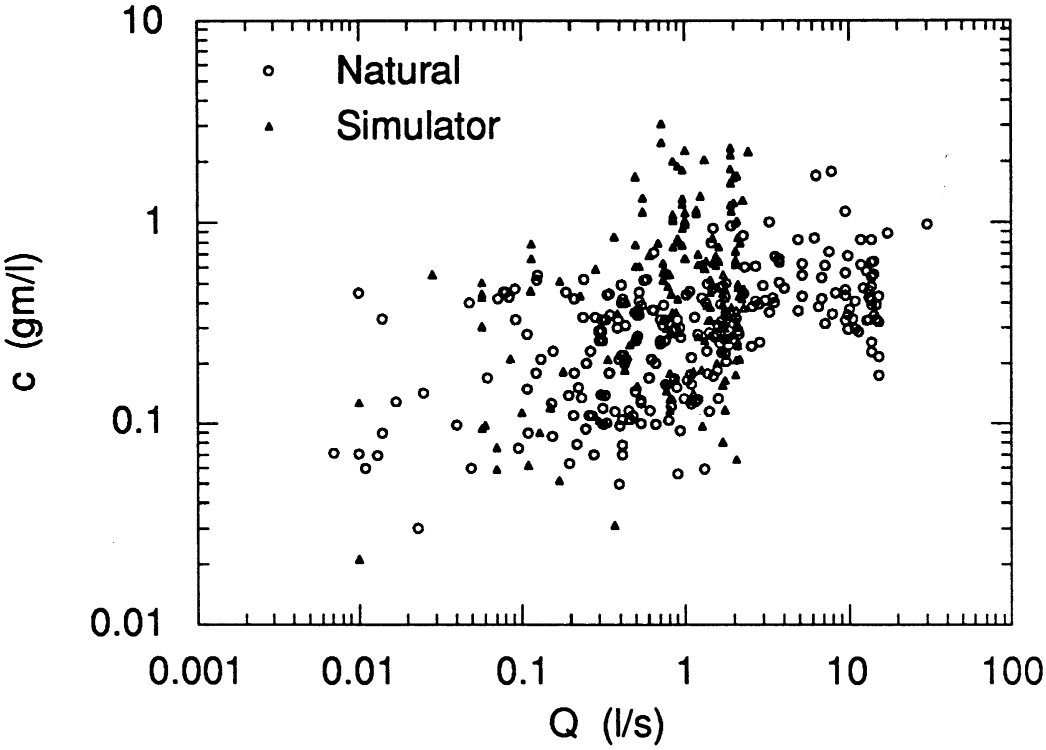

Figure 3.10 Concentration versus discharge for both the natural events and simulated data

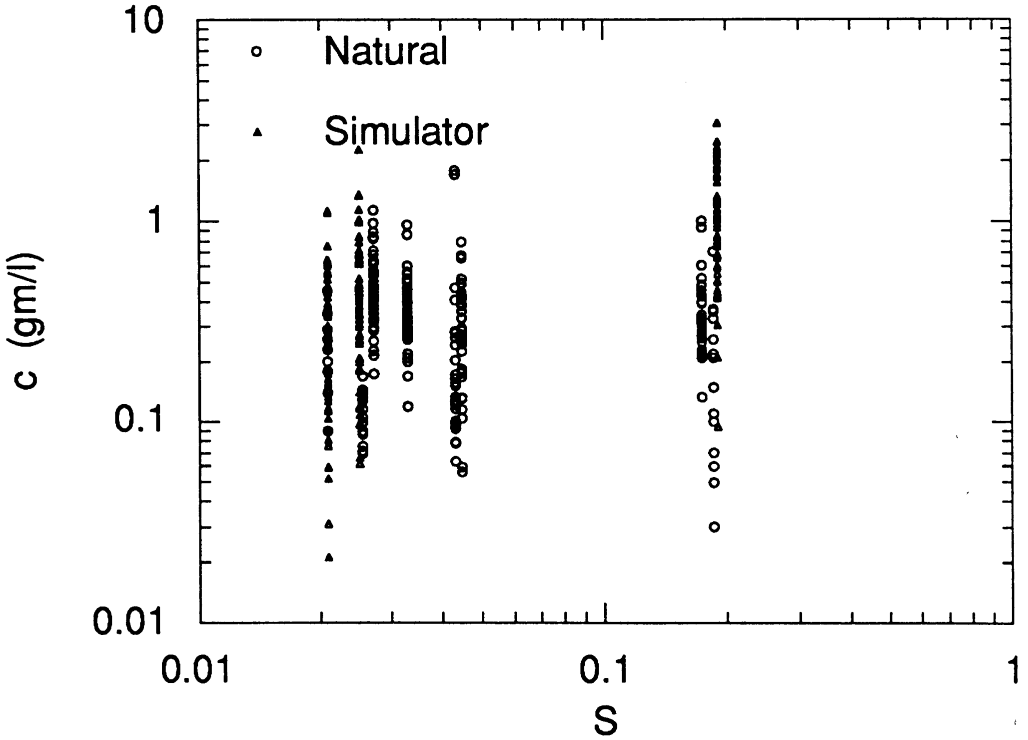

Figure 3.11 Concentration versus slope for both the natural events and simulated data

An examination indicates that the concentrations for the natural rainfall experiments are lower than the simulator results, particularly for high slopes. This behaviour is marked and suggests a bias in the natural data, as noted in section 3.2. In the graph of concentration versus discharge (fig 3.10) the results for the natural rainfall and simulated rainfall are little different, with the low discharge values for the natural event appearing to plot only slightly higher than the simulator.

Not surprisingly, a multiple regression of these data yields a result somewhat midway between the two results discussed in previous sections

$$c = 0.96\, q^{0.26}\, S^{0.34} \;\; ; \;\; r^2 = 0.29 \qquad 3.4.1$$

It is notable, however, that this fit is little better than that obtained for the natural data, and considerably worse than the fit for the simulation data. Furthermore, attempting to fit the diffusion coefficient, as was done for the simulated rainfall data, did not improve the significance of this fit. Given these considerations it was decided that the adopted sediment transport relation for this study should be the one fitted in equation 3.3.3 for the rainfall simulator experiments, ie

$$c = 3.59\, q^{0.68}\, S^{0.69} + \frac{0.178RS}{q} \;\; ; \;\; r^2 = 0.638 \qquad 3.4.2$$

4 Determination of parameters for SIBERIA

4.1 Overview

The parameter estimation of the hydrology and sediment transport models described in the previous section provide the basis for estimation of the parameters for SIBERIA. SIBERIA is a model of the long-term erosional behaviour of landscapes. Thus the parameters of SIBERIA characterise the average properties of the landscape and its processes, not the instantaneous or point values as calibrated in the hydrology and erosion studies above. However, there is very good reason to believe (Willgoose et al 1989, Huang & Willgoose 1992) that the requisite average parameters can be obtained from the hydrology and erosion models calibrated in previous sections. The parameters in SIBERIA can be considered in two groups.

The first group of parameters in SIBERIA define how the erosion varies with time, over periods of many years. This involves the averaging of the erosion that occurs in each runoff event, calibrated in section 3, to give the mean annual sediment yield. This mean annual sediment yield is not simply dependent on the sediment transport rate for a particular discharge and slope but also the range of discharges occurring during individual runoff events and the frequency at which these runoff events occur. Willgoose et al (1989) has shown that the simple concentration-discharge-slope dependence calibrated above in equation 3.4.2 is maintained in the mean annual formula but that the discharge used in the equation changes from being the discharge at that time to the mean peak discharge obtained from a frequency analysis of runoff events. This peak discharge can in turn be related to the contributing area to that point. This mean peak discharge is very similar in interpretation to the dominant discharge, or channel forming discharge, commonly used by river engineers in river sediment transport studies. The process that is followed in this report will be to simulate, using the hydrology model and observed pluviograph records for Jabiru, a runoff and erosion time series. The resulting erosion series will be averaged over the simulated record and the average sediment transport rate will be related to the mean peak discharge estimated by the hydrology model.

The second group of parameters define how the hydrology changes at different points within the catchment and, in particular, how the mean peak discharge varies with area—the scale dependence of the runoff hydrology. The hydrology model will use the digital terrain map of the proposed mine sites to simulate the variation of discharge with area for specified rainfall data. This model will then be used below to predict the scale dependence of the mean peak discharge; the variation of the discharge with increasing area and slope.

Finally, to predict the extent of potential gullying a gully threshold for the gully development module of the SIBERIA model is required. Data for a nearby natural site with similar regolith properties are used to estimate the magnitude of this threshold and its dependence on hillslope gradient and area.

This calibration process is summarised in figure 4.1.

4.2 Scale dependence of the hydrology

Some of the most important parameters in SIBERIA are those that define how the discharge used in the calculation of the sediment transport rate varies with catchment area. The general form of the relationship between discharge and area used in SIBERIA is given in equation 1.3.3. This relationship has been widely used in empirical studies of catchment hydrology and is the basis of mainly regional relationships for flood frequency.

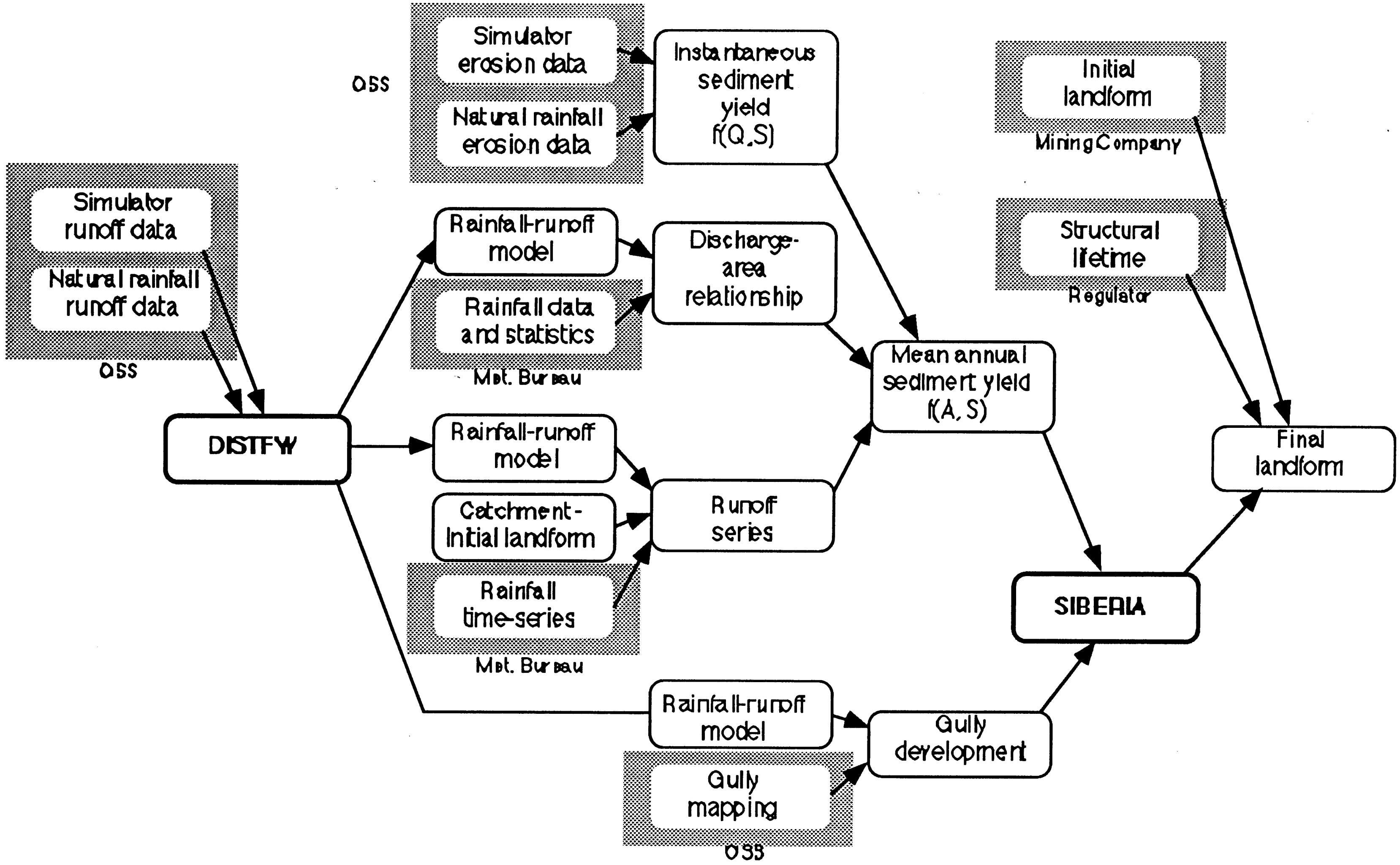

Figure 4.1 Schematic of the calibration process and use of SIBERIA

Recently, Huang and Willgoose (1992, 1993) have studied how the DISTFW rainfall-runoff model may be used to determine this relationship. This process is only valid for small catchment where it is reasonable to assume that the rainfall in all parts of the catchment are the same.

The process is as follows

1 Calibrate or select the parameters for the DISTFW model.

2 From Intensity-Frequency-Duration (IFD) curves of rainfall the 2 year storms of various durations are selected. Using the rainfall temporal patterns from Australian Rainfall and Runoff each of these storms is applied to the catchments and the peak discharge for every node in the catchment is noted for each storm.

3 The peak discharge at each node from the various duration 2 year storms is determined (smaller areas have highest discharge from short storms, larger from longer storms). These peak discharges are then plotted against area and the coefficients of the discharge-area relationship in SIBERIA are directly fitted from the graph. Huang and Willgoose (1992) have found that the correlation coefficient of this relationship is very high, and that the parameters in the relationship are a function primarily of the conveyance parameters in the rainfall-runoff model.

This process was followed to determine the area dependence of the discharge at RUM. It might be noted that equation 1.3.3 allows a slope dependence on discharge. Functionally, this dependence is only of importance when there are wholescale changes in the average slope of the catchment with time. This is not the case in this study so this dependence is ignored (ie n_3=0) and the discharge-area relationship is calibrated for the initial slopes.

Using the 30 m digital terrain map of the proposed rehabilitation strategy for the above-grade option the largest single catchment was defined (approx 1.6 km^2). This catchment was believed to have a hydrologic response typical of the other catchments on the rehabilitated area and is outlined in figure 4.2.

This digital terrain map was used as input to the digital terrain based version of DISTFW and a number of 1 in 2 year storms of different duration were simulated using IFD data for Jabiru. The 1 in 2 year storm was used because it is of about the same return period as the mean annual discharge (1 in 2.33 years), the discharge required by SIBERIA. The parameters used in DISTFW were those calibrated in section 2 with the exception of kinematic wave rate parameter as discussed below. For any node in the catchment the maximum peak discharge simulated from the different duration storms was calculated. This peak discharge was then plotted against area (fig 4.3) and the parameter m_3 calibrated. The adopted relationship for the 1 in 2 year discharge is

$$Q_2 = 0.000114\ A^{0.88} \tag{4.2.1}$$

The coefficient on this relationship, β_3, is not important as it only appears in SIBERIA in conjunction with the erosion rate parameter, β_1. These two parameters will be calibrated together in the next section where the mean annual erosion rate is determined.

As noted one parameter was changed from that in the calibrations of section 2. This was the kinematic wave rate parameter. This parameter is a function of the width of flow occurring (as well as Manning n). It was assumed in the work above that the width of flow in one node was half the grid spacing; ie 15 m. That is, that half of the surface area is flooded in a storm. For a rilled surface this is considered more reasonable than assuming that everywhere is flooded (ie classical overland sheet flow). Recent research in the US (Abrahams & Parsons 1991) has established that the classical model of overland sheet flow is unreasonable. The effect of this on the calibrated parameter, m_3, is relatively small as seen in figure 4.4. The general question of what proportion of the surface provides significant downslope flow (the so called rill area, as opposed to the remaining areas called interrill areas) is a major focus of research at this time (Willgoose & Riley 1993, Moore pers comm).

4.3 Long-term erosion rate and timescales for the simulation

For the determination of the long-term erosion rate a runoff series is created using the historical rainfall records at Jabiru and the calibrated rainfall-runoff model. Using the sediment transport equation previously calibrated and this runoff time-series an erosion time-series is generated and the average sediment transport per year can be determined.

The exceptionally large computational demands of generating a runoff series of sufficient accuracy for determining the average sediment transport rate from the engineered landform necessitated a multi-stage process for the generation of the runoff and erosion time-series.

1 The 1.6 km^2 catchment used in the hydrologic study of the previous section was used here for the sediment transport study.

2 This digital terrain map was used as input to the digital terrain based version of DISTFW and using a measured rainfall event a runoff event was simulated. Parameters used were those calibrated for the hydrology model in the previous section.

3 Using the plan of the catchment from the digital terrain map the conceptual subcatchment version of DISTFW with 10 subcatchments was calibrated to the simulated runoff event at the catchment outlet. Only one parameter was calibrated—the kinematic wave rate parameter; all other parameters are independent of whether the DTM or subcatchment version of DISTFW is used.

4 The subcatchment based model calibrated in 3 was then used to generate a 5 minute resolution runoff series for the catchment outlet from the 20 years of 30 minute pluviograph data for Jabiru.

5 Using the runoff data a time-series of the sediment yield from the catchment was then generated and averaged for each year. These results were then correlated to area and used as input to SIBERIA.

The key simplification in this process is in stage 3 which was required because to simulate the runoff data using the DTM rainfall-runoff model at 5 minute intervals would have required about 60 CPU hours per year on a high performance HP 710 workstation (about 3 times faster than a SUN SparcStation II workstation). The simplification of the runoff model did not significantly affect the accuracy and reduced the required computer time for the simulation of the 20 year runoff series to about 25 CPU minutes per year.

Figure 4.5 is a map based on the digital terrain map for the above-ground option. It shows the drainage network for the region including the engineered containment structure. The approximate boundary of the rehabilitated area is outlined on the map. The region selected for the hydrologic modeling is outlined on this figure. This region consists of 1773 nodes with area of 900 m^2 each for total catchment area of 1.6 km^2. The flow paths and the slopes were calculated by SIBERIA.

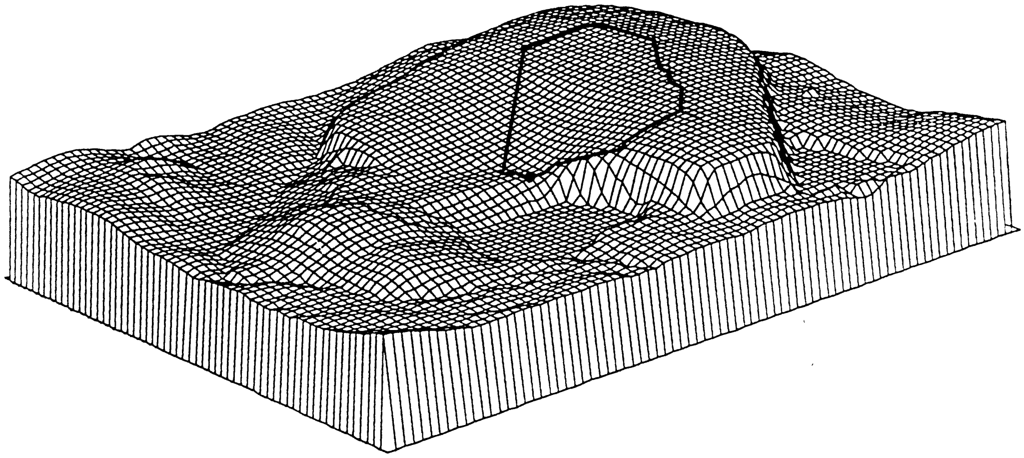

Figure 4.2 Perspective of the study catchment used for the hydrology study

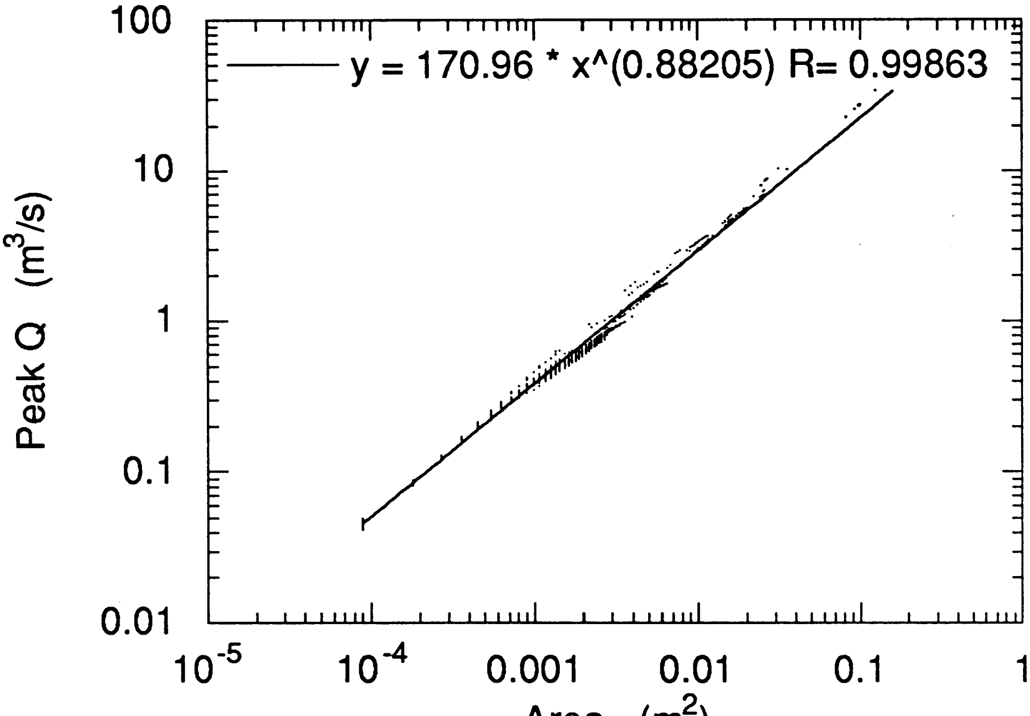

Figure 4.3 Discharge-area relationship for the 1 in 2 year storm
for each node in the study catchment

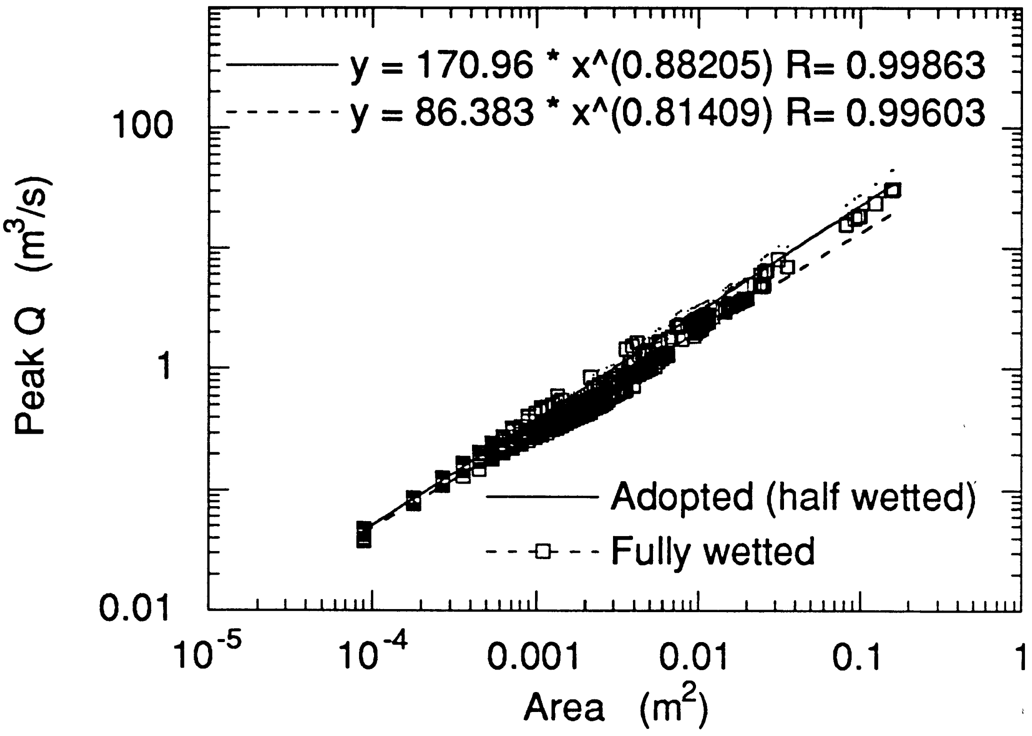

Figure 4.4 Sensitivity study on the discharge-area relationship for the 1 in 2 year storm for each node in the study catchment

The next stage was the calibration of the subcatchment model to the DTM model output. It was found on the work in the section 4.2 that the approximate time of concentration of the selected catchment was 60 minutes. The rainfall events that were collected and discussed as part of the calibration work (table 2.2) were examined and a storm that was close to the time of concentration was selected. The selected storm was the batter gauge on 21/1/91. The hydrograph from the catchment is shown in figure 4.6. The parameters used for this hydrograph are those for the adopted case used in the previous section with the exception of the sorptivity and the steady state infiltrations rate which were set to 0. The drainage paths within the catchment were then examined to select the 10 subcatchments for the subcatchment model. The selected subcatchments, together with the drainage pattern for the DTM model are shown in figure 4.5. As previously noted the only parameter that needed to be calibrated was the conveyance rate parameter, all others do not change (eg infiltration rates) from that in the DTM model. Figure 4.6 shows the satisfactory result of the calibration of the subcatchment model.

The final stage in the hydrology calculation was the simulation of the runoff time-series. For this ***eriss*** provided a pluviograph record for Jabiru at 30 minute resolution. This data series began in mid–1971 and ended in mid–1990. It is not possible to use the longer-term rainfall records at Darwin because it has significantly different rainfall statistics from Jabiru (Riley 1991). There is no evidence to suggest that the record at Jabiru is statistically different from that expected at the mine site. While individual storms may vary substantially from Jabiru to the mine-site, passing over one but not the other, it is the statistical characteristics of the rainfall and runoff series that are important in determining the mean runoff and sediment transport rates.

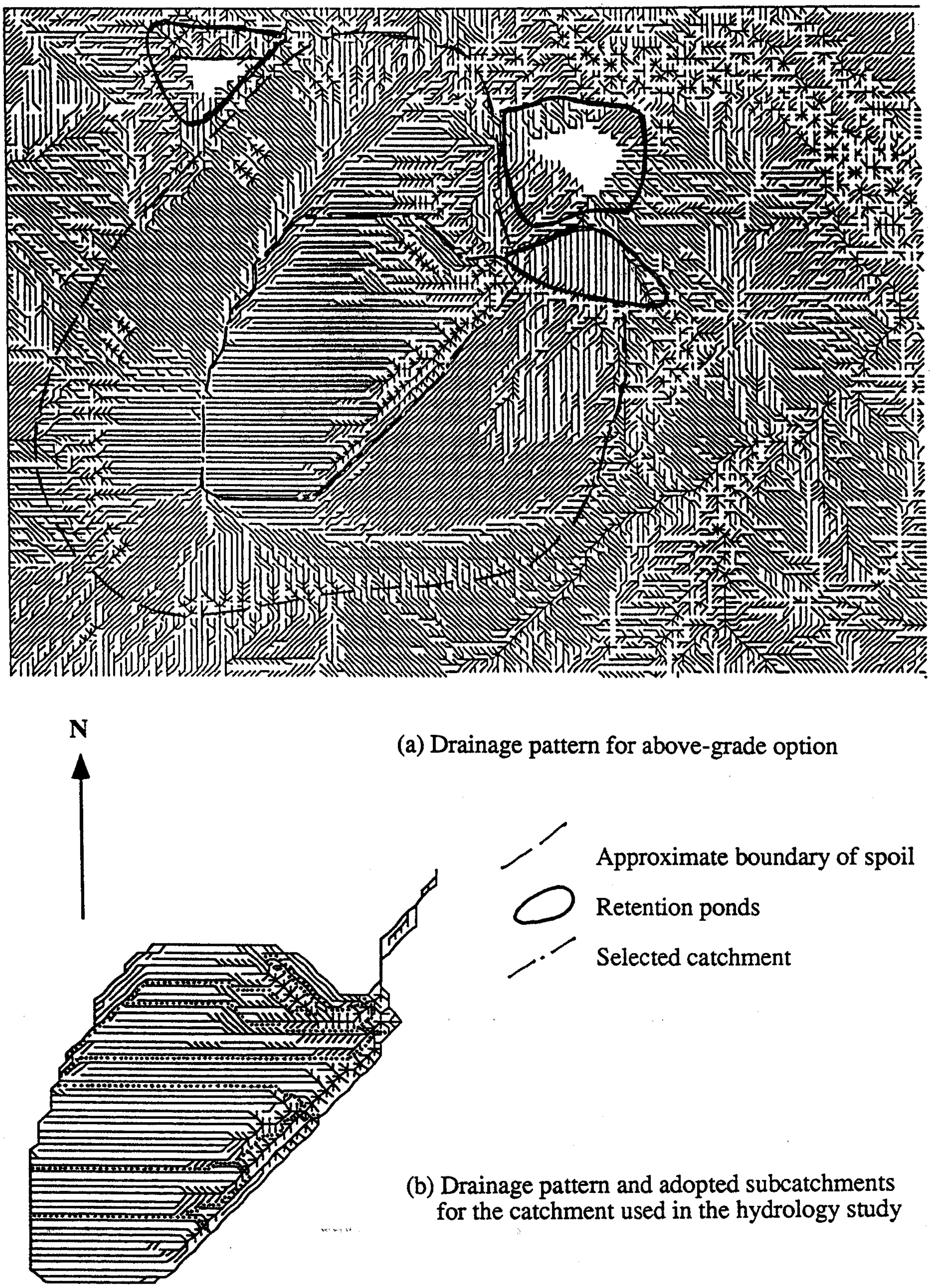

Figure 4.5 The drainage pattern of the study catchment used in the hydrology study

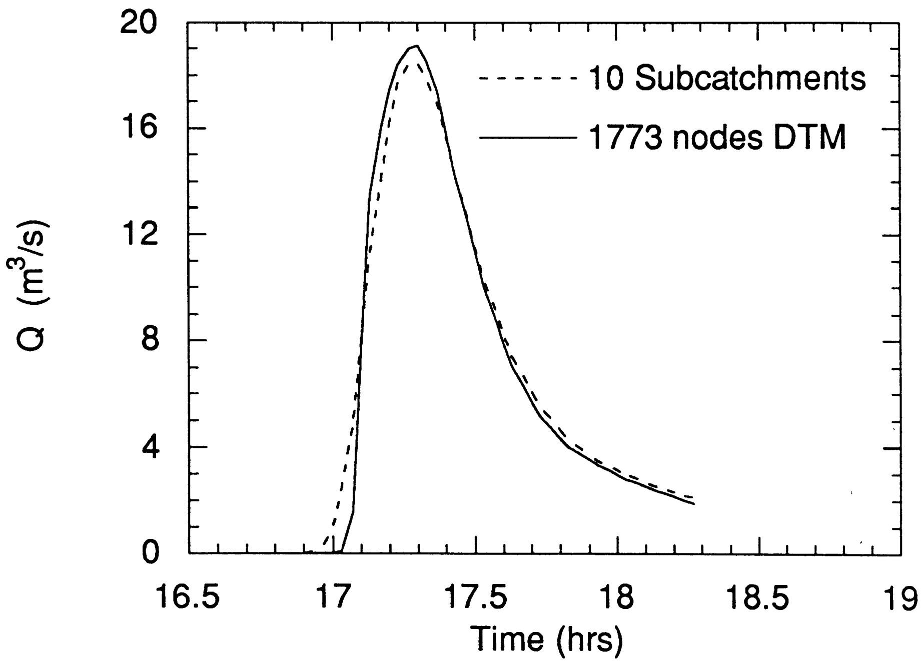

Figure 4.6 Calibration of the 10 subcatchment runoff model to the output of the 1773 node DTM runoff predictions for the event of 22/1/91

The Jabiru record is separated into two halves by a 3 year gap from 1980–1983. Data recovery from the early period was poor with substantial gaps in both the Dry and Wet seasons but data recovery is considerably better in the second half. It was necessary to simulate this runoff series at 5 minute intervals for almost 20 years of data. It was assumed that where rainfall data were missing during the Dry season rainfall did not occur.

Finally, this runoff series was used to simulate the erosion series. The adopted erosion model of equation 3.4.2 was used for this purpose. This erosion loss is considered to be indicative of losses that will occur from the cap of the engineered landform when it is in the unvegetated state. Losses from the batters are expected to be considerably higher because of the higher slopes. That there are higher losses on the batter compared with the caprock will be confirmed in the analysis of section 5.

4.4 Gully thresholds

One of the novel features of SIBERIA is its ability to model the dynamic development of gullies in response to hydrologic and erosional characteristics of the surface. Using a user-defined threshold, a gully occurs when that threshold is exceeded by a function called the channel initiation function (CIF). This CIF is a function of the hydrology upstream of the gully head. This hydrology is, in turn, a function of upslope area and slope. The CIF can be a function of the velocity of the overland flow, the shear stress of the overland flow, or, in areas dominated by groundwater flow, various functions of the groundwater head gradient. Most importantly, these functions are positively correlated with runoff and rainfall, area upstream of the gully head and the slope at the gully head (Willgoose et al 1989). Everything else being equal increases in rainfall, runoff, area and slope increase the tendency for a gully to erode at any given point in a catchment. This threshold behaviour based on area, slope and runoff has been widely observed in natural catchments (Patton & Schumm 1975, Montgomery & Dietrich 1988). At this time there is some inconclusive data for mine spoils (eg Elliott 1988) but the natural data suggest that similar mechanisms will occur in mine rehabilitation sites.

SIBERIA requires that this area-slope-runoff relation be determined *a priori* from field data and used as input parameters to the model. Once a gully is triggered, by exceeding the channel initiation threshold, the excavation of that channel proceeds using the sediment transport physics calibrated in section 3 of this report.

No data exist for the RUM rehabilitation site at this stage to allow the calibration of such a relationship. However, Williams and Riley (1992) have examined a natural area (Tin Camp Creek) derived from similar geologic material, schists. These data could be expected to be *reasonably indicative* of gullying behaviour of the mine site at some time in the future when the spoil site has developed a natural soil profile. However, without matching hydrologic data any conclusions on gully development on RUM must be made with extreme caution. Since the soils at both sites will be largely derived from the fast weathering schists in the outcropping rocks then it is likely that the soil profile will be similar. The main difference between the sites is that Tin Camp Creek is underlain at a relatively shallow depth by bed rock while the waste rock dump is not. This may affect the hydrology (and through it the channel initiation behaviour). The shape and size of the gullies will probably be only slightly different because it appears that most of the gullies at Tin Camp Creek do not excavate down to bedrock and where they do the bedrock is heavily weathered and friable; gully depth at Tin Camp Creek is not constrained by bedrock levels.

The form of the channel initiation function, $\boldsymbol{a}$, and its threshold, $\boldsymbol{a}_t$, used by SIBERIA is

$$\boldsymbol{a} = \beta_5\, \boldsymbol{q}^{m_5}\, \boldsymbol{S}^{n_5} \lesseqgtr \boldsymbol{a}_t \qquad 4.4.1$$

This function is both consistent with field data (Willgoose et al 1990) and justified from theoretical considerations (Willgoose et al 1989, Dietrich pers comm). If the discharge-area-slope relation of equation 1.3.3 ($\boldsymbol{q} = \beta_3 \boldsymbol{A}^{m_3} \boldsymbol{S}^{n_3}$) is adopted, then this relation can be re-expressed as

$$\boldsymbol{a} = \beta_5\, \boldsymbol{A}^{m_5} \boldsymbol{S}^{n_5} \lesseqgtr \boldsymbol{a}_t \qquad 4.4.2$$

where the primed variables are functions of the parameters of the CIF and the discharge relationships. Williams and Riley (1992) used discriminant analysis to identify two relationships, each with a threshold, that defined the transition from ungullied to knickpoint, and from knickpoint to gullied. The general form of their recommended relationship was of the form

$$\boldsymbol{a} = \beta_6 + \boldsymbol{AS} + l \lesseqgtr \boldsymbol{a}_t \qquad 4.4.3$$

where l was the slope length, which can be considered a surrogate of area (ie $l \sim A^{1/2}$). For this study it was necessary to reinterpret their data to develop a relationship of the form of equation 4.4.2.

Discriminant analysis (Mosteller & Tukey 1977) was used to identify the threshold between gully and ungullied. For this purpose, those points that were ungullied were given a discriminant value of 1, knickpoint 2, and gullied 3. A knickpoint is a gully head. At a gully head the channel initiation function equals the threshold (if it were less than the threshold then it would not be a gully, if it were greater than the threshold then it would not be the gully head—some point upstream with less area would be). Thus the line with discriminant value 2 defines the threshold between gullied and ungullied. The data analysis is plotted in figure 4.7 and the resulting channel initiation function is given as

$$\boldsymbol{a} = \boldsymbol{A}^{2.27} \boldsymbol{S} \lesseqgtr 23.6 \times 10^6 \qquad 4.4.4$$

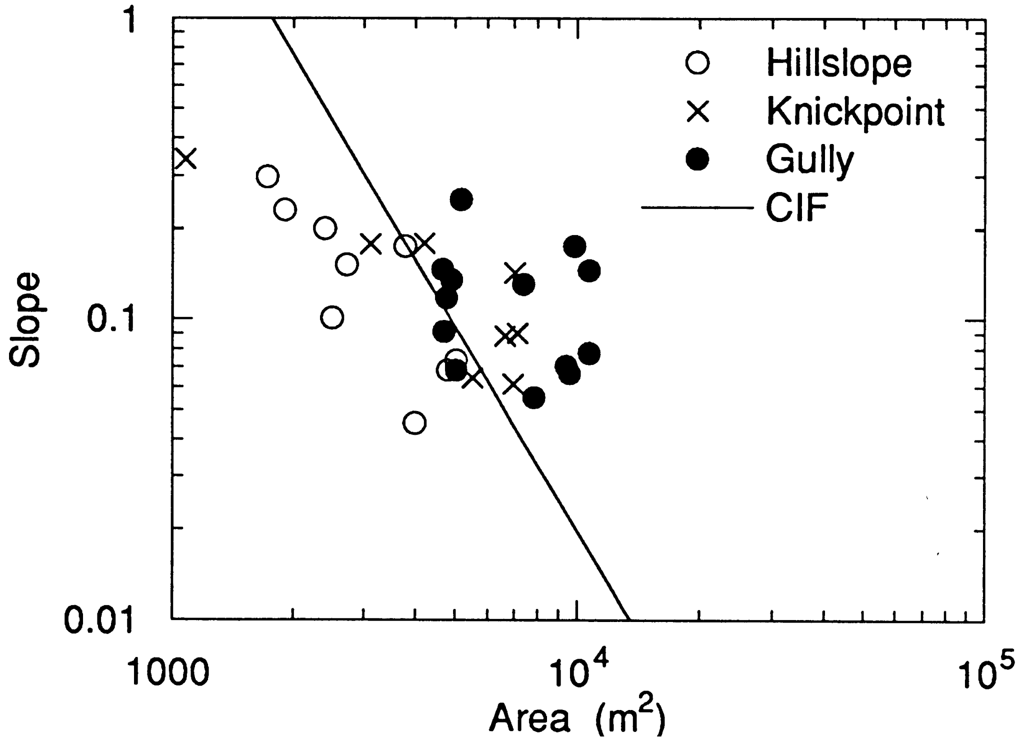

Figure 4.7 Adopted threshold for distinguishing gully from hillslope (data from Williams & Riley 1992)

The power on area in the above expression is in the range of values that have been observed for natural catchments and within the range of values predicted from theory. For a slope of 0.15 (approximately that of the waste rock batters) it predicts an area of about 4000 m^2 which for a planar slope is a slope length of about 65 m. For a slope of 0.02 (approximately that of the waste rock cap) it predicts an area of about 10 000 m^2 which for a planar slope is a slope length of about 100 m. It appears that the discriminating power of equation 4.4.4 and that of Williams and Riley (1992) are similar.

5 Assessment of proposed RUM landforms

5.1 Overview

The relationships that have been developed in the preceding sections were used to determine the parameters to be used by SIBERIA for the assessment of the various cases to be studied in this project. Two potential baseline designs were examined for the extent and location of erosion and deposition at the end of the design lifetime of 1000 years. They were the so-called above-grade and below-grade options as proposed by RUM where the tailings were stored above-grade and below-grade in a mine-pit, respectively.

A number of sensitivity studies have been carried out to assess the reliability of the predictions for the baseline above- and below-grade options.

Most importantly, the effect of settlement of the landform was examined. Richards (1987) believes that settlements of up to 1 m can be expected, randomly distributed in space. Random fluctuations on the initial elevations were imposed and the effect on the erosion was examined.

The gully threshold information from Tin Camp Creek is used to predict the extent of the gully erosion that will occur. The effect of gully erosion is to incise a localised gully into the surface so that the maximum depth of erosion is the depth of erosion determined in the baseline case plus the depth of gully incision.

The issue of greenhouse warming is discussed and its potential effect, through changes in rainfall, on the rate of erosion. Upper bound estimates are provided for infiltration which may assist in revegetation studies.

5.2 Above-grade option – baseline case

The above-grade option was run for the equivalent of 1000 years using the parameters calibrated in the previous sections. Perspectives of the waste rock dump are for the as-constructed year zero condition and for the 500 and 1000 year cases (fig 5.1 & 5.2). The grid used in this figure is a 60 m grid, ie since the calculations were done on a 30 m grid only every second elevation value is plotted. This was done to simplify the interpretation though inevitably some detail, particularly of the narrower valleys, is lost. While the differences in the surfaces for 0 and 1000 years may appear to be small, it must be remembered that the waste rock dump is almost 20 m high. The maximum valley depth is 7.7 m with the maximum deposition being 6.1 m. Note that while these valleys appear to be deeply incised in the figures this is simply a function of the vertical exaggeration of the figures. Even for the maximum depth of 7 m over the 30 grid resolution means that valley side slopes are still only 0.2, much less than for typical incised gullies.

Figure 5.1 also shows elevations at 500 years. Maximum erosion depth at 500 years is 5.7 m, 74% of the maximum 1000 year erosion. This indicates that incision of the valley proceeds very rapidly in early years. It is apparent from figure 5.1 that incision occurs most rapidly and that the extension of the developing valley network (triggered by the incision) occurs more uniformly over the 1000 year design period.

A plot of the initial elevations minus the 1000 year elevations (erosion positive upwards, deposition negative) is shown in figure 5.3. It is apparent from this figure that the maximum erosion occurs in the centrally draining part of the waste rock dump in three valleys that dissect the central plateau. Most of the eroded material from these areas appears to be deposited in the pit that the central area drains to. SIBERIA is currently limited in its capability to analyse deposition in dams so that interpretation of deposition in dams is particularly prone to errors. Note that the rate of erosion over most of the central spoil, outside of the gullies, is quite low and mostly less than 500 mm.

There is also significant erosion along the outside batters in the range of about 3–7 m. It fact, it is almost possible to define the extent of the waste rock dump from the peaks of gully development around the outside of the batters. Figure 5.3 plots the deposition and suggests that most of this eroded material is deposited in the region within about 100–200 m of the batter. The depth of deposition in those regions near the batter is approximately 5 m.

5.3 Above-grade option – effect of settlement

To assess the potential effect of settlements on the form of the erosion and the potential position of the valleys formed in the study of the baseline case some simulations were carried out where the initial elevations were randomly perturbed by 0 to -1 m. Because the settlement will occur randomly over the waste rock dump, the random application of settlement provides a sensitivity study of the potential location of valley and gully development. Two simulations were carried out and the final surfaces of the two realisations are plotted in figure 5.4. Maximum depths of erosion are 7.8 m and 8.5 m respectively—not significantly different from the 7.7 m depth predicted for the baseline case.

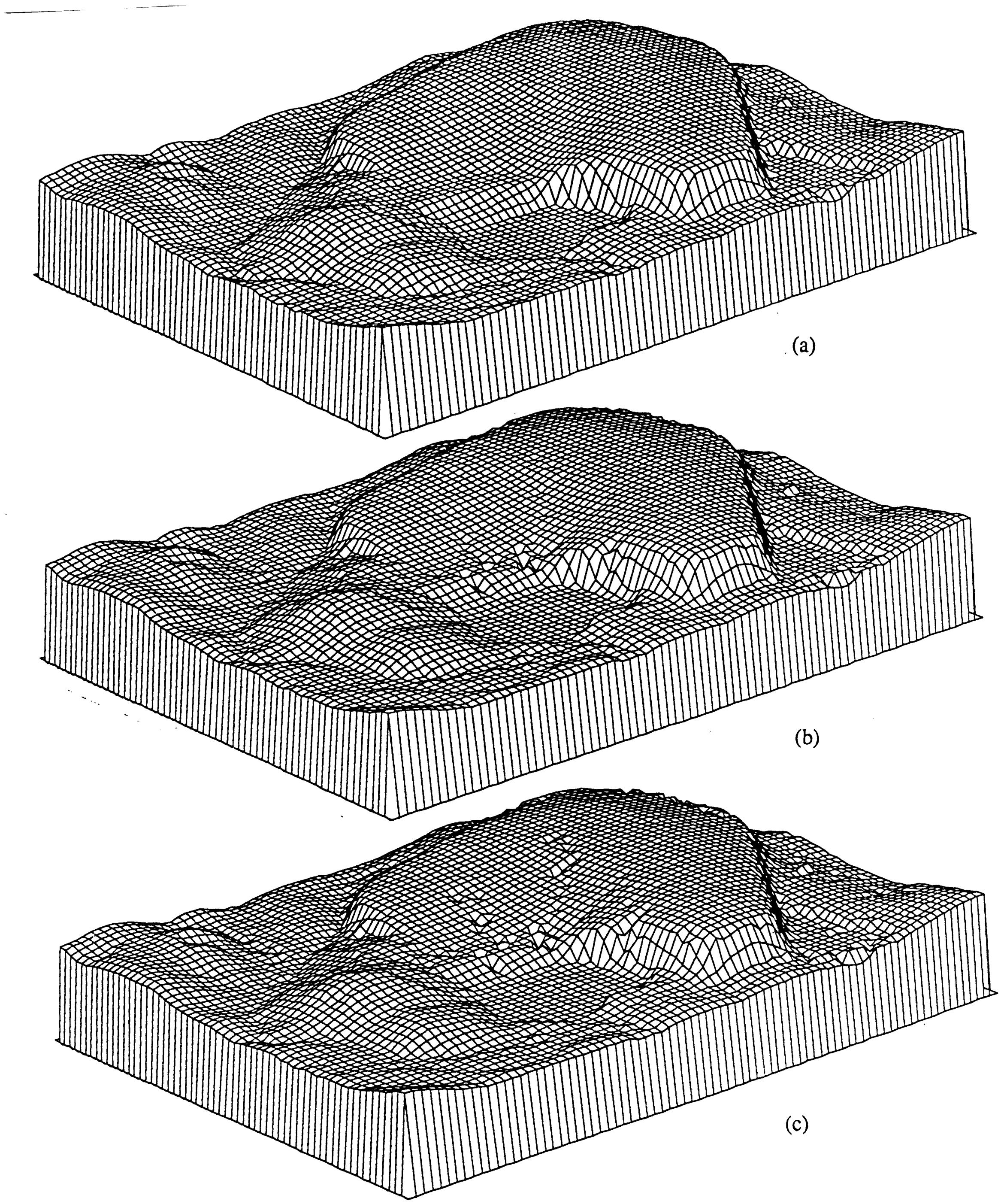

Figure 5.1 Above-grade option, baseline case: Elevations at (a) 0, (b) 500, (c) 1000 year viewed from the NE

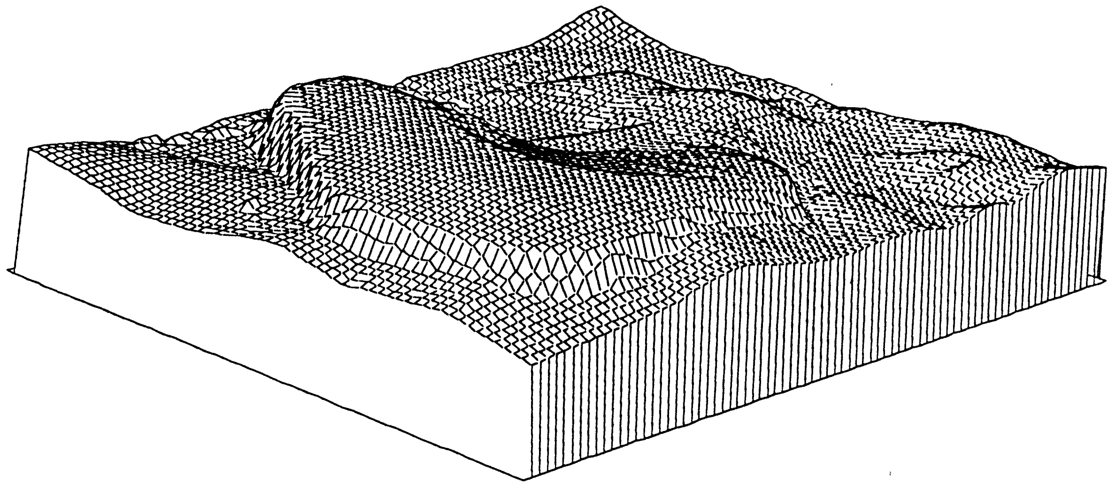

(a)

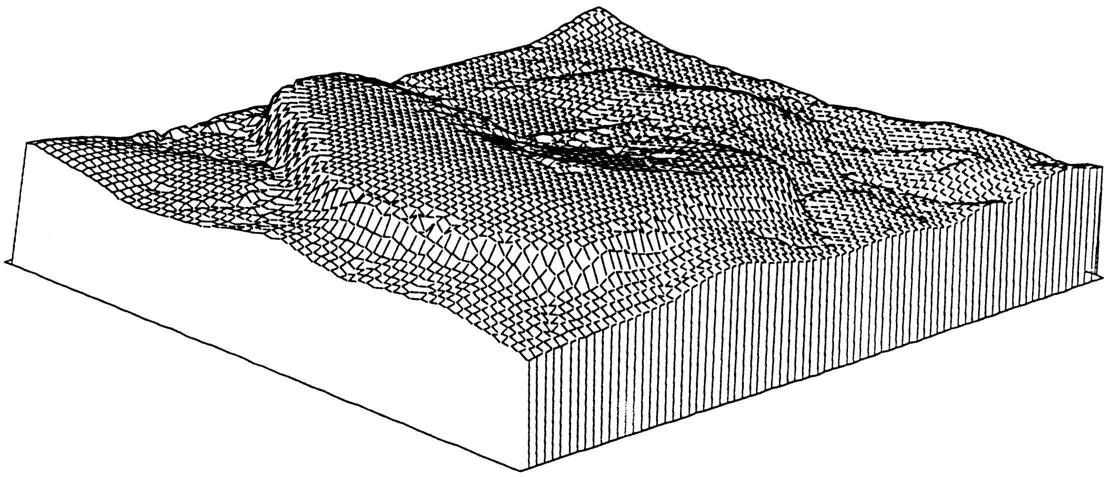

(b)

Figure 5.2 Above-grade option, baseline case: Elevations at (a) 0, (b) 1000 year viewed from the SW

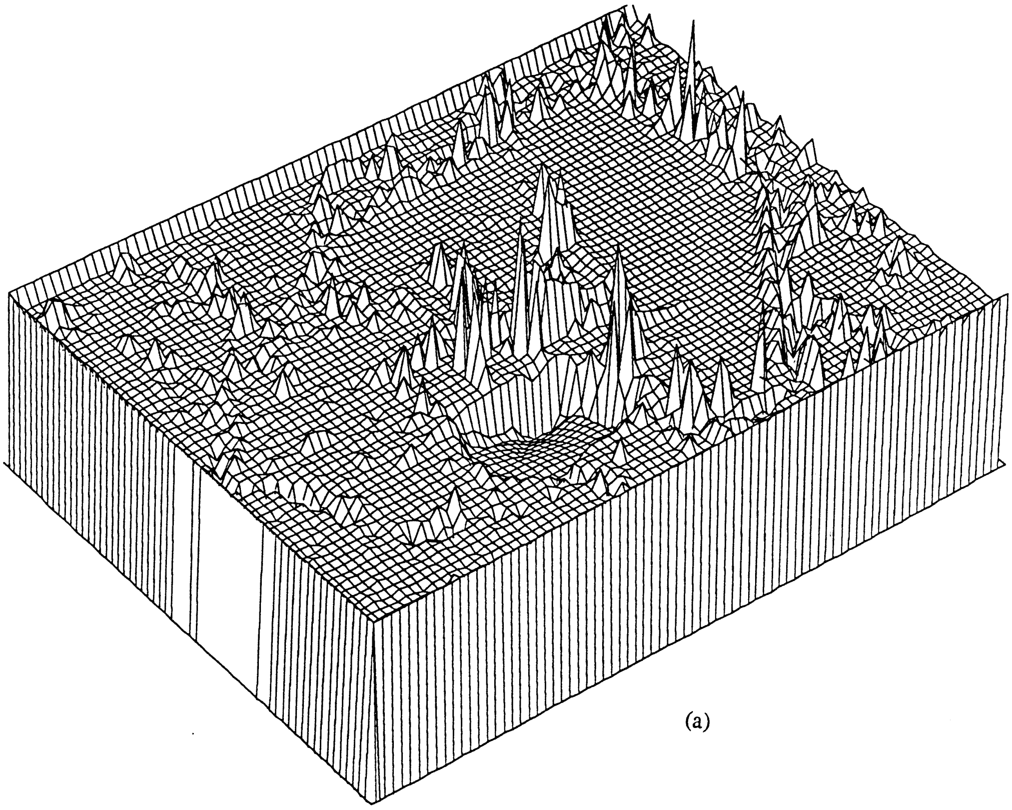

(a)

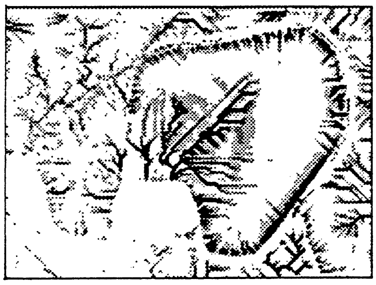

(b) Contours of erosion with 0m = white
to ≥ 1m = black

Figure 5.3 Above-grade option, baseline case: Erosion (upwards) and deposition at 1000 years

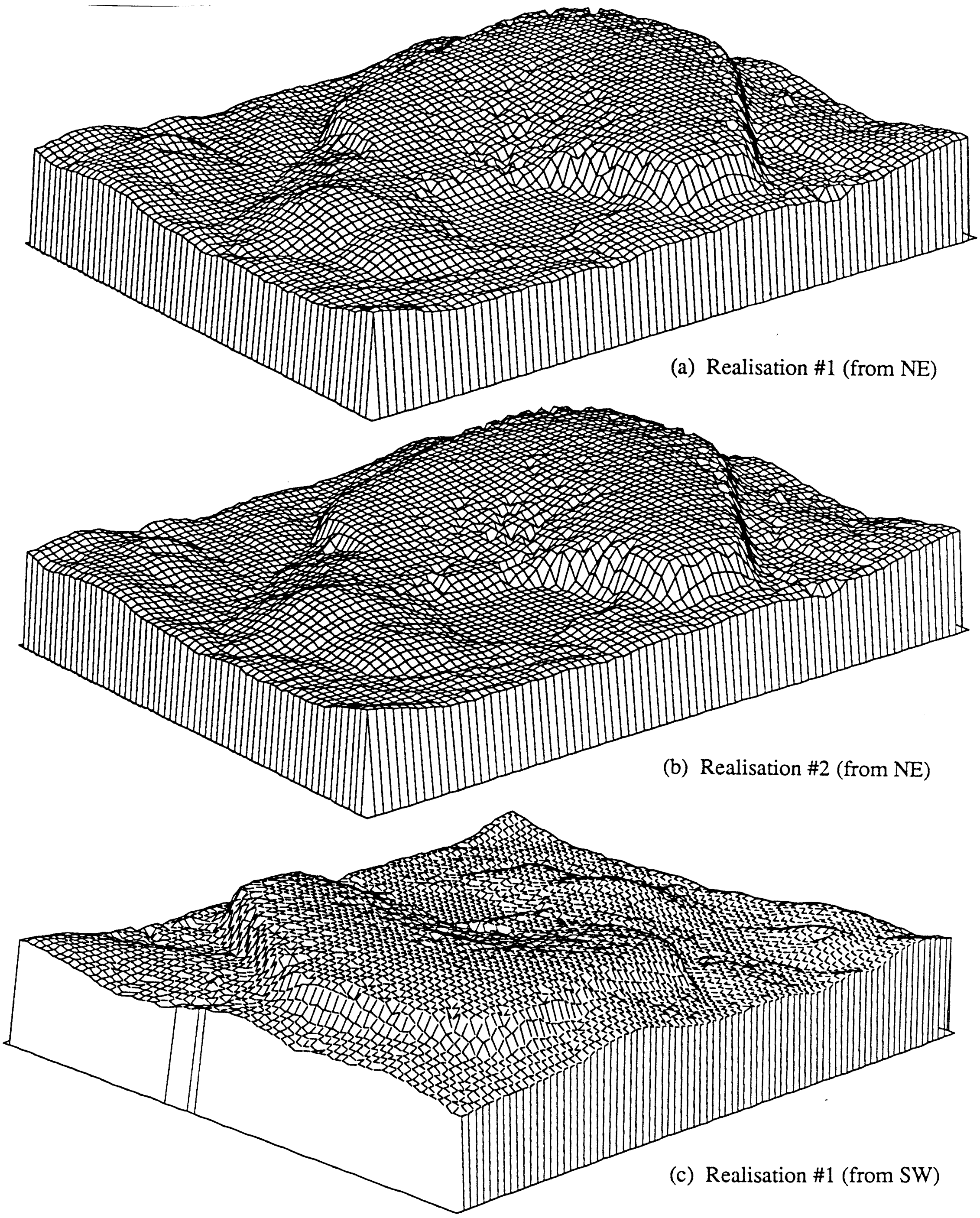

Figure 5.4 Above-grade option, with-random settlements cases: Elevations at 1000 years

Valley formation is much more widespread on the cap than it was under the baseline case. With careful inspection similarities in the valley patterns for the baseline case and the perturbed cases can be seen. The general areas where the valleys occur are the same in both cases—there is simply more widespread gullying in the with-settlement case.

On the batters there is also a significant change in the behaviour of the erosion when random settlement is allowed. Very significant and deep isolated valleys are formed in the with-settlement case, particularly on the north-western boundary. In the baseline case the erosion, though high, does not create the deep valleys that are apparent on the northwestern edge of the waste rock dump. Figure 5.4c shows a comparison of the extent of valley formation on the SW batters for the with- and without-settlement cases.

Figure 5.5 shows the spatial distribution of the erosion for the first of the with-settlement realisations. The most obvious difference with the baseline case (fig 5.3) is the widespread random background erosion of about 1 m. This is a direct consequence of the eroding and filling of the 1 m pits and hollows created by settlement. More detailed comparison shows that the regions of high erosion in the baseline case are maintained in the with-settlement case. As is observed in the elevation maps the high points of erosion are also more widespread.

The reason for the changes in behaviour on the caprock layer is very simple and has been observed in other situations. The baseline case is very initially smooth with the initial flow patterns consisting of long parallel flow paths (see for instance fig 4.5). The occurrence of the pits in the surface that result from settlement result in convergence of flow and the flow concentrates more readily. Flow is no longer uniformly spread over the surface but tends to flow along preferential flow paths. When flow concentrates in this way enhanced erosion occurs and valleys are more easily formed because velocities and shear stresses are increased. The first author's experience is that valley formation will inevitably occur in both cases; in the with-settlement case initial valley formation occurs somewhat earlier than in the smoother baseline case. Note that this flow concentration behaviour can result not only from settlement but has been observed to occur in the field as a result from any sort of perturbation that runs downslope (eg dozer tracks; Toy & Hadley 1987).

5.4 Above-grade option – with gullies

In this sensitivity study the potential for gully erosion, over and above the sheet erosion already discussed in the sections above, is examined for the above-grade case. The gully erosion threshold (called the CIF threshold) observed by Williams and Riley (1992) at Tin Camp Creek (discussed in section 4.4) is used to define the upper limits of gully erosion on the waste rock dump. In the absence of information of the sediment transport in the gullies at Tin Camp Creek, the sediment transport rate in the gullies is assumed to be equal to that on the hillslopes (eg SIBERIA's parameter O_t=1). The sensitivity of the gully development to the random settlements is also examined, particularly how the position of gullies change with the imposition of settlements. Here we do not predict the depth of gully development (that would require further data from studies at Tin Camp Creek), however, the gully incision can be simply added to the depths of sheet erosion discussed above; the two depths of erosion are believed to be largely independent over geomorphic timescales.

Figure 5.6 shows the gully positions for the baseline case at 1000 years. Figure 5.6a shows the gullies superimposed on a contour map of the site and figure 5.6b shows them superimposed on a map showing areas where slopes are greater than 0.04.

The gullies extend quite some distance into the central caprock area fanning out to fill the lower regions of the caprock. They do not extend all the way to the drainage divide on the caprock because there the contributing area and slopes are too low to trigger gully development. The gully development on the batters is largely constrained to the batters themselves although some do extend onto the caprock for a short distance in the south-west corner.

That most gullies stop at the top of the batters is not surprising since the slopes abruptly decrease at this point and on the caprock the CIF threshold in equation 4.4.4 is no longer exceeded. The extension onto the caprock in the south-west corner of the batter is possible because of the longer slope lengths on the caprock contributing to the batter at that point. However, even for those regions where gullies do not extend onto the caprock in 1000 years it is likely that for longer times they will as valleys incise and slopes near the divide increase.

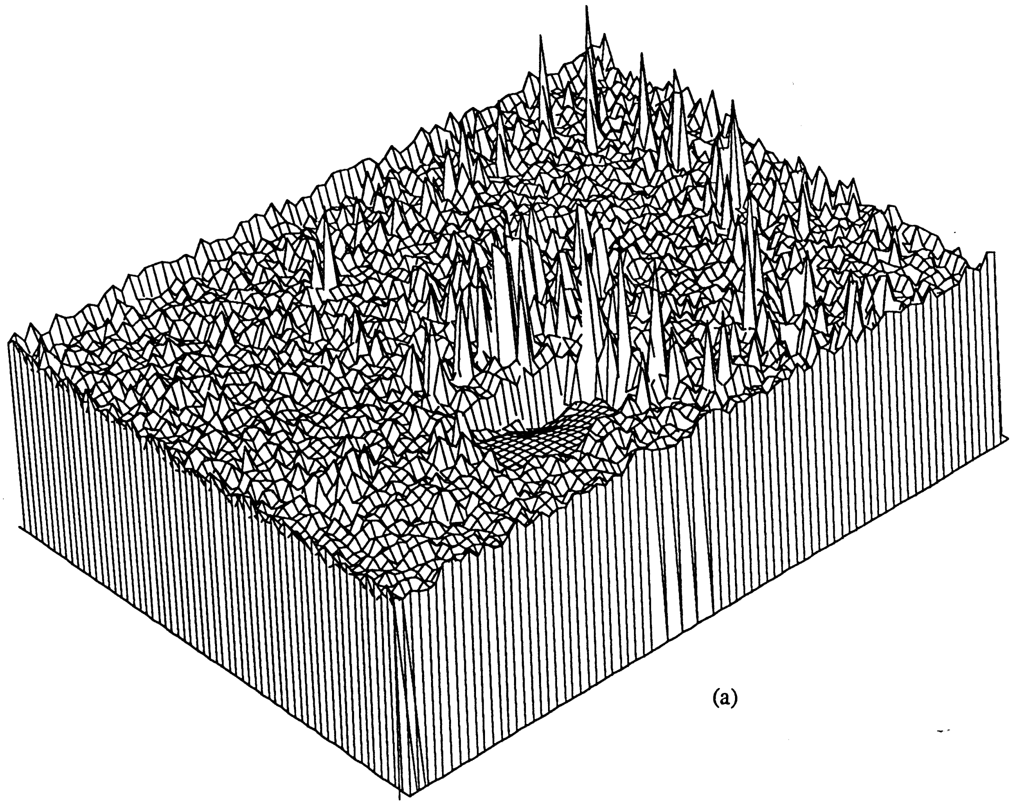

(a)

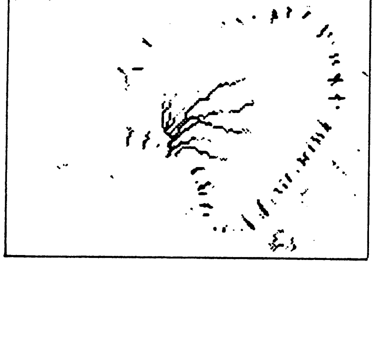

(b) Contours of erosion with 0m = white to ≥ 1m = black

Figure 5.5 Above-grade option, with-random settlements cases: Erosion (upwards) and deposition at 1000 years

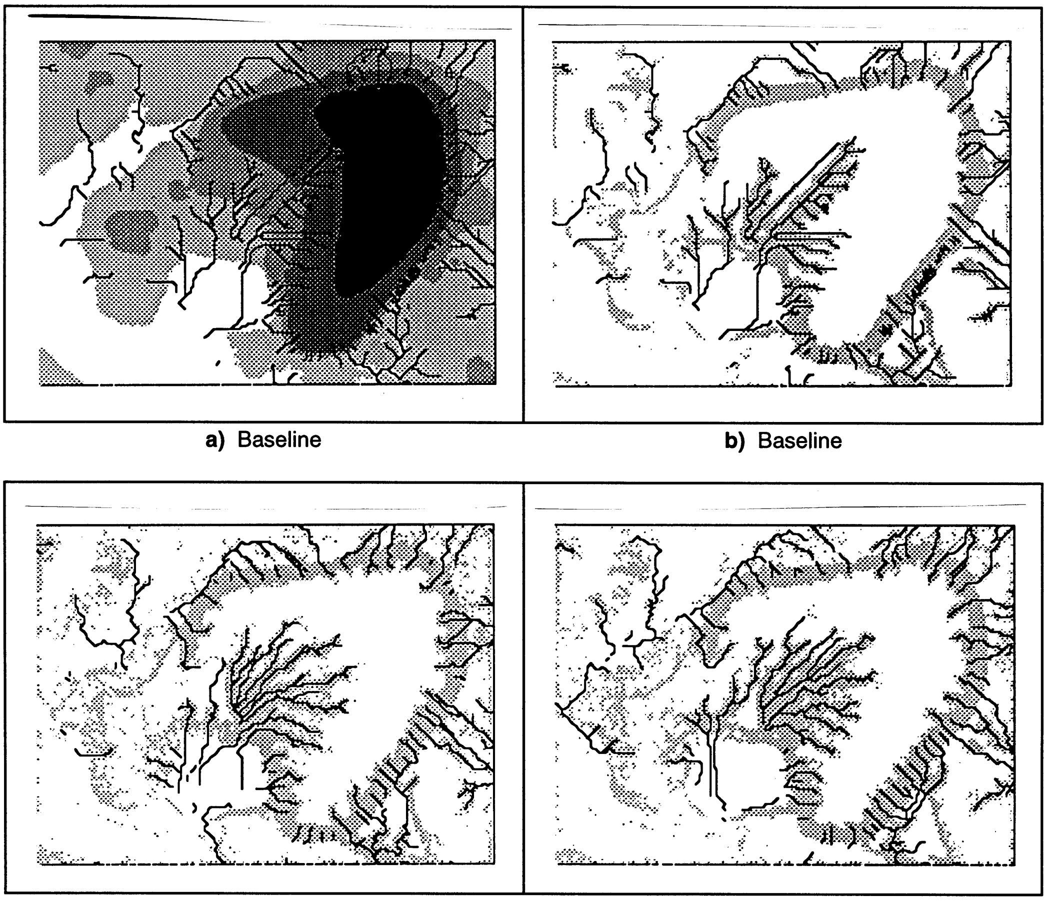

a) Baseline b) Baseline

c) Random settlements #1 d) Random settlements #2

Figure 5.6 Above-grade option, baseline and with-settlement cases: Preliminary estimates of gully development on the rehabilitation at 1000 years, overlaid on (a) elevations, (b), (c), (d) slopes greater than 0.05

Figure 5.6c,d shows the gully development for the two with-settlement cases discussed above. Most important is that the exact gully positions are different in both the with-settlement realisations, and that they are different from those in the baseline case. This is a result of the random fluctuations on the drainage pattern imposed by the settlements and is a direct result of a lack of imposed valley and drainage pattern in the baseline case. Despite these differences in the exact gully positions it can be clearly seen that all the figures show similarities in their average, overall, behaviour. Gullies are heavily concentrated in the central part of the caprock layer and they all terminate at about the same distance up the caprock layer. On the batters the gullies mostly stop at the batter top except in the south-west corner where once again gullies incise upstream onto the caprock upstream of the caprock layer. It is apparent that the gullies in the with-settlement case have advanced into the caprock more than in the baseline case, reflecting the increased erosion observed in the with-settlement case.

In all cases the drainage density of the gully development is about the same suggesting that settlements do not have a significant effect on the extent of gullying, only the location.

5.5 Below-grade option – baseline case

The below-grade option was run for the equivalent of 1000 years using the parameters calibrated in the previous sections. The procedure used was identical to that used in section 5.2 above for the above-grade option. Perspectives of the waste rock dump are for the as constructed year zero condition and for the 1000 year case in figures 5.7 and 5.8. As for section 5.2 these data are plotted on a 60 m grid though all erosion calculations were done on a 30 m grid.

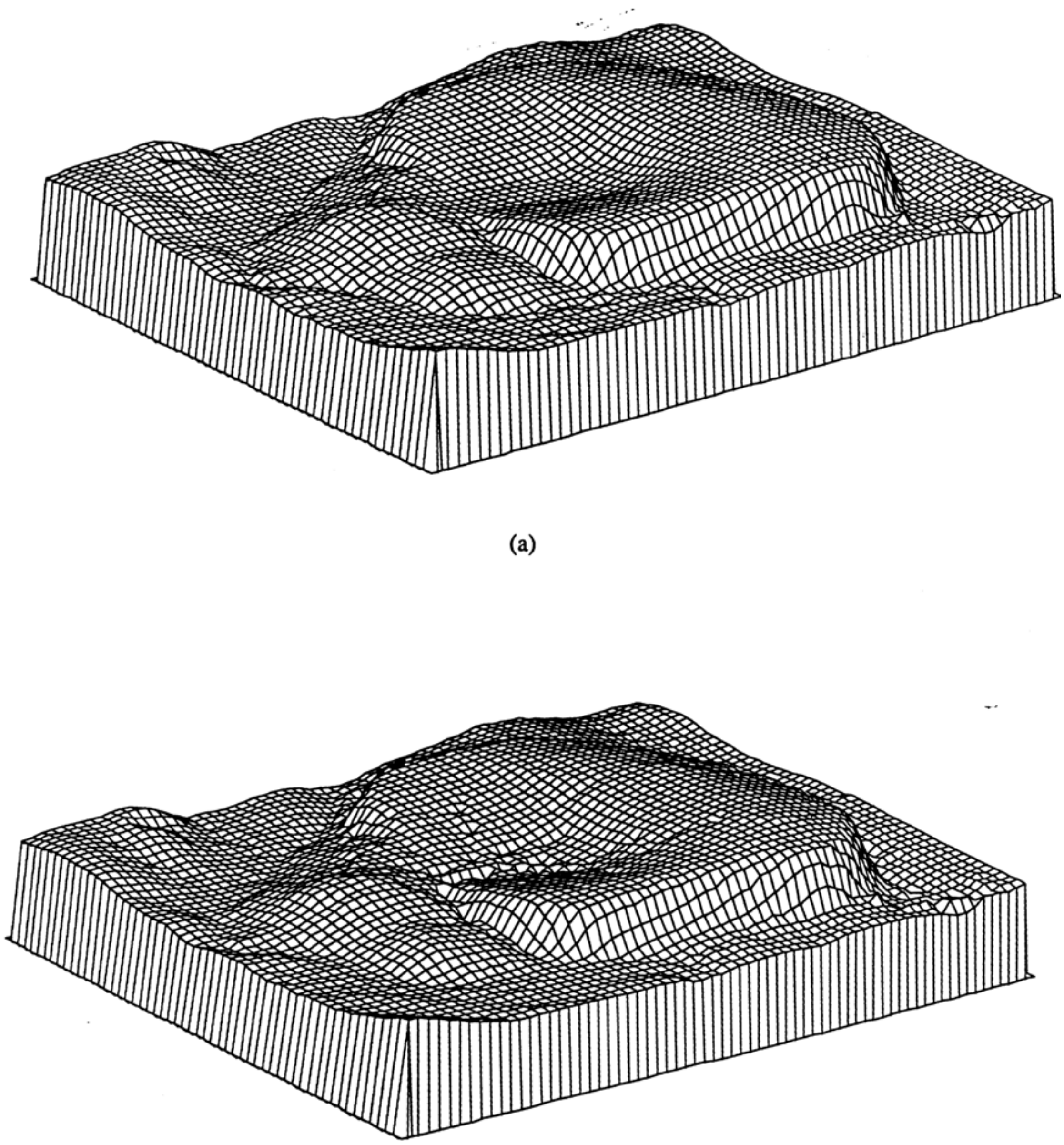

(a)

(b)

Figure 5.7 Below-grade option, baseline case: Elevations at (a) 0, (b) 1000 year viewed from the NE

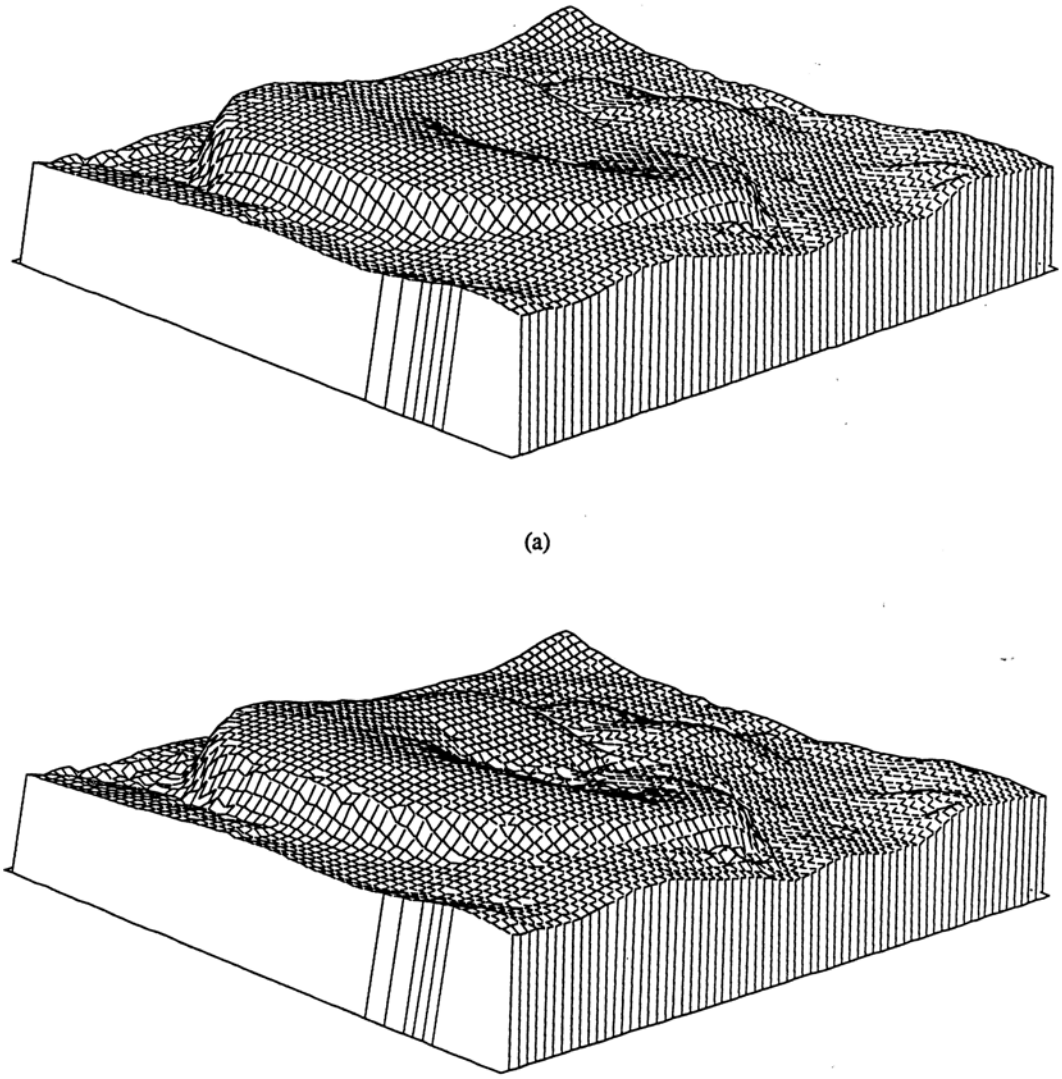

(a)

(b)

Figure 5.8 Below-grade option, baseline case: Elevations at (a) 0, (b) 1000 year viewed from the SW

The maximum depth of valley formation is 5.75 m and the maximum depth of deposition is 3.1 m. The maximum valley depths for the below-grade option are approximately 75% of those for the above-grade option. This reflects the smaller area draining to the central area and consequently the lower rate of erosion. The lower depths of deposition also reflect the lower rates of erosion.

In the centrally draining caprock region there are deep valleys forming in a similar fashion to those that occur in the above-ground case. These valleys radiate out in all directions from the dam in the centre of the caprock region. Note that these valleys propagate upwards from the gully that is formed by the intersection of the batters and the natural landscape on the north-east edge of the rehabilitation. The valley with maximum depth occurs in the central part of the rehabilitation and extends downstream in a northerly direction along the intersection of the NE batter and the natural surface. It thus seems likely that the dam that is proposed for the centrally draining area may be breached at some stage in the future by this valley propagating southwards along the NE batter bottom.

As in the above-grade option there is substantial erosion occurring along the batters on the northern, western and southern sides (fig 5.9). The peak erosion rates (about 3–4 m) occur on the western batter. The reason for this is similar to the reason for the severe batter erosion in the above-grade case. The 250 m slope length that flows west contributes flow to the batter tops so that erosion on the batters is enhanced. Again, as in the above-grade case, the uniformity of the erosion along the western edge means that structural protection works would be required for the complete length of the batter top. As in the above-grade case the deposition of the sediment eroded on the batters mostly occurs within 100–200 m downstream of the batters.

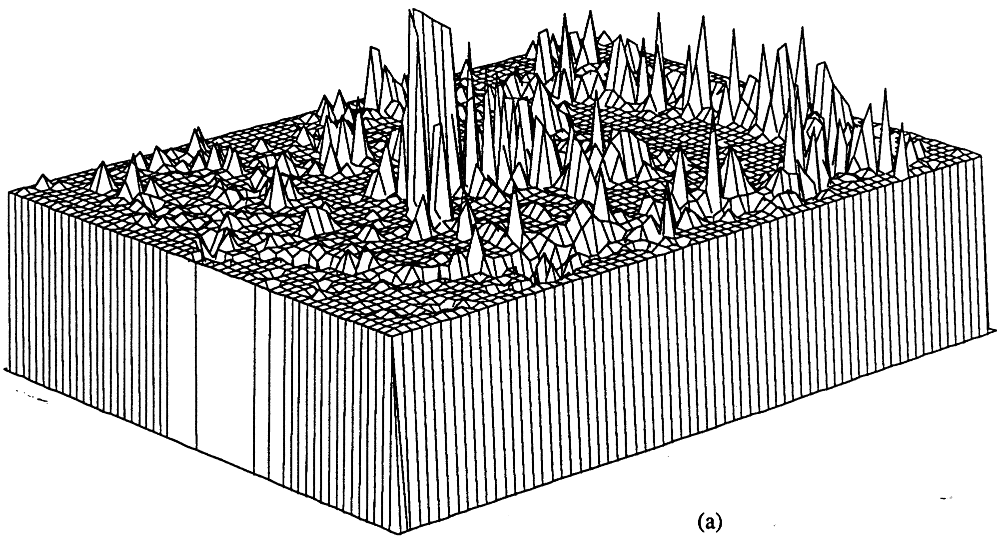

(a)

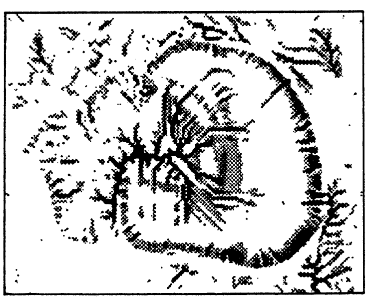

(b) Contours of erosion with 0m = white to ≥ 1m = black

Figure 5.9 Below-grade option, baseline case: Erosion (upwards) and deposition at 1000 years

The drainage density of the gully development for the below-grade option is about 15% less than that for the above grade option. That is, the total length of gullies/unit area in the below-grade case is 15% less than that in the above-grade case. This reduced gully development appears to be mainly a result of reduced gully development on the batters, which directly reflects the shorter hillslope lengths on the caprock contributing to the tops of the batters.

5.6 Below-grade option – effect of settlement

As in the above-grade case the sensitivity of the erosion pattern to random settlement effects was examined. The same procedure as for the above-grade was adopted and the erosion pattern simulated for 1000 years. Figures 5.10 and 5.11 shows the design landform subject to an initial 1 m random settlement at 1000 years. The maximum depths of erosion are 7.9 m and 6.1 m respectively—significantly higher than the 5.8 m observed in the baseline case.

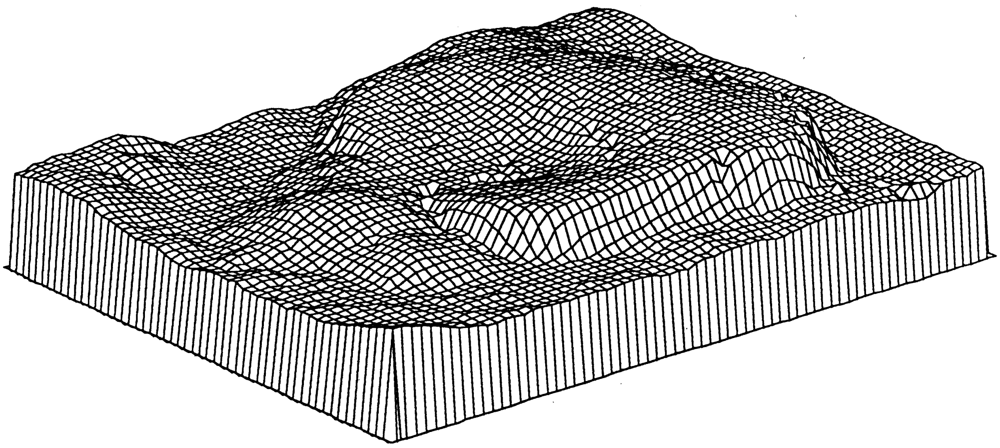

(a) Realisation #1

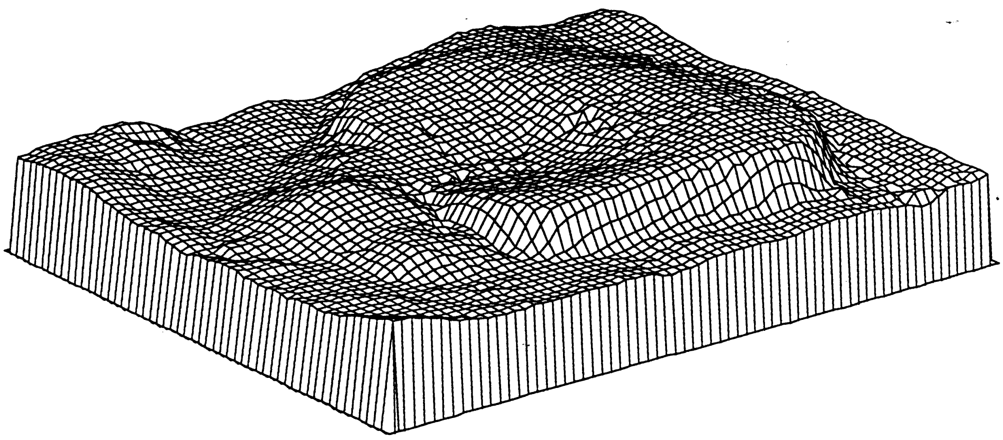

(b) Realisation #2

Figure 5.10 Below-grade option, with-random settlements cases: Elevations at 1000 years viewed from the NE

As for the above-grade with-settlement case the valley formation that occurs for the below-grade with-settlement case is more widespread than without settlement but the general region of valley formation is similar to the case of no settlement.

On the batters there is more widespread valley formation for the with-settlement case than the baseline case. As in the above-grade case this is a result of the convergence of flow on the caprock that the settlement triggers, which in turn concentrates the flow and erosion enhancing the valley formation process. Figure 5.11 shows the extent of valley formation on the batters for the with-settlement which can be compared with for the without-settlement baseline case (fig 5.8).

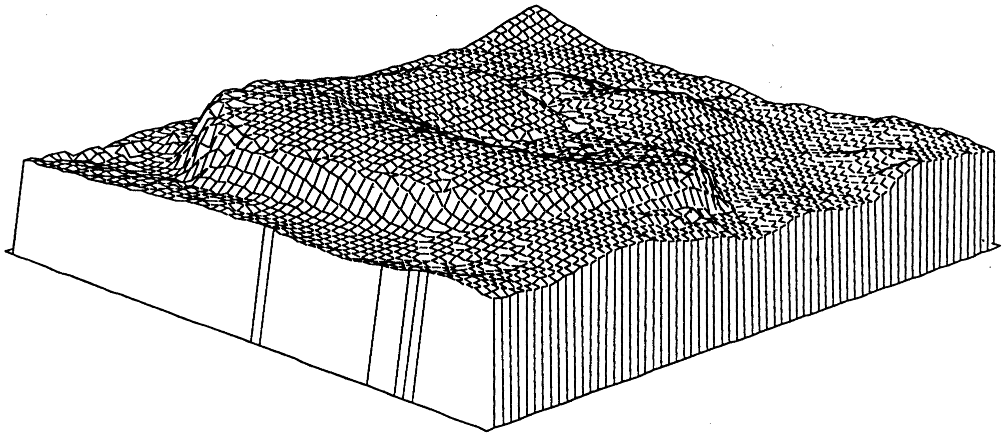

(a) Realisation #1

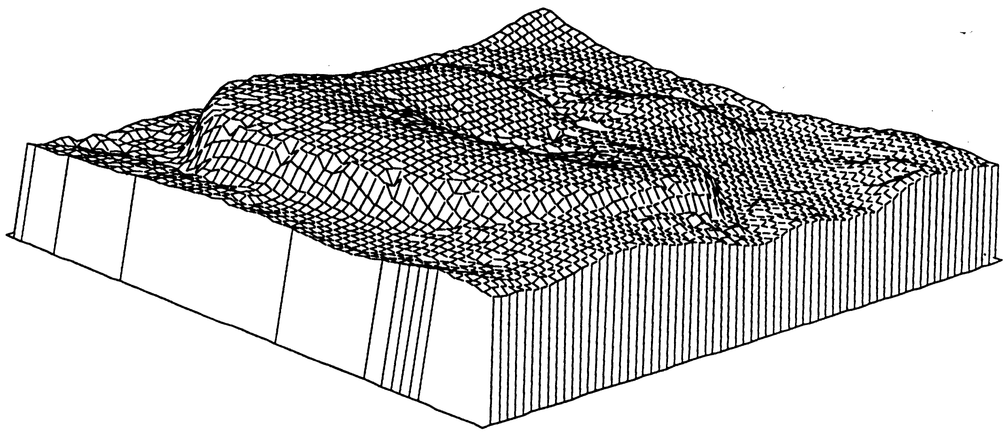

(b) Realisation #2

Figure 5.11 Below-grade option, with-random settlements cases:
Elevations at 1000 years viewed from the SW

Figure 5.12 shows the spatial distribution of the erosion for the first of the with-settlement realisations. The results here are qualitatively very similar to those observed for the above-grade case. Again the most obvious difference with the erosion for the baseline case (fig 5.9) is the widespread random background erosion of about 1 m. As in the above-grade case the regions of high erosion in the baseline case are maintained in the with-settlement case. The high points of erosion are also more widespread.

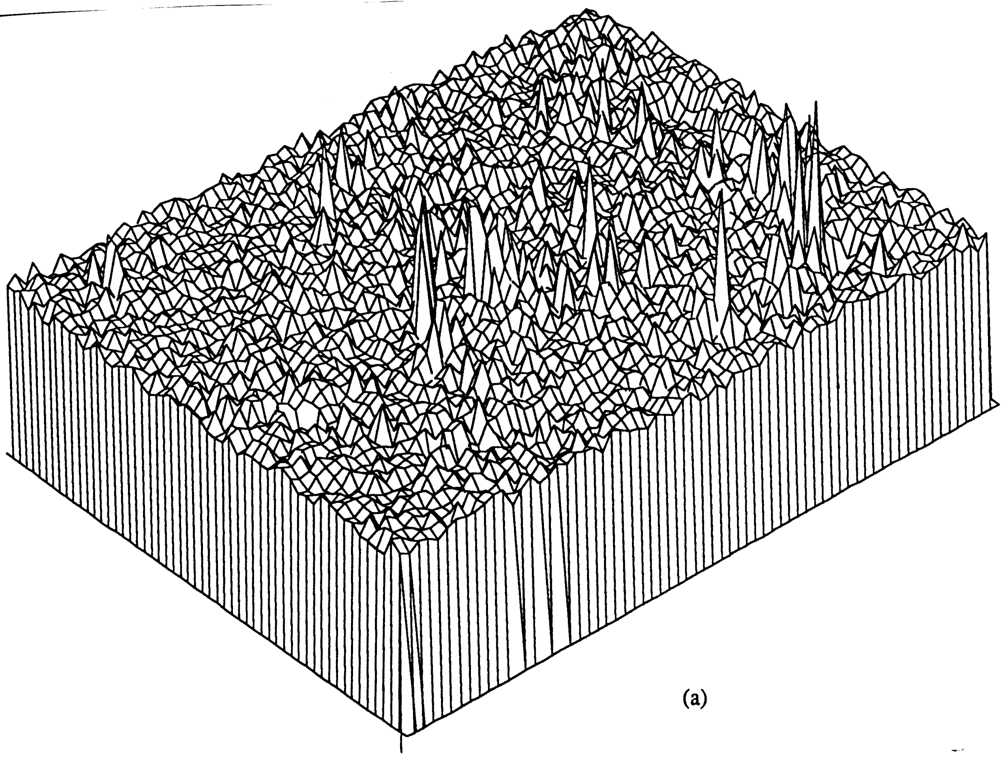

(a)

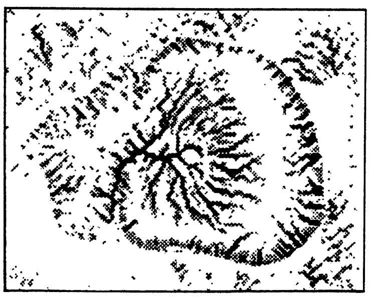

(b) Contours of erosion with 0m = white to ≥ 1m = black

Figure 5.12 Below-grade option, with-random settlements cases: Erosion (upwards) and deposition at 1000 years

5.7 Below-grade option – with gullies

In this sensitivity study the potential for gully erosion, over and above the sheet erosion already discussed in the sections above, is examined for the above-grade case. The gully erosion threshold (called the CIF threshold) observed by Williams and Riley (1992) at Tin Camp Creek (discussed in section 4.4) is used to define the upper limits of gully erosion on the waste rock dump. In the absence of information of the sediment transport in the gullies at Tin Camp Creek the sediment transport rate in the gullies is assumed to be equal to that on the hillslopes. The sensitivity of the gully development to the random settlements is also examined, particularly how the position of gullies change with the imposition of settlements. Here we do not predict the depth of gully development (that would require further data from studies at Tin Camp Creek), however, the gully incision can be simply added to the depths of sheet erosion discussed above; the two depths of erosion are believed to be largely independent over geomorphic timescales.

Figure 5.13a,b shows the gully positions for the below-grade baseline case at 1000 years. Figure 5.13a shows the gullies superimposed on a contour map of the site and 5.13b shows them superimposed on a map showing areas where slopes are greater than 0.04. The gullies extend quite some distance into the central caprock area fanning out to fill the lower regions of the caprock. They do not extend all the way to the drainage divide on the caprock because there the contributing area and slopes are too low to trigger gully development. The gully development on the batters is largely constrained to the batters themselves. Unlike the above-grade case no gullies extend onto the caprock region upstream of the batters, reflecting the shorter hillslopes upstream of the batters. As in the above-grade case, however, it is likely that for times greater than 1000 years, as the slopes at the top of the batter-caprock intersection begin to round, that the gullies will extend into the caprock region. The shorter slope lengths in the below-grade case mean that this extension will not occur as quickly as in the above-grade case.

Figure 5.13c,d shows the gully development for the two with-settlement cases discussed above. As in the above-grade case, the exact gully positions are different from those of the baseline case. This is a result of the random fluctuations on the drainage patterns imposed by the settlements and is a direct result of the lack of an imposed valley and drainage pattern in the baseline case. Despite these differences in the exact gully positions it can be seen that the average, overall, position of gullies is similar in all cases. Gullies are heavily concentrated in the central part of the caprock layer and they terminate at about the same distance up the caprock layer. On the batters the gullies no longer terminate at the top of the batter with some advancing onto the caprock, reflecting the increased erosion observed in the with-settlement case.

In all cases the drainage density of the gully development is about the same suggesting that settlements do not have a significant effect on the extent of gullying, only the location.

Finally note the gully that develops along the base of the NE batter, whose position is well known and independent of random settlements. This was discussed for the baseline case and poses a potential danger to the dam on the caprock.

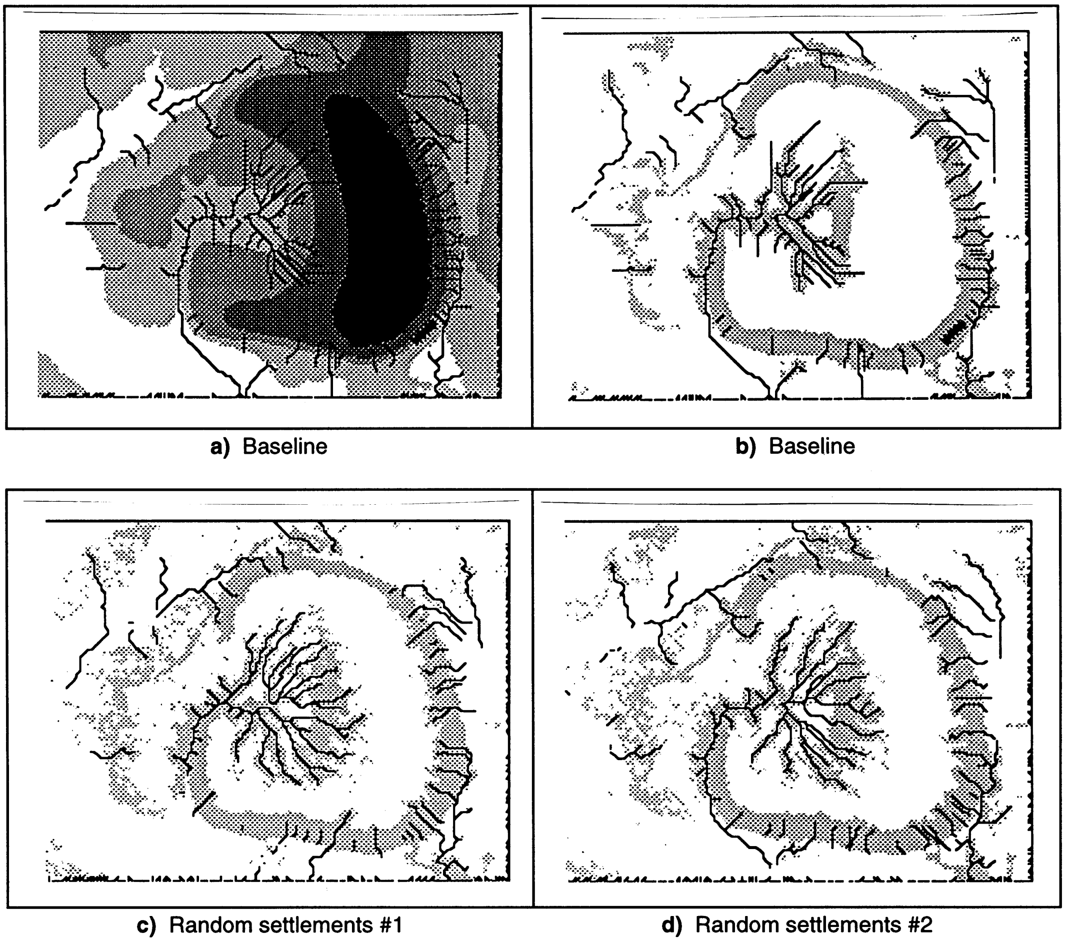

Figure 5.13 Below-grade option, baseline and with-settlement cases: Preliminary estimates of gully development on the rehabilitation at 1000 years, overlaid on (a) elevations, (b), (c), (d) slopes greater than 0.05

5.8 Other issues

5.8.1 Greenhouse warming

Changes in the rainfall occurring at Ranger as a result of enhanced greenhouse warming will change the runoff and thus the mean annual erosion. Systematic increases in rainfall will increase both runoff and erosion. It is unlikely that changes in the climate will modify the behaviour of these scenarios, so that gullies, etc, will still appear where predicted, but they will occur at earlier times.

The Intergovernmental Panel Report on Climate Change (IPCC 1990) is currently considered to be the most reliable source of information on the effects of enhanced greenhouse warming and the likely effects on climate. While there is considerable doubt about the ability of existing Global Circulation Models (GCMs) to provide accurate predictions of regional climate change, IPCC provides maps of changes in temperature, precipitation and soil moisture for the globe for a doubling of CO_2 as estimated by three models: the CCC (Canadian Climate Center), GFHI (Geophysical Fluid Dynamics Laboratory, Princeton) and UKHI (United Kingdom Meteorological Office).

IPCC provides estimates of the changes in precipitation. For the Darwin/Jabiru region it provides estimates of the change in precipitation for the months December to February ranging from +1 to 2 mm/day (CCC) to -1 to 2 mm/day (UKHI). For the months of June to August they universally predict 0 to 1 mm/day.

IPCC also provide predictions of changes in soil moisture. For the months December to February they predict a change in the soil moisture content ranging from a reduction of 10–20 mm (UKHI) to increases of more than 20 mm (CCC). For the months of June to August they predict increases in soil moisture ranging from 0 mm (GFHI) to 20 mm (CCC).

Clearly, there is substantial conflict between the predictions of the models. Also, it is clear from the maps provided that the values above are nowhere near the extremes predicted for other regions of the world.

It is recommended that until more convincing evidence appears, effects of enhanced greenhouse warming on the rainfall and erosion at Jabiru over the next 1000 years should be ignored.

5.8.2 Infiltration

Knowledge of the rates of infiltration is useful for assessing the availability of moisture to the plants used in revegetation. The runoff time-series simulation of the section 4.2 can be used to provide an upper bound on the amount of moisture that would have been available under historical conditions. This *upper bound* is the amount of water that does not runoff, and consists of both infiltration from the surface to lower layers and evaporation from the surface. More accurate assessment of the net infiltration requires accurate assessment of evaporation and evapotranspiration losses which is outside of the scope of this project. The yearly average upper bound figures are listed in table 5.1. Note that in some years rainfall for only part of the Wet season was collected, while for other years large parts of the Dry season were not recorded. In these years the upper bound on infiltration may well be higher. These years are noted accordingly.

Table 5.1 Simulated runoff yield for waste rock dump

Year	Rainfall (mm)	Runoff (mm)	Year	Rainfall (mm)	Runoff (mm)
1971[(a)]	173	90	1983[(a)]	184	108
1972	1163	548	1984	2082	1026
1973	1353	656	1985[(a)]	378	207
1974	1604	586	1986	1145	414
1975	1642	693	1987	1277	531
1976	1144[(b)]	444	1988	1135	515
1977	928	445	1989	1152	484
1978	1467	744	1990[(a)]	748	355
1979	1193	559			
1980	1663	782			

[(a)] Year incomplete; [(b)] Dry season incomplete

The runoff *yield* for the engineered landform is approximately 0.45. However, this should not be mistaken for the runoff coefficient from the engineered landform, which is also a function of the rainfall volume and temporal pattern, and overland flow hydraulics. Hydrological studies of natural areas near Jabiru (eg Tin Camp Creek) and revegetated/ripped areas on the existing waste rock dump should provide useful comparative runoff yield data.

5.8.3 Long-term versus short-term erosion modelling

Traditional methods of erosion assessment used by agricultural engineers, such as USLE, RUSLE and CREAMS, determine the erosion at any given time for a particular landform. They are unable to predict the change in shape of the landscape as a result of the erosion that occurs on it, nor are they able to predict the effect that the change in the landform has on the future erosion patterns. These methods are implicitly short-term techniques. If erosion predictions are only required for a small time in the future, over which the erosion doesn't change the landform much, then they provide good predictions of erosion patterns.

Over longer periods of time, however, the change of landform shape cannot be ignored. This is the rationale for the use of the SIBERIA landscape evolution model for the erosion assessment in this report. Localised erosion results in localised convergence of flow with further increases in erosion. Thus valleys will deepen over time as the natural process of drainage development occurs. While over the short-term the predictions of the short-term and long-term models will be little different, as the landform erodes the short-term models will progressively provide poorer estimates of the erosion. In particular, the spatial *pattern* of erosion, where the localised high erosion occurs on the rehabilitation, will be poorly estimated.

Figure 5.14 demonstrates the difference between the two modelling approaches, showing the patterns of erosion for three cases for the above-grade baseline proposal. The first case (figure 5.14b) shows the pattern of erosion for the first 3 years after the rehabilitation is complete (assuming that the surface of the rehabilitation was completed at the same time, rather than progressively during mine operation); the second case (figure 5.14c) shows the pattern of erosion for the 3 years after the end of the design life (ie years 1000 to 1003). Both of these cases can be considered to be indicative of the results from short-term modelling exercises with specified landforms. The second case, of course, assumes that we know the result of the long-term modeling exercise. The third case (figure 5.14d) shows the pattern of erosion for the 1000 year long-term modeling described in section 5.

The pattern of erosion is different in both cases. Both of the short-term results predict a more uniform erosion distribution than the well defined, localised, erosion apparent in the long-term result. The 1000 year short-term result does exhibit some localised erosion but only in the valleys already created by the long-term model; it does not predict the localised erosion upstream that will probably occur after 1000 years in the long-term case.

The reason for this result lies in the way valleys are incised over time. Valleys do not gradually downcut over their whole length with time. If they did, then erosion depth estimates from the short-term models could be factored up for the design life of the landform. Rather, valleys rapidly incise at the valley head as it propagates upstream from the highwall around the central retention pond with proportionally less erosion both upstream and downstream of the headcut. This is apparent in figure 5.14c where the highest erosion rates are at the valley heads. Short-term methods can predict where the areas of localised high erosion will occur at any given time for any specified landform, however, they are unable to predict how this region of localised high erosion will move over time. They are thus unable to accurately estimate the spatial distribution of the regions of high erosion.

While the *pattern* of erosion is different in the short-term and long-term results, the average rate of erosion over the domain (caprock, batters and the portions of undisturbed natural surface illustrated in fig 5.1) is much the same (about 0.3 m over the 1000 years). The difference between the short-term and long-term results is that much more of the long-term erosion is concentrated in deep valleys; the short-term results would predict more uniform, less concentrated, erosion depths. In short, the short-term modelling results would be non-conservative with lower values for maximum erosion depths, even though average depths of erosion appear to similar for both short-term and long-term results.

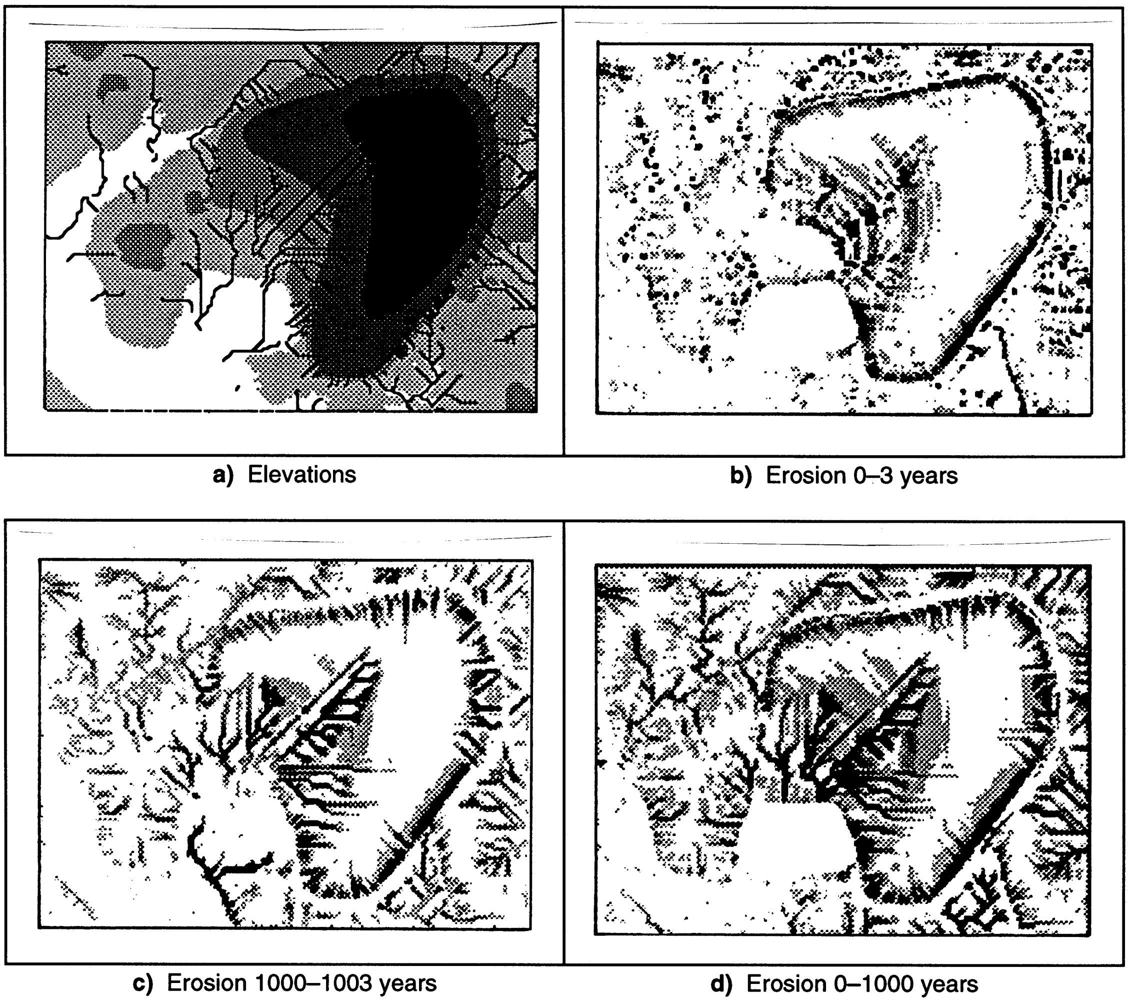

Figure 5.14 Comparison of the patterns of erosion for the short-term and long-term erosion modelling methods

6 Conclusions

6.1 Discussion

The simulations herein have clearly showed that significant erosion will occur in the next 1000 years in the caprock region of both the above-ground and below-ground options. Peak erosion depths without gully development are predicted to be in the range of 7–8 m. Gully development potentially increases the maximum penetration of the caprock layer further. It is predicted that a number of valleys will dissect the central region of the caprock. The exact position of these valleys is subject to some doubt because of the poor definition of an initial drainage structure on the proposed designs. It thus appears difficult to design localised protective measures for these gullies because the position of these potential gullies cannot be predicted *a priori*. Drainage network development is a chaotic process (Willgoose et al 1991c, Ijjasz-Vasquez 1990) but if an initial drainage pattern is imposed some predicability should be imposed on the eroding system.

In addition, it has also been shown that the steep (slope≈ 0.15) batter slopes will suffer severe degradation of the order of 5–7 m. The valleys on the batters do not occur in predictable places but occur along all the batter extremities of the waste rock dump. The erosion problem is thus not localised to one place, where it potentially may be protected, but it occurs across broad areas making it difficult to design reliable protective measures. The fundamental cause of this problem is that there are substantial slope lengths (>200 m) on the caprock that contribute flow to the upper end of the batters. When this flow reaches the batter it cascades over the batter causing severe degradation. One solution, bund walls around the top of the batter, is unlikely to solve this problem. The widespread nature of the erosion on the batters indicates that there appear to be few safe locations where this flow can be diverted to.

The substantial erosion on the batters results in deposition in the surrounding areas. The deepest depths of deposition (about 5 m over 1000 years) appear to very close (within 150–200 m of the batters) to the batters, although it is apparent that some deposition does occur at greater distances. Computational limitations meant that it was necessary to restrict the study area to that immediately surrounding the proposed waste rock dump so that more exact comments of the region of deposition cannot be made at this stage. Moreover, without knowledge of erosion rates on the natural areas surrounding the waste rock dump such a study may be subject to significant error.

Finally, in the absence of random settlements, the rates of erosional loss on the majority of the caprock layer away from the gullies appear to be relatively small (less than 500 mm). In fact, the low erosional loss on the portion of that caprock region contributing to the batters enhances the gully erosion that occurs on the batters. Addition of random settlements with a range of 0−1 m induces erosion and deposition on the caprock of about 1 m depth. There is no apparent systematic pattern to this erosion.

This deep sheet erosion in isolated regions with little erosion in intervening areas suggests a solution strategy for the problem and involves considering the geomorphology of the entire waste rock dump. As previously noted, the major problem with the existing designs is that their slopes decrease as drainage area increases in a different fashion from that observed in natural catchments, which are closer to their equilibrium form. This characteristic of natural catchment arises from the balance of erosion, drainage patterns and elevations that catchments tend towards over geologic timescales (Gilbert 1909, Willgoose et al 1991d, Willgoose 1993). Figure 6.1 is a schematic showing how this natural adjustment process works.

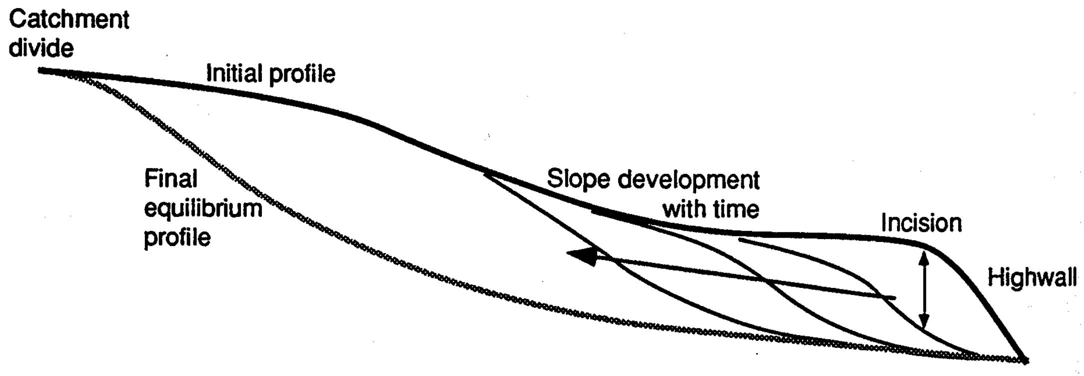

Figure 6.1 Schematic of erosion incision when the initial profile is far from the long-term equilibrium profile

The closer that the starting profile is to the final equilibrium profile the less incision will occur. These equilibrium profiles can be described mathematically by (Willgoose 1993)

$$\frac{A^{\alpha_1} S}{Z - Z_d{}^{\alpha_2}} = \text{constant} \qquad 6.1.1$$

where A is the drainage area, S the slope, Z the elevation and Z_d the datum elevation and the parameters α_1 and α_2 are a function of the runoff and erosion physics. These long-term equilibria results (published by the first author and others) should be examined as a criteria to redesign the slopes and landform of the waste rock dump. Effort should be concentrated on reducing slope lengths and gradients near the base of the dump in the central area. Emphasis should also be placed on imposing a drainage structure that is appropriate to the runoff and erosion from the waste rock dump. The long flat hillslopes that characterise the proposed design bear little resemblance to natural conditions and should be replaced with hills and valleys of the kind observed in natural catchments. This imposed drainage structure could maintain the key internal drainage feature of the existing design and would allow the use of the proposed pits and dams to trap sediment.

Thus, in summary, there are a three problems with the proposals that should be addressed.

The first problem is that the slope gradient does not decrease downslope as it does in natural catchments. This feature means that sediment transport increase much faster downslope than occurs in natural catchments. The long-term effect of this is for gully erosion to develop at the bottom of the slopes as the lower parts of the catchment trend towards the low slope condition in the lower reaches of the catchment which is the long-term equilibria.

The second problem is that the wide flat hillslopes allow gullies to concentrate flow (and thus increase the discharges and erosion) with great ease. By imposing a drainage structure of valleys with interceding hills it becomes very difficult for a gully to capture adjacent areas (first they must erode away the interceding hill). Discharges are then unlikely to change much as erosion proceeds from that designed. A secondary advantage is that if a gully does occur it will be localised and its growth will be controlled. A key feature controlling the rate of growth of gullies is their ability to capture area; reduce this ability and gullies grow less quickly.

The third problem is that the long caprock hillslopes contribute flow to the tops of the batters, inducing deep erosion at the tops of the batters around the emplacement area.

6.2 Recommendations for future work

6.2.1 Increasing the reliability of SIBERIA parameters

- **Checking of data**: Further reliability checks are required on available monitoring data and the data for the simulator trials should be carefully compared with the data from natural storms to solve the apparent conflict in the fitted ϕ value for these two data sources.
- **Sediment yield data from natural rainfall events**: For sediment yield data that have no matching discharges, the discharge data should be reconstructed from the hydrology model and recorded rainfall records. These data could then be used to increase the reliability of the sediment transport model calibrated here.
- **Erosion studies**: Erosion studies should be carried out over slopes intermediate between that of the caprock and the batter to better define and explain the slope dependence of the sediment transport equation.

- **Runoff studies for other conditions 1**: Rainfall simulator or natural runoff data should be collected for abandoned mine workings where spoil heaps are derived from similar schist material as at Ranger. This would allow the estimation of the effect of soil development on runoff and erosion properties.

- **Runoff studies for other conditions 2**: Rainfall simulator or natural runoff data should be collected for the vegetated areas of the spoil heap at RUM. This would allow the estimation of the effect of vegetation development on runoff and erosion properties.

- **Analysis of existing data not considered here**: The data collected during 1991/1992 for the deep ripped sites on the caprock should be analysed and compared with the analysis in this report for unripped sites. This will allow assessment of the short-term effects on infiltration, runoff and erosion.

- **Gully erosion at Tin Camp Creek**: The gully geometry of the gullies proceeding downstream should be correlated with area and slope. This will give reliable indicators of the amount of sediment delivered by these gullies to the catchment during their formation. This can be then be used to predict the depth of gullying likely at RUM, for design of the depth of the upper cap layer.

- **Gully erosion at abandoned mine sites**: The threshold above which gully erosion occurs should be examined and hydrologic studies carried out to consider the hydrologic generality of the threshold behaviour for abandoned mine sites in the region. These studies will increase confidence in the thresholds derived from the natural catchment at Tin Camp Creek. Gully cross-sections should be correlated to area and slope as for Tin Camp Creek.

6.2.2 Further simulations with SIBERIA

- **Long-term equilibria** (beyond 1000 years) of the sites should be examined to provide information on the long-term form of the landscape.

- **SIBERIA and natural landforms**: The efficacy of SIBERIA should be examined for the ability to predict the form of the nearby terrain (eg Tin Camp Creek area) using the hydrology and erosion data collected by ***eriss***.

- **Spatial variability of rainfall**: The radar data for rainfall of Krawjewski et al (1991) should be closely examined for its possible effect on the parameters of SIBERIA and predictions herein.

- **Sediment storage in dams**: Detailed data regarding the three dams that the waste rock dump drains into should be used for input to SIBERIA to assess the timescales over which these dams will fill and understand their usefulness for stopping off-site deposition over geomorphologic timescales.

Appendixes

Appendix A Maps of field sites

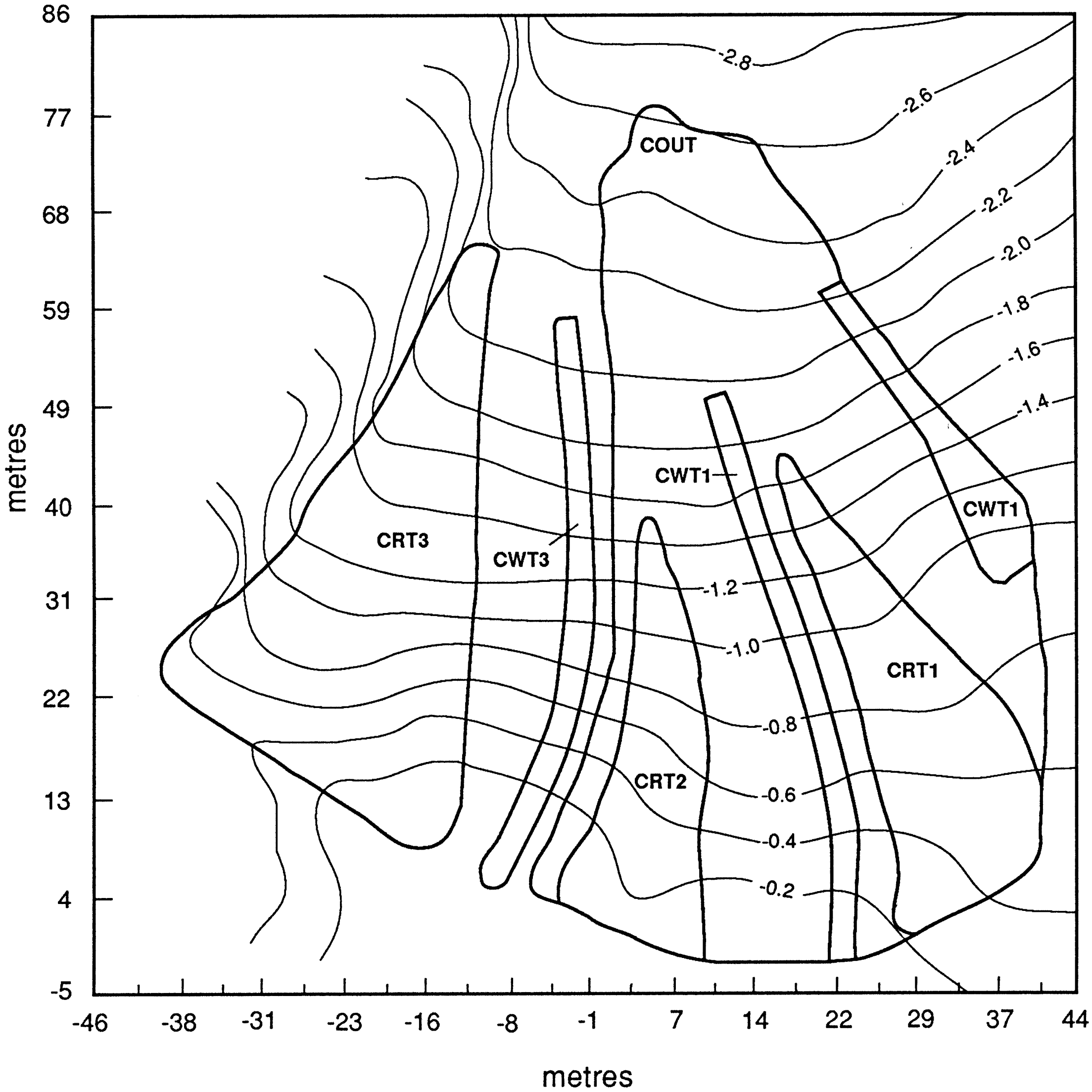

Figure A.1 Caprock monitoring sites and contours

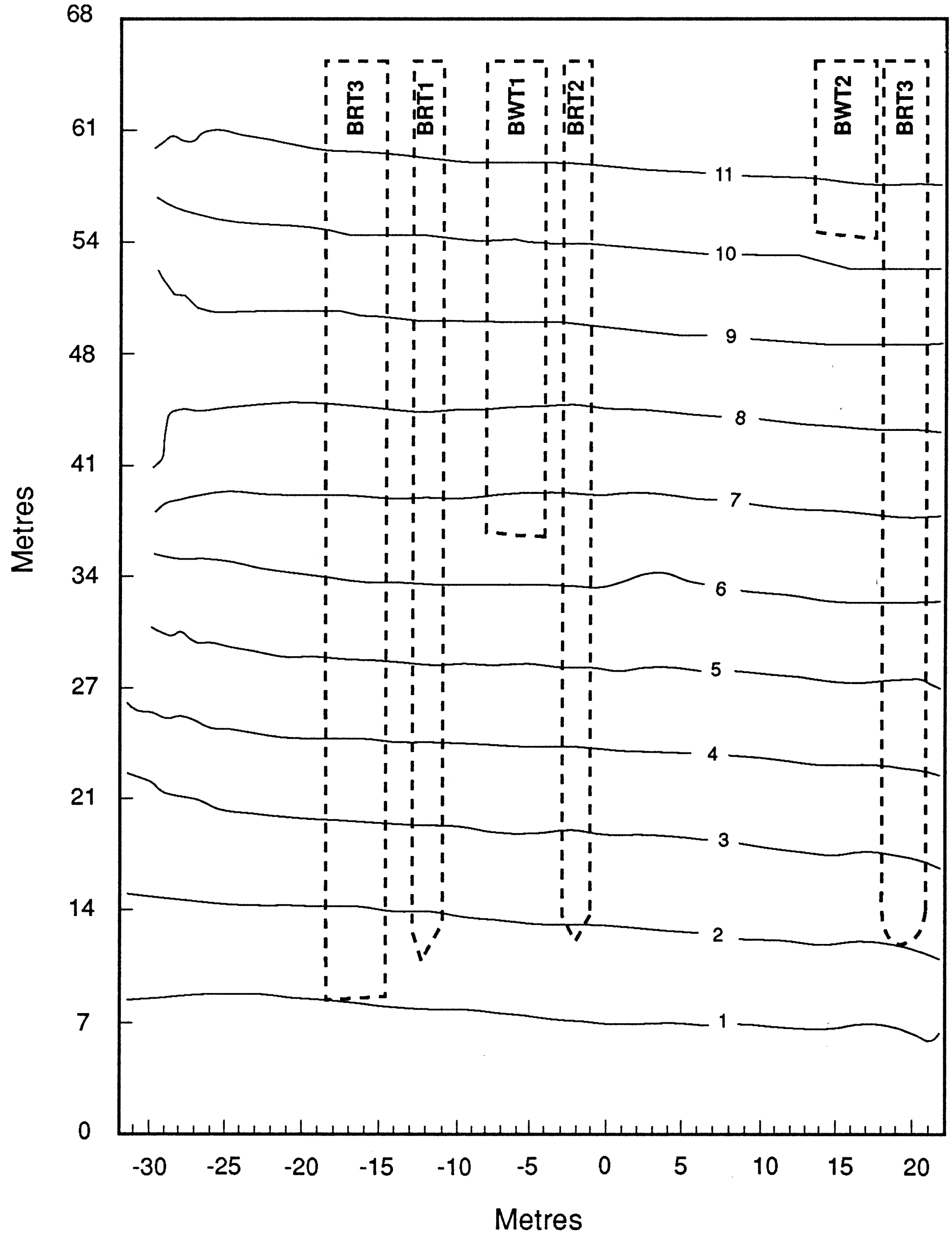

Figure A.2 Batter monitoring sites and contours

Appendix B Runoff data

B.1 Natural rainfall

The following data are pluviograph records for the storms used in the calibration of the hydrology model for the natural rainfall experiments. Times are in the format 24 hour time and date, and rainfall is mm.

Caprock pluviograph

time	rainfall	time	rainfall	time	rainfall
14:50_07/01/1991	0.000	20:40_07/01/1991	0.000	07:45_10/01/1991	0.000
14:51_07/01/1991	0.000	20:41_07/01/1991	0.000	07:46_10/01/1991	0.000
14:52_07/01/1991	0.000	20:42_07/01/1991	0.000	07:47_10/01/1991	0.000
14:53_07/01/1991	2.000	20:43_07/01/1991	0.000	07:48_10/01/1991	0.000
14:54_07/01/1991	3.000	20:44_07/01/1991	0.200	07:49_10/01/1991	0.000
14:55_07/01/1991	6.000	20:45_07/01/1991	0.200	07:50_10/01/1991	0.000
14:56_07/01/1991	7.000	20:46_07/01/1991	0.200	07:51_10/01/1991	0.000
14:57_07/01/1991	2.000	20:47_07/01/1991	0.400	07:52_10/01/1991	0.000
14:58_07/01/1991	1.000	20:48_07/01/1991	0.800	07:53_10/01/1991	0.000
14:59_07/01/1991	1.000	20:49_07/01/1991	1.000	07:54_10/01/1991	0.000
15:00_07/01/1991	0.000	20:50_07/01/1991	1.000	07:55_10/01/1991	0.000
15:01_07/01/1991	1.000	20:51_07/01/1991	0.600	07:56_10/01/1991	0.600
15:02_07/01/1991	0.000	20:52_07/01/1991	0.200	07:57_10/01/1991	1.000
15:03_07/01/1991	0.000	20:53_07/01/1991	0.200	07:58_10/01/1991	0.800
15:04_07/01/1991	0.000	20:54_07/01/1991	0.200	07:59_10/01/1991	0.400
15:05_07/01/1991	0.000	20:55_07/01/1991	0.000	08:00_10/01/1991	0.200
15:06_07/01/1991	0.000	20:56_07/01/1991	0.000	08:01_10/01/1991	0.000
15:07_07/01/1991	0.000	20:57_07/01/1991	0.000	08:02_10/01/1991	0.600
15:08_07/01/1991	0.000	20:58_07/01/1991	0.400	08:03_10/01/1991	0.800
15:09_07/01/1991	0.000	20:59_07/01/1991	0.200	08:04_10/01/1991	1.000
15:10_07/01/1991	0.000	21:00_07/01/1991	0.000	08:05_10/01/1991	1.200
15:11_07/01/1991	0.000	21:01_07/01/1991	0.400	08:06_10/01/1991	0.800
15:12_07/01/1991	0.000	21:02_07/01/1991	0.600	08:07_10/01/1991	0.600
15:13_07/01/1991	0.000	21:03_07/01/1991	0.600	08:08_10/01/1991	1.000
15:14_07/01/1991	0.000	21:04_07/01/1991	0.800	08:09_10/01/1991	0.800
15:15_07/01/1991	0.000	21:05_07/01/1991	0.600	08:10_10/01/1991	0.600
15:16_07/01/1991	0.000	21:06_07/01/1991	0.400	08:11_10/01/1991	0.400
15:17_07/01/1991	0.000	21:07_07/01/1991	0.400	08:12_10/01/1991	0.400
15:18_07/01/1991	0.000	21:08_07/01/1991	0.400	08:13_10/01/1991	0.400
15:19_07/01/1991	0.000	21:09_07/01/1991	0.200	08:14_10/01/1991	0.400
15:20_07/01/1991	0.000	21:10_07/01/1991	0.200	08:15_10/01/1991	0.200
15:21_07/01/1991	0.000	21:11_07/01/1991	0.200	08:16_10/01/1991	0.200
15:22_07/01/1991	0.000	21:12_07/01/1991	0.000	08:17_10/01/1991	0.200
15:23_07/01/1991	0.000	21:13_07/01/1991	0.200	08:18_10/01/1991	0.000

time	rainfall	time	rainfall	time	rainfall
15:24_07/01/1991	0.000	21:14_07/01/1991	0.200	08:19_10/01/1991	0.200
15:25_07/01/1991	0.000	21:15_07/01/1991	0.000	08:20_10/01/1991	0.000
		21:16_07/01/1991	0.000	08:21_10/01/1991	0.200
		21:17_07/01/1991	0.000	08:22_10/01/1991	0.200
		21:18_07/01/1991	0.200	08:23_10/01/1991	0.200
		21:19_07/01/1991	0.000	08:24_10/01/1991	0.000
		21:20_07/01/1991	0.000	08:25_10/01/1991	0.400
		21:21_07/01/1991	0.000	08:26_10/01/1991	0.400
		21:22_07/01/1991	0.000	08:27_10/01/1991	0.200
		21:23_07/01/1991	0.000	08:28_10/01/1991	0.400
		21:24_07/01/1991	0.000	08:29_10/01/1991	0.200
		21:25_07/01/1991	0.000	08:30_10/01/1991	0.200
		21:26_07/01/1991	0.000	08:31_10/01/1991	0.200
		21:27_07/01/1991	0.000	08:32_10/01/1991	0.000
		21:28_07/01/1991	0.000	08:33_10/01/1991	0.200
		21:29_07/01/1991	0.000	08:34_10/01/1991	0.200
		21:30_07/01/1991	0.000	08:35_10/01/1991	0.000
				08:36_10/01/1991	0.200
				08:37_10/01/1991	0.000
				08:38_10/01/1991	0.000
				08:39_10/01/1991	0.000
				08:40_10/01/1991	0.000
				08:41_10/01/1991	0.200
				08:42_10/01/1991	0.000
				08:43_10/01/1991	0.000
				08:44_10/01/1991	0.000
				08:45_10/01/1991	0.000
				08:46_10/01/1991	0.000
				08:47_10/01/1991	0.000
				08:48_10/01/1991	0.000
				08:49_10/01/1991	0.000
				08:50_10/01/1991	0.000
14:00_10/01/1991	0.000	16:40_21/01/1991	0.000	11:40_06/02/1991	0.000
14:01_10/01/1991	0.000	16:41_21/01/1991	0.000	11:41_06/02/1991	0.000
14:02_10/01/1991	0.000	16:42_21/01/1991	0.000	11:42_06/02/1991	0.000
14:03_10/01/1991	0.200	16:43_21/01/1991	0.000	11:43_06/02/1991	0.200
14:04_10/01/1991	0.000	16:44_21/01/1991	0.000	11:44_06/02/1991	0.800
14:05_10/01/1991	0.000	16:45_21/01/1991	0.000	11:45_06/02/1991	2.200
14:06_10/01/1991	0.000	16:46_21/01/1991	0.000	11:46_06/02/1991	1.400
14:07_10/01/1991	0.000	16:47_21/01/1991	0.000	11:47_06/02/1991	1.200

time	rainfall	time	rainfall	time	rainfall
14:08_10/01/1991	0.000	16:48_21/01/1991	0.000	11:48_06/02/1991	0.800
14:09_10/01/1991	0.200	16:49_21/01/1991	0.000	11:49_06/02/1991	0.600
14:10_10/01/1991	0.000	16:50_21/01/1991	0.400	11:50_06/02/1991	0.600
14:11_10/01/1991	0.000	16:51_21/01/1991	0.200	11:51_06/02/1991	0.400
14:12_10/01/1991	0.000	16:52_21/01/1991	0.400	11:52_06/02/1991	0.000
14:13_10/01/1991	0.000	16:53_21/01/1991	0.400	11:53_06/02/1991	0.000
14:14_10/01/1991	0.000	16:54_21/01/1991	0.600	11:54_06/02/1991	0.000
14:15_10/01/1991	0.200	16:55_21/01/1991	0.600		
14:16_10/01/1991	0.000	16:56_21/01/1991	0.800		
14:17_10/01/1991	0.200	16:57_21/01/1991	1.400		
14:18_10/01/1991	0.400	16:58_21/01/1991	1.400		
14:19_10/01/1991	0.000	16:59_21/01/1991	1.400		
14:20_10/01/1991	0.000	17:00_21/01/1991	1.600		
14:21_10/01/1991	0.000	17:01_21/01/1991	1.600		
14:22_10/01/1991	0.000	17:02_21/01/1991	1.600		
14:23_10/01/1991	0.000	17:03_21/01/1991	1.400		
14:24_10/01/1991	0.200	17:04_21/01/1991	1.400		
14:25_10/01/1991	0.000	17:05_21/01/1991	1.000		
14:26_10/01/1991	0.400	17:06_21/01/1991	1.200		
14:27_10/01/1991	0.600	17:07_21/01/1991	1.200		
14:28_10/01/1991	1.000	17:08_21/01/1991	1.000		
14:29_10/01/1991	0.600	17:09_21/01/1991	1.000		
14:30_10/01/1991	0.600	17:10_21/01/1991	0.800		
14:31_10/01/1991	0.800	17:11_21/01/1991	0.800		
14:32_10/01/1991	0.400	17:12_21/01/1991	0.800		
14:33_10/01/1991	0.600	17:13_21/01/1991	0.800		
14:34_10/01/1991	0.200	17:14_21/01/1991	0.600		
14:35_10/01/1991	0.200	17:15_21/01/1991	0.800		
14:36_10/01/1991	0.400	17:16_21/01/1991	0.800		
14:37_10/01/1991	0.400	17:17_21/01/1991	0.800		
14:38_10/01/1991	0.200	17:18_21/01/1991	0.600		
14:39_10/01/1991	0.800	17:19_21/01/1991	0.200		
14:40_10/01/1991	1.000	17:20_21/01/1991	0.400		
14:41_10/01/1991	0.800	17:21_21/01/1991	0.200		
14:42_10/01/1991	0.800	17:22_21/01/1991	0.200		
14:43_10/01/1991	0.600	17:23_21/01/1991	0.200		
14:44_10/01/1991	0.400	17:24_21/01/1991	0.000		
14:45_10/01/1991	0.400	17:25_21/01/1991	0.200		
14:46_10/01/1991	0.600	17:26_21/01/1991	0.000		
14:47_10/01/1991	0.200	17:27_21/01/1991	0.000		

time	rainfall	time	rainfall
14:48_10/01/1991	0.000	17:28_21/01/1991	0.000
14:49_10/01/1991	0.200	17:29_21/01/1991	0.200
14:50_10/01/1991	0.400	17:30_21/01/1991	0.000
14:51_10/01/1991	0.200	17:31_21/01/1991	0.000
14:52_10/01/1991	0.200	17:32_21/01/1991	0.200
14:53_10/01/1991	0.400	17:33_21/01/1991	0.200
14:54_10/01/1991	0.200	17:34_21/01/1991	0.000
14:55_10/01/1991	0.200	17:35_21/01/1991	0.000
14:56_10/01/1991	0.200	17:36_21/01/1991	0.200
14:57_10/01/1991	0.200	17:37_21/01/1991	0.000
14:58_10/01/1991	0.000	17:38_21/01/1991	0.200
14:59_10/01/1991	0.200	17:39_21/01/1991	0.000
15:00_10/01/1991	0.200	17:40_21/01/1991	0.000
15:01_10/01/1991	0.000	17:41_21/01/1991	0.200
15:02_10/01/1991	0.200	17:42_21/01/1991	0.000
15:03_10/01/1991	0.000	17:43_21/01/1991	0.000
15:04_10/01/1991	0.200	17:44_21/01/1991	0.200
15:05_10/01/1991	0.000	17:45_21/01/1991	0.200
15:06_10/01/1991	0.200	17:46_21/01/1991	0.000
15:07_10/01/1991	0.200	17:47_21/01/1991	0.200
15:08_10/01/1991	0.200	17:48_21/01/1991	0.000
15:09_10/01/1991	0.200	17:49_21/01/1991	0.200
15:10_10/01/1991	0.000	17:50_21/01/1991	0.200
15:11_10/01/1991	0.200	17:51_21/01/1991	0.000
15:12_10/01/1991	0.000	17:52_21/01/1991	0.200
15:13_10/01/1991	0.000	17:53_21/01/1991	0.200
15:14_10/01/1991	0.000	17:54_21/01/1991	0.000
15:15_10/01/1991	0.000	17:55_21/01/1991	0.200
15:16_10/01/1991	0.000	17:56_21/01/1991	0.000
15:17_10/01/1991	0.000	17:57_21/01/1991	0.200
15:18_10/01/1991	0.000	17:58_21/01/1991	0.000
15:19_10/01/1991	0.200	17:59_21/01/1991	0.000
15:20_10/01/1991	0.000	18:00_21/01/1991	0.200
15:21_10/01/1991	0.200	18:01_21/01/1991	0.000
15:22_10/01/1991	0.200	18:02_21/01/1991	0.000
15:23_10/01/1991	0.200	18:03_21/01/1991	0.000
15:24_10/01/1991	0.000	18:04_21/01/1991	0.200
15:25_10/01/1991	0.200	18:05_21/01/1991	0.000
15:26_10/01/1991	0.200	18:06_21/01/1991	0.000
15:27_10/01/1991	0.200	18:07_21/01/1991	0.000

time	rainfall	time	rainfall
15:28_10/01/1991	0.000	18:08_21/01/1991	0.000
15:29_10/01/1991	0.200	18:09_21/01/1991	0.000
15:30_10/01/1991	0.000	18:10_21/01/1991	0.000
15:31_10/01/1991	0.400	18:11_21/01/1991	0.000
15:32_10/01/1991	0.000	18:12_21/01/1991	0.000
15:33_10/01/1991	0.000	18:13_21/01/1991	0.000
15:34_10/01/1991	0.000	18:14_21/01/1991	0.200
15:35_10/01/1991	0.000	18:15_21/01/1991	0.000
15:36_10/01/1991	0.000		
15:37_10/01/1991	0.200		
15:38_10/01/1991	0.000		
15:39_10/01/1991	0.000		
15:40_10/01/1991	0.200		
15:41_10/01/1991	0.000		
15:42_10/01/1991	0.000		
15:43_10/01/1991	0.000		
15:44_10/01/1991	0.000		
15:45_10/01/1991	0.000		
14:35_16/02/1991	0.000		
14:36_16/02/1991	0.000		
14:37_16/02/1991	0.000		
14:38_16/02/1991	0.000		
14:39_16/02/1991	0.000		
14:40_16/02/1991	0.000		
14:41_16/02/1991	0.000		
14:42_16/02/1991	0.200		
14:43_16/02/1991	1.600		
14:44_16/02/1991	1.600		
14:45_16/02/1991	1.600		
14:46_16/02/1991	1.800		
14:47_16/02/1991	1.400		
14:48_16/02/1991	1.000		
14:49_16/02/1991	1.200		
14:50_16/02/1991	1.200		
14:51_16/02/1991	1.200		
14:52_16/02/1991	1.200		
14:53_16/02/1991	1.200		
14:54_16/02/1991	0.800		
14:55_16/02/1991	0.600		
14:56_16/02/1991	0.600		

time	rainfall
14:57_16/02/1991	0.600
14:58_16/02/1991	0.200
14:59_16/02/1991	0.400
15:00_16/02/1991	0.400
15:01_16/02/1991	0.200
15:02_16/02/1991	0.200
15:03_16/02/1991	0.000
15:04_16/02/1991	0.200
15:05_16/02/1991	0.000
15:06_16/02/1991	0.000
15:07_16/02/1991	0.200
15:08_16/02/1991	0.000
15:09_16/02/1991	0.000
15:10_16/02/1991	0.200
15:11_16/02/1991	0.000
15:12_16/02/1991	0.000
15:13_16/02/1991	0.000
15:14_16/02/1991	0.000
15:15_16/02/1991	0.000
15:16_16/02/1991	0.000
15:17_16/02/1991	0.000
15:18_16/02/1991	0.000
15:19_16/02/1991	0.200
15:20_16/02/1991	0.000
15:21_16/02/1991	0.000
15:22_16/02/1991	0.000
15:23_16/02/1991	0.000
15:24_16/02/1991	0.000
15:25_16/02/1991	0.000

Batter pluviograph

time	rainfall	time	rainfall
11:40_06/02/1991	0.000	13:30_22/02/1991	0.000
11:41_06/02/1991	0.000	13:31_22/02/1991	0.000
11:42_06/02/1991	0.000	13:32_22/02/1991	0.000
11:43_06/02/1991	0.200	13:33_22/02/1991	0.000
11:44_06/02/1991	0.400	13:34_22/02/1991	1.400
11:45_06/02/1991	1.600	13:35_22/02/1991	2.000
11:46_06/02/1991	1.200	13:36_22/02/1991	2.200
11:47_06/02/1991	0.800	13:37_22/02/1991	2.400
11:48_06/02/1991	0.800	13:38_22/02/1991	2.200
11:49_06/02/1991	0.800	13:39_22/02/1991	1.200
11:50_06/02/1991	0.000	13:40_22/02/1991	0.000
11:51_06/02/1991	0.000	13:41_22/02/1991	0.000
11:52_06/02/1991	0.000	13:42_22/02/1991	0.000
11:53_06/02/1991	0.000	13:43_22/02/1991	0.000
11:54_06/02/1991	0.000	13:44_22/02/1991	0.000
11:55_06/02/1991	0.000	13:45_22/02/1991	0.000
11:56_06/02/1991	0.000	13:46_22/02/1991	0.000
11:57_06/02/1991	0.200	13:47_22/02/1991	0.000
11:58_06/02/1991	0.000	13:48_22/02/1991	0.000
11:59_06/02/1991	0.000	13:49_22/02/1991	0.000
12:00_06/02/1991	0.000	13:50_22/02/1991	0.000
12:01_06/02/1991	0.000	13:51_22/02/1991	0.000
12:02_06/02/1991	0.000	13:52_22/02/1991	0.000
12:03_06/02/1991	0.000	13:53_22/02/1991	0.000
12:04_06/02/1991	0.000	13:54_22/02/1991	0.000
12:05_06/02/1991	0.000	13:55_22/02/1991	0.000
12:06_06/02/1991	0.000	13:56_22/02/1991	0.000
12:07_06/02/1991	0.000	13:57_22/02/1991	0.000
12:08_06/02/1991	0.000	13:58_22/02/1991	0.000
12:09_06/02/1991	0.000	13:59_22/02/1991	0.000
12:10_06/02/1991	0.000	14:00_22/02/1991	0.000
		14:01_22/02/1991	0.200
		14:02_22/02/1991	0.000
		14:03_22/02/1991	0.000
		14:04_22/02/1991	0.000
		14:05_22/02/1991	0.000
		14:06_22/02/1991	0.200
		14:07_22/02/1991	0.200
		14:08_22/02/1991	0.200

time	rainfall	time	rainfall
		14:09_22/02/1991	0.000
		14:10_22/02/1991	0.000
		14:11_22/02/1991	0.000
		14:12_22/02/1991	0.200
		14:13_22/02/1991	0.000
		14:14_22/02/1991	0.000
		14:15_22/02/1991	0.000

The data below are the measured runoffs for the storms used in the calibration of the hydrology model. Times are in the format 24 hour time and date, and runoff litres/second.

CWT1		CWT1		CWT2	
time	**runoff**	**time**	**runoff**	**time**	**runoff**
14:25_10/01/91	0.0000	14:43_16/02/91	0.0000	20:45_07/01/1991	0.000
14:26_10/01/91	0.0907	14:44_16/02/91	0.0025	20:46_07/01/1991	0.000
14:27_10/01/91	0.1643	14:45_16/02/91	0.0102	20:47_07/01/1991	0.000
14:28_10/01/91	0.4740	14:46_16/02/91	0.0178	20:48_07/01/1991	0.000
14:29_10/01/91	1.1145	14:47_16/02/91	0.0254	20:49_07/01/1991	0.004
14:30_10/01/91	1.5001	14:48_16/02/91	0.0806	20:50_07/01/1991	0.136
14:31_10/01/91	1.4792	14:49_16/02/91	0.2604	20:51_07/01/1991	0.597
14:32_10/01/91	1.4862	14:50_16/02/91	0.5208	20:52_07/01/1991	0.610
14:33_10/01/91	1.4184	14:51_16/02/91	0.8362	20:53_07/01/1991	0.525
14:34_10/01/91	1.2397	14:52_16/02/91	1.1248	20:54_07/01/1991	0.410
14:35_10/01/91	0.9634	14:53_16/02/91	1.3419	20:55_07/01/1991	0.295
14:36_10/01/91	0.7687	14:54_16/02/91	1.5538	20:56_07/01/1991	0.210
14:37_10/01/91	0.7565	14:55_16/02/91	1.6263	20:57_07/01/1991	0.126
14:38_10/01/91	0.7525	14:56_16/02/91	1.6388	20:58_07/01/1991	0.091
14:39_10/01/91	0.7152	14:57_16/02/91	1.6015	20:59_07/01/1991	0.072
14:40_10/01/91	1.0053	14:58_16/02/91	1.5400	21:00_07/01/1991	0.081
14:41_10/01/91	1.4629	14:59_16/02/91	1.3471	21:01_07/01/1991	0.078
14:42_10/01/91	1.6801	15:00_16/02/91	1.0688	21:02_07/01/1991	0.092
14:43_10/01/91	1.8360	15:01_16/02/91	0.9281	21:03_07/01/1991	0.124
14:44_10/01/91	1.7770	15:02_16/02/91	0.7650	21:04_07/01/1991	0.238
14:45_10/01/91	1.4935	15:03_16/02/91	0.6016	21:05_07/01/1991	0.418
14:46_10/01/91	1.2131	15:04_16/02/91	0.3978	21:06_07/01/1991	0.528
14:47_10/01/91	1.1122	15:05_16/02/91	0.2686	21:07_07/01/1991	0.510
14:48_10/01/91	0.8143	15:06_16/02/91	0.1931	21:08_07/01/1991	0.492
14:49_10/01/91	0.5728	15:07_16/02/91	0.1558	21:09_07/01/1991	0.473
14:50_10/01/91	0.4965	15:08_16/02/91	0.1296	21:10_07/01/1991	0.451
14:51_10/01/91	0.5113	15:09_16/02/91	0.1034	21:11_07/01/1991	0.314
14:52_10/01/91	0.4761	15:10_16/02/91	0.0772	21:12_07/01/1991	0.211
14:53_10/01/91	0.4559	15:11_16/02/91	0.0572	21:13_07/01/1991	0.160
14:54_10/01/91	0.4701	15:12_16/02/91	0.0496	21:14_07/01/1991	0.120
14:55_10/01/91	0.4692	15:13_16/02/91	0.0420	21:15_07/01/1991	0.091
14:56_10/01/91	0.4453	15:14_16/02/91	0.0345	21:16_07/01/1991	0.079
14:57_10/01/91	0.4214	15:15_16/02/91	0.0269	21:17_07/01/1991	0.066
14:58_10/01/91	0.3976	15:16_16/02/91	0.0193	21:18_07/01/1991	0.054
14:59_10/01/91	0.3737	15:17_16/02/91	0.0117	21:19_07/01/1991	0.042
15:00_10/01/91	0.3498	15:18_16/02/91	0.0064	21:20_07/01/1991	0.030
15:01_10/01/91	0.3259	15:19_16/02/91	0.0057	21:21_07/01/1991	0.017

time	runoff	time	runoff	time	runoff
15:02_10/01/91	0.3021	15:20_16/02/91	0.0051	21:22_07/01/1991	0.006
15:03_10/01/91	0.2782	15:21_16/02/91	0.0044	21:23_07/01/1991	0.005
15:04_10/01/91	0.2543	15:22_16/02/91	0.0037	21:24_07/01/1991	0.004
15:05_10/01/91	0.2305	15:23_16/02/91	0.0031	21:25_07/01/1991	0.004
15:06_10/01/91	0.2066	15:24_16/02/91	0.0024	21:26_07/01/1991	0.003
15:07_10/01/91	0.1827	15:25_16/02/91	0.0018	21:27_07/01/1991	0.003
15:08_10/01/91	0.1886	15:26_16/02/91	0.0011	21:28_07/01/1991	0.002
15:09_10/01/91	0.2309	15:27_16/02/91	0.0004	21:29_07/01/1991	0.002
15:10_10/01/91	0.2489	15:28_16/02/91	0.0000	21:30_07/01/1991	0.001
15:11_10/01/91	0.2449	15:29_16/02/91	0.0000		
15:12_10/01/91	0.2228				
15:13_10/01/91	0.1829				
15:14_10/01/91	0.1430				
15:15_10/01/91	0.1032				
15:16_10/01/91	0.0761				
15:17_10/01/91	0.0684				
15:18_10/01/91	0.0606				
15:19_10/01/91	0.0529				
15:20_10/01/91	0.0451				
15:21_10/01/91	0.0514				
15:22_10/01/91	0.0787				
15:23_10/01/91	0.1061				
15:24_10/01/91	0.1334				
15:25_10/01/91	0.1607				
15:26_10/01/91	0.1881				
15:27_10/01/91	0.2154				
15:28_10/01/91	0.2427				
15:29_10/01/91	0.2469				
15:30_10/01/91	0.2112				
15:31_10/01/91	0.2024				
15:32_10/01/91	0.2248				
15:33_10/01/91	0.2020				
15:34_10/01/91	0.1595				
15:35_10/01/91	0.1197				
15:36_10/01/91	0.0891				
15:37_10/01/91	0.0732				
15:38_10/01/91	0.0680				
15:39_10/01/91	0.0629				
15:40_10/01/91	0.0577				
15:41_10/01/91	0.0525				
15:42_10/01/91	0.0473				

time	runoff
15:43_10/01/91	0.0421
15:44_10/01/91	0.0369
15:45_10/01/91	0.0317
15:46_10/01/91	0.0265
15:47_10/01/91	0.0214
15:48_10/01/91	0.0162
15:49_10/01/91	0.0110
15:50_10/01/91	0.0058
15:51_10/01/91	0.0025
15:52_10/01/91	0.0019
15:53_10/01/91	0.0014
15:54_10/01/91	0.0009
15:55_10/01/91	0.0003
15:56_10/01/91	0.0000
15:57_10/01/91	0.0000

CWT2		CWT2		CWT3	
time	**runoff**	**time**	**runoff**	**time**	**runoff**
14:20_10/01/1991	0.000	16:50_21/01/1991	0.000	11:42_06/02/1991	0.000
14:21_10/01/1991	0.000	16:51_21/01/1991	0.000	11:43_06/02/1991	0.000
14:22_10/01/1991	0.000	16:52_21/01/1991	0.000	11:44_06/02/1991	0.000
14:23_10/01/1991	0.000	16:53_21/01/1991	0.000	11:45_06/02/1991	0.001
14:24_10/01/1991	0.000	16:54_21/01/1991	0.000	11:46_06/02/1991	0.080
14:25_10/01/1991	0.000	16:55_21/01/1991	0.000	11:47_06/02/1991	0.202
14:26_10/01/1991	0.000	16:56_21/01/1991	0.000	11:48_06/02/1991	0.293
14:27_10/01/1991	0.000	16:57_21/01/1991	0.000	11:49_06/02/1991	0.350
14:28_10/01/1991	0.142	16:58_21/01/1991	0.261	11:50_06/02/1991	0.345
14:29_10/01/1991	0.397	16:59_21/01/1991	1.159	11:51_06/02/1991	0.313
14:30_10/01/1991	0.628	17:00_21/01/1991	1.924	11:52_06/02/1991	0.282
14:31_10/01/1991	0.707	17:01_21/01/1991	2.230	11:53_06/02/1991	0.250
14:32_10/01/1991	0.735	17:02_21/01/1991	2.290	11:54_06/02/1991	0.218
14:33_10/01/1991	0.706	17:03_21/01/1991	2.334	11:55_06/02/1991	0.187
14:34_10/01/1991	0.632	17:04_21/01/1991	2.335	11:56_06/02/1991	0.155
14:35_10/01/1991	0.510	17:05_21/01/1991	2.126	11:57_06/02/1991	0.123
14:36_10/01/1991	0.428	17:06_21/01/1991	1.782	11:58_06/02/1991	0.102
14:37_10/01/1991	0.411	17:07_21/01/1991	1.905	11:59_06/02/1991	0.085
14:38_10/01/1991	0.391	17:08_21/01/1991	1.775	12:00_06/02/1991	0.069
14:39_10/01/1991	0.386	17:09_21/01/1991	1.555	12:01_06/02/1991	0.052
14:40_10/01/1991	0.528	17:10_21/01/1991	1.349	12:02_06/02/1991	0.036
14:41_10/01/1991	0.761	17:11_21/01/1991	1.279	12:03_06/02/1991	0.027

time	runoff	time	runoff	time	runoff
14:42_10/01/1991	0.936	17:12_21/01/1991	1.141	12:04_06/02/1991	0.022
14:43_10/01/1991	1.020	17:13_21/01/1991	1.015	12:05_06/02/1991	0.017
14:44_10/01/1991	0.946	17:14_21/01/1991	0.792	12:06_06/02/1991	0.012
14:45_10/01/1991	0.760	17:15_21/01/1991	0.666	12:07_06/02/1991	0.007
14:46_10/01/1991	0.661	17:16_21/01/1991	0.762	12:08_06/02/1991	0.002
14:47_10/01/1991	0.601	17:17_21/01/1991	0.743	12:09_06/02/1991	0.000
14:48_10/01/1991	0.428	17:18_21/01/1991	0.742	12:10_06/02/1991	0.000
14:49_10/01/1991	0.315	17:19_21/01/1991	0.591		
14:50_10/01/1991	0.244	17:20_21/01/1991	0.494		
14:51_10/01/1991	0.204	17:21_21/01/1991	0.399		
14:52_10/01/1991	0.189	17:22_21/01/1991	0.304		
14:53_10/01/1991	0.188	17:23_21/01/1991	0.208		
14:54_10/01/1991	0.190	17:24_21/01/1991	0.113		
14:55_10/01/1991	0.182	17:25_21/01/1991	0.079		
14:56_10/01/1991	0.174	17:26_21/01/1991	0.056		
14:57_10/01/1991	0.166	17:27_21/01/1991	0.034		
14:58_10/01/1991	0.159	17:28_21/01/1991	0.033		
14:59_10/01/1991	0.140	17:29_21/01/1991	0.032		
15:00_10/01/1991	0.114	17:30_21/01/1991	0.031		
15:01_10/01/1991	0.101	17:31_21/01/1991	0.029		
15:02_10/01/1991	0.090	17:32_21/01/1991	0.028		
15:03_10/01/1991	0.085	17:33_21/01/1991	0.027		
15:04_10/01/1991	0.081	17:34_21/01/1991	0.026		
15:05_10/01/1991	0.076	17:35_21/01/1991	0.025		
15:06_10/01/1991	0.071				
15:07_10/01/1991	0.067				
15:08_10/01/1991	0.062				
15:09_10/01/1991	0.064				
15:10_10/01/1991	0.072				
15:11_10/01/1991	0.067				
15:12_10/01/1991	0.056				
15:13_10/01/1991	0.048				
15:14_10/01/1991	0.040				
15:15_10/01/1991	0.032				
15:16_10/01/1991	0.024				
15:17_10/01/1991	0.016				
15:18_10/01/1991	0.008				
15:19_10/01/1991	0.006				
15:20_10/01/1991	0.012				
15:21_10/01/1991	0.019				
15:22_10/01/1991	0.025				

time	runoff
15:23_10/01/1991	0.032
15:24_10/01/1991	0.039
15:25_10/01/1991	0.045
15:26_10/01/1991	0.057
15:27_10/01/1991	0.075
15:28_10/01/1991	0.084
15:29_10/01/1991	0.078
15:30_10/01/1991	0.070
15:31_10/01/1991	0.062
15:32_10/01/1991	0.053
15:33_10/01/1991	0.045
15:34_10/01/1991	0.037
15:35_10/01/1991	0.028
15:36_10/01/1991	0.020
15:37_10/01/1991	0.015
15:38_10/01/1991	0.013
15:39_10/01/1991	0.012
15:40_10/01/1991	0.011
15:41_10/01/1991	0.010
15:42_10/01/1991	0.009
15:43_10/01/1991	0.008
15:44_10/01/1991	0.007
15:45_10/01/1991	0.006
15:46_10/01/1991	0.005
15:47_10/01/1991	0.004
15:48_10/01/1991	0.003
15:49_10/01/1991	0.002
15:50_10/01/1991	0.001

CWT3		COUT		COUT	
time	**runoff**	**time**	**runoff**	**time**	**runoff**
14:40_16/02/1991	0.000	20:50_07/01/1991	0.207	07:55_10/01/1991	0.000
14:41_16/02/1991	0.000	20:51_07/01/1991	3.262	07:56_10/01/1991	0.000
14:42_16/02/1991	0.000	20:52_07/01/1991	7.569	07:57_10/01/1991	0.000
14:43_16/02/1991	0.000	20:53_07/01/1991	11.859	07:58_10/01/1991	0.013
14:44_16/02/1991	0.000	20:54_07/01/1991	13.740	07:59_10/01/1991	0.944
14:45_16/02/1991	0.000	20:55_07/01/1991	13.740	08:00_10/01/1991	3.516
14:46_16/02/1991	0.021	20:56_07/01/1991	11.859	08:01_10/01/1991	6.513
14:47_16/02/1991	0.134	20:57_07/01/1991	9.499	08:02_10/01/1991	8.317
14:48_16/02/1991	0.300	20:58_07/01/1991	6.856	08:03_10/01/1991	9.908

time	runoff	time	runoff	time	runoff
14:49_16/02/1991	0.351	20:59_07/01/1991	5.214	08:04_10/01/1991	10.117
14:50_16/02/1991	0.342	21:00_07/01/1991	3.780	08:05_10/01/1991	10.540
14:51_16/02/1991	0.311	21:01_07/01/1991	3.780	08:06_10/01/1991	14.227
14:52_16/02/1991	0.307	21:02_07/01/1991	3.015	08:07_10/01/1991	15.234
14:53_16/02/1991	0.345	21:03_07/01/1991	3.516	08:08_10/01/1991	15.234
14:54_16/02/1991	0.325	21:04_07/01/1991	5.214	08:09_10/01/1991	15.234
14:55_16/02/1991	0.306	21:05_07/01/1991	7.208	08:10_10/01/1991	13.739
14:56_16/02/1991	0.287	21:06_07/01/1991	9.499	08:11_10/01/1991	10.117
14:57_16/02/1991	0.265	21:07_07/01/1991	13.256	08:12_10/01/1991	12.782
14:58_16/02/1991	0.238	21:08_07/01/1991	13.740	08:13_10/01/1991	14.727
14:59_16/02/1991	0.211	21:09_07/01/1991	13.740	08:14_10/01/1991	15.234
15:00_16/02/1991	0.184	21:10_07/01/1991	13.740	08:15_10/01/1991	15.234
15:01_16/02/1991	0.157	21:11_07/01/1991	13.256	08:16_10/01/1991	15.234
15:02_16/02/1991	0.131	21:12_07/01/1991	10.970	08:17_10/01/1991	12.316
15:03_16/02/1991	0.109	21:13_07/01/1991	9.096	08:18_10/01/1991	9.498
15:04_16/02/1991	0.097	21:14_07/01/1991	7.938	08:19_10/01/1991	7.569
15:05_16/02/1991	0.085	21:15_07/01/1991	6.856	08:20_10/01/1991	6.513
15:06_16/02/1991	0.074	21:16_07/01/1991	5.214	08:21_10/01/1991	5.527
15:07_16/02/1991	0.062	21:17_07/01/1991	4.329	08:22_10/01/1991	6.175
15:08_16/02/1991	0.050	21:18_07/01/1991	3.015	08:23_10/01/1991	5.214
15:09_16/02/1991	0.041	21:19_07/01/1991	2.325	08:24_10/01/1991	4.615
15:10_16/02/1991	0.035	21:20_07/01/1991	2.219	08:25_10/01/1991	4.051
15:11_16/02/1991	0.030	21:21_07/01/1991	1.809	08:26_10/01/1991	3.516
15:12_16/02/1991	0.024	21:22_07/01/1991	1.433	08:27_10/01/1991	4.329
15:13_16/02/1991	0.019	21:23_07/01/1991	1.173	08:28_10/01/1991	5.214
15:14_16/02/1991	0.013	21:24_07/01/1991	0.944	08:29_10/01/1991	6.175
15:15_16/02/1991	0.009	21:25_07/01/1991	0.744	08:30_10/01/1991	6.855
15:16_16/02/1991	0.009	21:26_07/01/1991	0.426	08:31_10/01/1991	7.569
15:17_16/02/1991	0.008	21:27_07/01/1991	0.305	08:32_10/01/1991	6.855
15:18_16/02/1991	0.007	21:28_07/01/1991	0.207	08:33_10/01/1991	6.855
15:19_16/02/1991	0.007	21:29_07/01/1991	0.207	08:34_10/01/1991	6.855
15:20_16/02/1991	0.006	21:30_07/01/1991	0.131	08:35_10/01/1991	6.175
15:21_16/02/1991	0.005			08:36_10/01/1991	5.214
15:22_16/02/1991	0.005			08:37_10/01/1991	4.329
15:23_16/02/1991	0.004			08:38_10/01/1991	3.516
15:24_16/02/1991	0.003			08:39_10/01/1991	3.015
15:25_16/02/1991	0.003			08:40_10/01/1991	2.325
15:26_16/02/1991	0.002			08:41_10/01/1991	1.809
15:27_16/02/1991	0.001			08:42_10/01/1991	1.614
15:28_16/02/1991	0.000			08:43_10/01/1991	1.433
15:29_16/02/1991	0.000			08:44_10/01/1991	1.173

time	runoff	time	runoff	time	runoff
15:30_16/02/1991	0.000			08:45_10/01/1991	0.744
				08:46_10/01/1991	0.744
				08:47_10/01/1991	0.305
				08:48_10/01/1991	0.207
				08:49_10/01/1991	0.131
				08:50_10/01/1991	0.131
				08:51_10/01/1991	0.075
				08:52_10/01/1991	0.075
				08:53_10/01/1991	0.037
				08:54_10/01/1991	0.013
				08:55_10/01/1991	0.013

CRT1		BRT2		BRT2	
time	**runoff**	**time**	**runoff**	**time**	**runoff**
20:40_07/01/1991	0.000	11:40_06/02/1991	0.000	13:30_22/02/1991	0.000
20:41_07/01/1991	0.000	11:41_06/02/1991	0.000	13:31_22/02/1991	0.000
20:42_07/01/1991	0.000	11:42_06/02/1991	0.000	13:32_22/02/1991	0.000
20:43_07/01/1991	0.000	11:43_06/02/1991	0.000	13:33_22/02/1991	0.000
20:44_07/01/1991	0.000	11:44_06/02/1991	0.000	13:34_22/02/1991	0.000
20:45_07/01/1991	0.000	11:45_06/02/1991	0.000	13:35_22/02/1991	0.618
20:46_07/01/1991	0.000	11:46_06/02/1991	0.011	13:36_22/02/1991	3.174
20:47_07/01/1991	0.000	11:47_06/02/1991	0.638	13:37_22/02/1991	4.240
20:48_07/01/1991	0.000	11:48_06/02/1991	1.112	13:38_22/02/1991	4.334
20:49_07/01/1991	0.000	11:49_06/02/1991	1.317	13:39_22/02/1991	4.334
20:50_07/01/1991	0.046	11:50_06/02/1991	1.477	13:40_22/02/1991	4.024
20:51_07/01/1991	1.464	11:51_06/02/1991	1.428	13:41_22/02/1991	3.308
20:52_07/01/1991	3.546	11:52_06/02/1991	1.092	13:42_22/02/1991	2.697
20:53_07/01/1991	3.798	11:53_06/02/1991	0.629	13:43_22/02/1991	2.301
20:54_07/01/1991	3.094	11:54_06/02/1991	0.440	13:44_22/02/1991	1.793
20:55_07/01/1991	2.044	11:55_06/02/1991	0.325	13:45_22/02/1991	1.207
20:56_07/01/1991	1.377	11:56_06/02/1991	0.218	13:46_22/02/1991	0.687
20:57_07/01/1991	0.898	11:57_06/02/1991	0.133	13:47_22/02/1991	0.420
20:58_07/01/1991	0.560	11:58_06/02/1991	0.076	13:48_22/02/1991	0.240
20:59_07/01/1991	0.411	11:59_06/02/1991	0.041	13:49_22/02/1991	0.143
21:00_07/01/1991	0.337	12:00_06/02/1991	0.016	13:50_22/02/1991	0.058
21:01_07/01/1991	0.302	12:01_06/02/1991	0.006	13:51_22/02/1991	0.030
21:02_07/01/1991	0.344	12:02_06/02/1991	0.003	13:52_22/02/1991	0.026
21:03_07/01/1991	0.513	12:03_06/02/1991	0.001	13:53_22/02/1991	0.023
21:04_07/01/1991	0.885	12:04_06/02/1991	0.000	13:54_22/02/1991	0.020
21:05_07/01/1991	1.654	12:05_06/02/1991	0.000	13:55_22/02/1991	0.018

time	runoff	time	runoff	time	runoff
21:06_07/01/1991	2.830	12:06_06/02/1991	0.000	13:56_22/02/1991	0.015
21:07_07/01/1991	3.439	12:07_06/02/1991	0.000	13:57_22/02/1991	0.012
21:08_07/01/1991	3.274	12:08_06/02/1991	0.000	13:58_22/02/1991	0.009
21:09_07/01/1991	2.884	12:09_06/02/1991	0.000	13:59_22/02/1991	0.006
21:10_07/01/1991	2.587	12:10_06/02/1991	0.000	14:00_22/02/1991	0.003
21:11_07/01/1991	2.124	12:11_06/02/1991	0.000	14:01_22/02/1991	0.001
21:12_07/01/1991	1.667	12:12_06/02/1991	0.000	14:02_22/02/1991	0.000
21:13_07/01/1991	1.271	12:13_06/02/1991	0.000	14:03_22/02/1991	0.000
21:14_07/01/1991	0.853	12:14_06/02/1991	0.000	14:04_22/02/1991	0.000
21:15_07/01/1991	0.660	12:15_06/02/1991	0.000	14:05_22/02/1991	0.000
21:16_07/01/1991	0.496				
21:17_07/01/1991	0.334				
21:18_07/01/1991	0.211				
21:19_07/01/1991	0.120				
21:20_07/01/1991	0.092				
21:21_07/01/1991	0.064				
21:22_07/01/1991	0.036				
21:23_07/01/1991	0.009				
21:24_07/01/1991	0.007				
21:25_07/01/1991	0.004				
21:26_07/01/1991	0.002				
21:27_07/01/1991	0.000				
21:28_07/01/1991	0.000				
21:29_07/01/1991	0.000				
21:30_07/01/1991	0.000				

B.2 Simulated rainfall

The data below are the rainfall data for the comparison of the hydrology model with the data from the rainfall simulation experiments (fig 2.16), plot 4 run2 from data set B1RF2QSS. Time is measured in minutes from the start of the rainfall. Rainfall measurements are in cumulative mm from the start of the experiment (the rainfall used in the comparison was the average of the two pluviographs measurements). Runoff measurements are in litres/second.

Time	Pluvio 1	Pluvio 2	Time	q
8:20:30	0	0	8:29:30	0.11500
8:20:40	0.2	0.2	8:30:00	0.49950
8:20:50	0.4	0.2	8:30:30	0.55280
8:21:00	0.6	0.4	8:31:00	0.55280
8:21:10	1	0.6	8:32:00	0.97120
8:21:20	1.2	0.8	8:34:00	0.90670
8:21:30	1.4	1	8:35:00	0.97120
8:21:40	1.8	1.2	8.36:00	0.84210
8:21:50	2.2	1.4	8.38:00	0.84210
8:22:00	2.4	1.6	8.40:00	0.90670
8:22:10	2.8	1.8	8.42:00	0.97120
8:22:20	3.2	2	8.45:00	0.84210
8:22:30	3.4	2.2	8.50:00	0.97120
8:22:40	3.8	2.4	8.55:00	0.90670
8:22:50	4.2	2.6	9.00:00	0.90670
8:23:00	4.4	2.8	9.05:00	0.84210
8:23:10	4.8	3	9.15:00	0.84210
8:23:20	5	3.2	9.20:00	0.72030
8:23:30	5.4	3.6	9.24:30	0.72030
8:23:40	5.8	3.8	9.25:00	
8:23:50	6.2	4	9.25:30	0.49950
8:24:00	6.6	4.2	9.25:30	0.22880
8:24:10	7	4.4	9.26:00	0.11500
8:24:20	7.4	4.8	9.26:30	0.057200
8:24:30	7.6	5	9.27:00	0.057200
8:24:40	8	5.2	9.27:30	0.057200
8:24:50	8.2	5.4	9.28:00	0.057200
8:25:00	8.2	5.4	9.28:30	0.057200
8:25:10	8.6	5.6	9.29:00	0.0000
8:25:20	8.8	5.8		
8:25:30	9	6		
8:25:40	9.4	6.2		
8:25:50	9.8	6.4		
8:26:00	10.2	6.6		
8:26:10	10.4	7		
8:26:20	10.8	7.2		

Time	Pluvio 1	Pluvio 2	Time	q
8:26:30	11	7.4		
8:26:40	11.4	7.6		
8:26:50	11.6	7.8		
8:27:00	12	8		
8:27:10	12.6	8		
8:27:20	12.8	8.2		
8:27:30	13	8.4		
8:27:40	13.4	8.6		
8:27:50	13.4	8.8		
8:28:00	13.6	9		
8:28:10	13.8	9		
8:28:20	14	9.2		
8:28:30	14.2	9.4		
8:28:40	14.2	9.6		
8:28:50	14.6	9.8		
8:29:00	14.8	10		
8:29:10	15	10.2		
8:29:20	15.4	10.4		
8:29:30	15.6	10.6		
8:29:40	15.8	10.8		
8:29:50	16	11		
8:30:00	16.2	11.2		
8:30:10	16.2	11.4		
8:30:20	16.6	11.6		
8:30:30	16.8	12		
8:30:40	17	12.2		
8:30:50	17.2	12.4		
8:31:00	17.4	12.8		
8:31:10	17.6	13		
8:31:20	17.8	13.4		
8:31:30	18	13.6		
8:31:40	18.2	13.8		
8:31:50	18.6	14.2		
8:32:00	18.8	14.4		
8:32:10	19	14.8		
8:32:20	19.2	15		
8:32:30	19.4	15.2		
8:32:40	19.6	15.4		
8:32:50	19.8	15.6		
8:33:00	20	15.8		

Time	Pluvio 1	Pluvio 2	Time	q
8:33:10	20.2	16		
8:33:20	20.4	16		
8:33:30	20.8	16.2		
8:33:40	21	16.4		
8:33:50	21.4	16.6		
8:34:00	21.8	16.8		
8:34:10	22.4	16.8		
8:34:20	22.6	17		
8:34:30	22.8	17.2		
8:34:40	23	17.4		
8:34:50	23.2	17.6		
8:35:00	23.4	17.6		
8:35:10	23.8	17.8		
8:35:20	24.2	18		
8:35:30	24.6	18.2		
8:35:40	25	18.4		
8:35:50	25.2	18.6		
8:36:00	25.6	18.8		
8:36:10	25.8	19.2		
8:36:20	26.2	19.4		
8:36:30	26.6	19.6		
8:36:40	27	19.8		
8:36:50	27.4	20		
8:37:00	27.8	20.2		
8:37:10	28	20.4		
8:37:20	28.4	20.6		
8:37:30	28.8	20.8		
8:37:40	29.2	21.2		
8:37:50	29.4	21.4		
8:38:00	29.8	21.6		
8:38:10	30.2	22		
8:38:20	30.6	22.2		
8:38:30	30.8	22.4		
8:38:40	31.2	22.6		
8:38:50	31.4	22.8		
8:39:00	31.8	23		
8:39:10	32	23.2		
8:39:20	32.2	23.4		
8:39:30	32.4	23.6		
8:39:40	32.6	23.8		

Time	Pluvio 1	Pluvio 2	Time	q
8:39:50	33	23.8		
8:40:00	33.2	24		
8:40:10	33.6	24.2		
8:40:20	33.8	24.4		
8:40:30	34.2	24.6		
8:40:40	34.4	24.8		
8:40:50	34.6	25		
8:41:00	34.8	25.2		
8:41:10	35	25.2		
8:41:20	35.2	25.4		
8:41:30	35.6	25.6		
8:41:40	35.8	25.8		
8:41:50	36	26		
8:42:00	36.2	26		
8:42:10	36.6	26.2		
8:42:20	36.6	26.4		
8:42:30	36.8	26.6		
8:42:40	37	26.6		
8:42:50	37.4	26.8		
8:43:00	37.4	27		
8:43:10	37.8	27.2		
8:43:20	38	27.4		
8:43:30	38.4	27.6		
8:43:40	38.6	27.6		
8:43:50	38.6	27.8		
8:44:00	38.8	28		
8:44:10	39	28.2		
8:44:20	39	28.4		
8:44:30	39.4	28.4		
8:44:40	39.6	28.6		
8:44:50	40	28.8		
8:45:00	40.2	29		
8:45:10	40.4	29.2		
8:45:20	40.6	29.2		
8:45:30	40.6	29.4		
8:45:40	41	29.6		
8:45:50	41.2	29.8		
8:46:00	41.6	30		
8:46:10	41.8	30.2		
8:46:20	42.2	30.2		

Time	Pluvio 1	Pluvio 2	Time	q
8:46:30	42.4	30.4		
8:46:40	42.6	30.6		
8:46:50	42.8	30.8		
8:47:00	43	30.8		
8:47:10	43.4	31.2		
8:47:20	43.6	31.2		
8:47:30	43.8	31.6		
8:47:40	44.2	31.6		
8:47:50	44.4	31.8		
8:48:00	44.8	32		
8:48:10	45	32.2		
8:48:20	45.2	32.4		
8:48:30	45.4	32.4		
8:48:40	45.6	32.6		
8:48:50	45.8	32.8		
8:49:00	46.2	33		
8:49:10	46.4	33.2		
8:49:20	46.6	33.4		
8:49:30	46.8	33.6		
8:49:40	47	33.6		
8:49:50	47.2	33.8		
8:50:00	47.4	34		
8:50:10	47.6	34.4		
8:50:20	47.8	34.8		
8:50:30	48	35		
8:50:40	48.2	35.4		
8:50:50	48.6	35.6		
8:51:00	48.6	35.8		
8:51:10	49	36.2		
8:51:20	49	36.4		
8:51:30	49.2	36.6		
8:51:40	49.4	36.8		
8:51:50	49.6	37.2		
8:52:00	49.8	37.6		
8:52:10	50	37.8		
8:52:20	50.2	38		
8:52:30	50.4	38.2		
8:52:40	50.6	38.4		
8:52:50	50.6	38.6		
8:53:00	50.8	38.8		

Time	Pluvio 1	Pluvio 2	Time	q
8:53:10	51	39		
8:53:20	51.2	39.2		
8:53:30	51.4	39.4		
8:53:40	51.6	39.6		
8:53:50	51.8	39.8		
8:54:00	51.8	39.8		
8:54:10	52.2	40		
8:54:20	52.4	40.2		
8:54:30	52.8	40.4		
8:54:40	53	40.6		
8:54:50	53.4	40.8		
8:55:00	53.8	41		
8:55:10	54.2	41.2		
8:55:20	54.6	41.4		
8:55:30	55	41.6		
8:55:40	55.4	41.6		
8:55:50	55.8	41.8		
8:56:00	56.2	42		
8:56:10	56.6	42		
8:56:20	56.8	42.2		
8:56:30	57.2	42.4		
8:56:40	57.6	42.4		
8:56:50	57.8	42.8		
8:57:00	58.2	43		
8:57:10	58.4	43.2		
8:57:20	58.6	43.2		
8:57:30	59	43.4		
8:57:40	59.2	43.6		
8:57:50	59.4	43.8		
8:58:00	59.6	44		
8:58:10	59.6	44.2		
8:58:20	59.8	44.4		
8:58:30	59.8	44.6		
8:58:40	60	44.8		
8:58:50	60.2	45		
8:59:00	60.2	45.2		
8:59:10	60.4	45.4		
8:59:20	60.6	45.6		
8:59:30	60.8	45.8		
8:59:40	61	46		

Time	Pluvio 1	Pluvio 2	Time	q
8:59:50	61.4	46		
9:00:00	61.6	46.2		
9:00:10	62	46.4		
9:00:20	62.2	46.6		
9:00:30	62.4	46.8		
9:00:40	62.6	47		
9:00:50	62.8	47.2		
9:01:00	63	47.2		
9:01:10	63.4	47.4		
9:01:20	63.6	47.6		
9:01:30	63.8	47.8		
9:01:40	64.2	48		
9:01:50	64.4	48.2		
9:02:00	64.6	48.4		
9:02:10	64.8	48.6		
9:02:20	65.2	48.8		
9:02:30	65.6	48.8		
9:02:40	66	49		
9:02:50	66.2	49.2		
9:03:00	66.6	49.4		
9:03:10	67	49.6		
9:03:20	67.4	50		
9:03:30	67.8	50.2		
9:03:40	68.2	50.4		
9:03:50	68.4	50.6		
9:04:00	68.8	51		
9:04:10	69	51.2		
9:04:20	69.4	51.4		
9:04:30	69.8	51.6		
9:04:40	70.2	51.8		
9:04:50	70.6	52		
9:05:00	71	52.2		
9:05:10	71.4	52.4		
9:05:20	71.6	52.6		
9:05:30	71.8	52.8		
9:05:40	72.2	53		
9:05:50	72.2	53.2		
9:06:00	72.4	53.2		
9:06:10	72.6	53.4		
9:06:20	72.6	53.8		

Time	Pluvio 1	Pluvio 2	Time	q
9:06:30	72.8	54		
9:06:40	73	54		
9:06:50	73.2	54.2		
9:07:00	73.4	54.4		
9:07:10	73.6	54.6		
9:07:20	73.8	54.8		
9:07:30	74.2	55		
9:07:40	74.6	55.2		
9:07:50	75	55.2		
9:08:00	75.4	55.4		
9:08:10	75.8	55.4		
9:08:20	76.2	55.6		
9:08:30	76.6	55.8		
9:08:40	76.8	55.8		
9:08:50	77.2	56		
9:09:00	77.6	56.2		
9:09:10	78	56.4		
9:09:20	78.4	56.6		
9:09:30	78.6	56.8		
9:09:40	79	56.8		
9:09:50	79.4	57		
9:10:00	79.8	57.2		
9:10:10	80.2	57.2		
9:10:20	80.6	57.4		
9:10:30	81	57.6		
9:10:40	81.4	57.6		
9:10:50	81.8	57.6		
9:11:00	82.4	57.8		
9:11:10	82.8	58		
9:11:20	83	58		
9:11:30	83.4	58.2		
9:11:40	83.6	58.4		
9:11:50	84	58.6		
9:12:00	84.2	58.8		
9:12:10	84.4	58.8		
9:12:20	84.8	59		
9:12:30	85	59.2		
9:12:40	85.4	59.2		
9:12:50	85.8	59.4		
9:13:00	86.2	59.4		

Time	Pluvio 1	Pluvio 2	Time	q
9:13:10	86.6	59.6		
9:13:20	86.8	59.6		
9:13:30	87.2	59.8		
9:13:40	87.6	59.8		
9:13:50	88	60		
9:14:00	88.4	60		
9:14:10	88.6	60.2		
9:14:20	89	60.2		
9:14:30	89.4	60.4		
9:14:40	89.8	60.6		
9:14:50	90.2	60.8		
9:15:00	90.6	60.8		
9:15:10	91	61		
9:15:20	91.2	61.2		
9:15:30	91.6	61.4		
9:15:40	92	61.4		
9:15:50	92.2	61.6		
9:16:00	92.6	61.8		
9:16:10	93.2	62		
9:16:20	93.6	62		
9:16:30	94	62.2		
9:16:40	94.4	62.2		
9:16:50	94.6	62.4		
9:17:00	95	62.6		
9:17:10	95	62.6		
9:17:20	95	62.6		
9:17:30	95	62.6		
9:17:40	95	62.6		
9:17:50	95	62.6		
9:18:00	95	62.6		
9:18:10	95	62.8		
9:18:20	95	62.8		

Appendix C Erosion data

C.1 Natural rainfall

All data in the tables below are in units of 24 hour time to a resolution of a minute and date (time), litres/s (discharge, q) and grams/litre (concentration, c).

Batter sites

BRT2			BWT1		
time	q	c	time	q	c
11:52_06/02/1991	1.092	0.21484100	09:52_30/01/1991	0.500	0.25999999
11:54_06/02/1991	0.440	0.21011100	09:54_30/01/1991	0.644	0.36999999
15:00_13/02/1991	1.996	0.31634700	09:56_30/01/1991	0.536	0.09999999
15:02_13/02/1991	1.664	0.39329200	09:58_30/01/1991	0.393	0.04999999
15:03_13/02/1991	1.628	0.25276900	10:00_30/01/1991	0.272	0.10999999
15:04_13/02/1991	1.596	0.30710800	17:04_04/02/1991	0.258	0.10999999
15:05_13/02/1991	1.559	0.28204100	17:06_04/02/1991	0.425	0.21999999
15:06_13/02/1991	1.526	0.26848500	17:08_04/02/1991	0.479	0.10999999
15:07_13/02/1991	1.599	0.30445500	17:10_04/02/1991	0.415	0.06999999
15:08_13/02/1991	1.664	0.28513600	17:12_04/02/1991	0.279	0.06999999
15:09_13/02/1991	1.743	0.30613700	17:14_04/02/1991	0.207	0.10999999
15:10_13/02/1991	1.773	0.22229700	17:16_04/02/1991	0.108	0.14999999
15:12_13/02/1991	1.559	0.27697500	17:18_04/02/1991	0.049	0.05999999
15:14_13/02/1991	1.672	0.32365100	17:20_04/02/1991	0.023	0.02999999
15:16_13/02/1991	1.811	0.26394300	17:22_04/02/1991	0.011	0.05999999
15:18_13/02/1991	1.590	0.31170600	11:48_06/02/1991	0.494	0.35999999
15:20_13/02/1991	1.367	0.22980100	11:50_06/02/1991	0.645	0.70999999
15:22_13/02/1991	0.991	0.13327000	11:52_06/02/1991	0.310	0.32999999
14:50_16/02/1991	1.777	0.22740400	11:54_06/02/1991	0.132	0.20999999
14:51_16/02/1991	1.713	0.48569600			
14:52_16/02/1991	1.640	0.47978000			
14:53_16/02/1991	1.498	0.93804600			
14:54_16/02/1991	1.069	0.45763700			
14:56_16/02/1991	0.583	0.52107700			
14:58_16/02/1991	0.243	0.52351600			
15:00_16/02/1991	0.084	0.43003200			
15:02_16/02/1991	0.048	0.40051400			
15:04_16/02/1991	0.014	0.33303600			
15:06_16/02/1991	0.010	0.44691700			
13:41_22/02/1991	3.308	1.0051030			
13:42_22/02/1991	2.697	0.60572000			
13:43_22/02/1991	2.301	0.44268500			
13:44_22/02/1991	1.793	0.34495600			
13:45_22/02/1991	1.207	0.28009800			

Caprock sites

CWT2			CWT3		
time	q	c	time	q	c
20:53_07/01/1991	0.525	0.45000000	11:49_06/02/1991	0.350	0.35000000
20:54_07/01/1991	0.410	0.40000000	11:51_06/02/1991	0.313	0.26000000
20:55_07/01/1991	0.295	0.29000000	11:53_06/02/1991	0.250	0.20000000
20:56_07/01/1991	0.210	0.42000000	11:55_06/02/1991	0.187	0.45000000
20:57_07/01/1991	0.126	0.55000000	11:57_06/02/1991	0.123	0.18000000
20:58_07/01/1991	0.091	0.47000000	14:51_16/02/1991	0.311	0.29000000
20:59_07/01/1991	0.072	0.42000000	14:53_16/02/1991	0.345	0.18000000
21:00_07/01/1991	0.081	0.45000000	14:55_16/02/1991	0.306	0.14000000
21:01_07/01/1991	0.078	0.45000000	14:57_16/02/1991	0.265	0.23000000
21:02_07/01/1991	0.092	0.33000000	14:59_16/02/1991	0.211	0.18000000
21:03_07/01/1991	0.124	0.52000000	15:01_16/02/1991	0.157	0.23000000
21:04_07/01/1991	0.238	0.34000000	15:03_16/02/1991	0.109	0.09000000
21:05_07/01/1991	0.418	0.42000000			
21:06_07/01/1991	0.528	0.35000000			
21:07_07/01/1991	0.510	0.35000000			
21:08_07/01/1991	0.492	0.36000000			
14:29_10/01/1991	0.397	0.21000000			
14:30_10/01/1991	0.628	0.21000000			
14:31_10/01/1991	0.707	0.26000000			
14:32_10/01/1991	0.735	0.31000000			
14:33_10/01/1991	0.706	0.33000000			
14:34_10/01/1991	0.632	0.37000000			
14:35_10/01/1991	0.510	0.27000000			
14:36_10/01/1991	0.428	0.40000000			
14:37_10/01/1991	0.411	0.22000000			
14:38_10/01/1991	0.391	0.33000000			
14:39_10/01/1991	0.386	0.30000000			
14:40_10/01/1991	0.528	0.41000000			
14:41_10/01/1991	0.761	0.26000000			
14:42_10/01/1991	0.936	0.30000000			
14:43_10/01/1991	1.020	0.44000000			
14:44_10/01/1991	0.946	0.27000000			
14:45_10/01/1991	0.760	0.33000000			
14:46_10/01/1991	0.661	0.20000000			
14:47_10/01/1991	0.601	0.17000000			
14:48_10/01/1991	0.428	0.20000000			
14:49_10/01/1991	0.315	0.12000000			
17:00_21/01/1991	1.924	0.96000000			
17:02_21/01/1991	2.290	0.86000000			

CWT2			CWT3		
time	**q**	**c**	**time**	**q**	**c**
17:04_21/01/1991	2.335	0.60000000			
17:06_21/01/1991	1.782	0.50000000			
17:08_21/01/1991	1.775	0.43000000			
17:10_21/01/1991	1.349	0.40000000			
17:12_21/01/1991	1.141	0.34000000			
17:14_21/01/1991	0.792	0.32000000			
17:16_21/01/1991	0.762	0.56000000			
17:18_21/01/1991	0.742	0.39000000			
17:06_04/02/1991	0.522	0.37000000			
17:08_04/02/1991	0.542	0.39000000			
17:10_04/02/1991	0.432	0.31000000			
17:12_04/02/1991	0.330	0.33000000			
17:14_04/02/1991	0.285	0.34000000			
17:16_04/02/1991	0.108	0.28000000			

CRT1			CRT2		
time	**q**	**c**	**time**	**q**	**c**
20:51_07/01/1991	1.464	0.79473000	14:28_10/01/1991	0.000	0.07169600
20:52_07/01/1991	3.546	0.68102400	14:29_10/01/1991	0.222	0.15238100
20:53_07/01/1991	3.798	0.66075600	14:30_10/01/1991	0.762	0.15728100
20:54_07/01/1991	3.094	0.41398800	14:31_10/01/1991	1.090	0.15876700
20:55_07/01/1991	2.044	0.33409400	14:32_10/01/1991	1.097	0.12496500
20:56_07/01/1991	1.377	0.49845100	14:33_10/01/1991	1.031	0.16542000
20:57_07/01/1991	0.898	0.32978500	14:34_10/01/1991	0.889	0.15252300
20:58_07/01/1991	0.560	0.52054700	14:35_10/01/1991	0.665	0.09958900
20:59_07/01/1991	0.411	0.49276000	14:36_10/01/1991	0.402	0.09770400
21:00_07/01/1991	0.337	0.44134000	14:37_10/01/1991	0.247	0.09392000
21:01_07/01/1991	0.302	0.25933800	14:38_10/01/1991	0.219	0.07885600
21:02_07/01/1991	0.344	0.44371200	14:39_10/01/1991	0.197	0.06324600
21:03_07/01/1991	0.513	0.27446800	14:40_10/01/1991	0.413	0.07800700
21:04_07/01/1991	0.885	0.29710000	14:41_10/01/1991	0.935	0.09283200
21:05_07/01/1991	1.654	0.28733500	14:42_10/01/1991	1.488	0.17298100
21:06_07/01/1991	2.830	0.39422400	14:43_10/01/1991	1.799	0.20474800
21:07_07/01/1991	3.439	0.42346900	14:44_10/01/1991	1.601	0.13333600
21:08_07/01/1991	3.274	0.35967200	14:45_10/01/1991	1.157	0.12882000
21:09_07/01/1991	2.884	0.25528900	14:46_10/01/1991	0.818	0.12172700
21:10_07/01/1991	2.587	0.38363300	14:47_10/01/1991	0.611	0.11661500
21:11_07/01/1991	2.124	0.28951200	14:48_10/01/1991	0.333	0.10134700

time	q	c	time	q	c
21:12_07/01/1991	1.667	0.22524800	14:49_10/01/1991	0.153	0.12645900
21:13_07/01/1991	1.271	0.42242600	14:50_10/01/1991	0.040	0.09865400
14:30_10/01/1991	0.857	0.16850000	12:04_11/01/1991	1.401	0.28605000
14:31_10/01/1991	1.203	0.13229800	12:06_11/01/1991	1.472	0.46782600
14:32_10/01/1991	1.383	0.17744500	12:07_11/01/1991	1.727	0.26398900
14:33_10/01/1991	1.409	0.11567200	12:08_11/01/1991	2.145	0.27902600
14:34_10/01/1991	1.309	0.05928400	12:09_11/01/1991	2.558	0.24399300
14:35_10/01/1991	1.092	0.13183900	12:10_11/01/1991	2.696	0.40747100
14:36_10/01/1991	0.898	0.05614600	12:27_11/01/1991	7.820	1.7933880
14:37_10/01/1991	0.794	0.10383100	12:32_11/01/1991	6.308	1.7120430
14:39_10/01/1991	0.709	0.24974200			
14:41_10/01/1991	1.077	0.17614400			
14:43_10/01/1991	1.853	0.24668300			
14:45_10/01/1991	1.582	0.18447200			

CRT3			COUT		
time	q	c	time	q	c
20:52_07/01/1991	0.062	0.17045400	20:52_07/01/1991	7.569	0.71877800
20:53_07/01/1991	0.234	0.13516000	20:53_07/01/1991	11.859	0.82385400
20:54_07/01/1991	0.374	0.11517700	20:54_07/01/1991	13.740	0.82337000
20:55_07/01/1991	0.416	0.10505300	20:55_07/01/1991	13.740	0.53798400
20:56_07/01/1991	0.315	0.09925100	20:56_07/01/1991	11.859	0.62038400
20:57_07/01/1991	0.154	0.08699000	20:57_07/01/1991	9.499	0.56104500
20:58_07/01/1991	0.096	0.07591300	20:58_07/01/1991	6.856	0.53534200
20:59_07/01/1991	0.013	0.06974800	20:59_07/01/1991	5.214	0.62442700
21:00_07/01/1991	0.007	0.07167000	21:00_07/01/1991	3.780	0.63653700
21:01_07/01/1991	0.010	0.07053500	21:01_07/01/1991	3.780	0.50348600
21:02_07/01/1991	0.014	0.08993100	21:02_07/01/1991	3.015	0.48536400
21:03_07/01/1991	0.017	0.12837000	21:03_07/01/1991	3.516	0.40200800
21:04_07/01/1991	0.025	0.14296700	21:04_07/01/1991	5.214	0.54777700
21:05_07/01/1991	0.195	0.13833200	21:05_07/01/1991	7.208	0.61003700
21:06_07/01/1991	0.325	0.13925000	21:06_07/01/1991	9.499	0.46305200
21:07_07/01/1991	0.458	0.10556200	21:07_07/01/1991	13.256	0.46248900
21:08_07/01/1991	0.499	0.14522200	21:08_07/01/1991	13.740	0.48320100
21:09_07/01/1991	0.539	0.13055000	21:09_07/01/1991	13.740	0.38976900
21:10_07/01/1991	0.539	0.13171100	21:10_07/01/1991	13.740	0.41254400
21:11_07/01/1991	0.536	0.12790300	21:11_07/01/1991	13.256	0.42201900
21:12_07/01/1991	0.456	0.11641000	21:12_07/01/1991	10.970	0.40847700
			21:14_07/01/1991	7.938	0.35126200
			21:15_07/01/1991	6.856	0.41902400

CRT3			COUT		
time	q	c	time	q	c
			21:16_07/01/1991	5.214	0.43113700
			15:00_08/01/1991	4.913	0.81976900
			15:01_08/01/1991	9.909	0.68467700
			15:02_08/01/1991	13.740	0.63772200
			15:03_08/01/1991	14.228	0.64145900
			15:04_08/01/1991	14.228	0.55482800
			15:05_08/01/1991	12.317	0.47215000
			15:06_08/01/1991	8.318	0.44769200
			15:07_08/01/1991	6.176	0.83739800
			15:08_08/01/1991	4.051	0.47319400
			08:10_10/01/1991	13.739	0.25497900
			08:12_10/01/1991	12.782	0.57277400
			08:14_10/01/1991	15.234	0.17540200
			08:16_10/01/1991	15.234	0.43323500
			08:18_10/01/1991	9.498	1.1408720
			08:20_10/01/1991	6.513	0.38401600
			14:31_10/01/1991	11.410	0.28784300
			14:37_10/01/1991	14.727	0.38872900
			14:39_10/01/1991	10.117	0.37154500
			14:41_10/01/1991	12.782	0.32780200
			12:01_11/01/1991	15.234	0.32108100
			12:02_11/01/1991	15.234	0.21702000
			12:03_11/01/1991	13.255	0.33143600
			12:04_11/01/1991	10.969	0.29784800
			12:05_11/01/1991	9.908	0.29705600
			12:06_11/01/1991	9.498	0.43392400
			12:07_11/01/1991	9.498	0.32619700
			12:08_11/01/1991	10.540	0.33387300
			12:27_11/01/1991	17.355	0.88824700
			12:32_11/01/1991	30.452	0.97785000
			17:37_28/12/1990	2.325	1.3592980
			17:38_28/12/1990	3.780	1.2045150
			17:39_28/12/1990	4.329	1.2912300
			17:40_28/12/1990	4.329	1.1151860
			17:41_28/12/1990	4.051	1.2154910
			17:42_28/12/1990	3.015	1.3565480
			17:43_28/12/1990	2.219	1.2297690
			17:44_28/12/1990	1.614	1.2769350
			17:45_28/12/1990	1.173	1.1490480

CRT3			COUT		
time	**q**	**c**	**time**	**q**	**c**
			17:46_28/12/1990	0.744	1.3126110
			17:47_28/12/1990	0.571	1.2212900
			17:48_28/12/1990	0.426	1.5949080
			17:49_28/12/1990	0.305	1.2021710
			17:50_28/12/1990	0.132	1.2104180
			17:51_28/12/1990	0.075	1.1574080
			17:52_28/12/1990	0.037	1.4027180
			18:05_28/12/1990	0.004	1.1369710
			17:06_04/02/1991	13.739	0.22890900
			17:08_04/02/1991	14.727	0.32923000
			17:10_04/02/1991	14.227	0.34632300
			17:12_04/02/1991	9.908	0.34863000
			17:14_04/02/1991	7.208	0.31404800
			17:16_04/02/1991	4.912	0.36601000

C.2 Simulated rainfall

The data below are those for calibration of the sediment transport equation from simulated rainfall equation 3.3.1. Times, t, are in minutes from the start of the experiment, discharge, q, in litres/second, and concentrations, c, in grams/litre.

Batter sites

Plot 4 Run 2			**Plot 4 Run 3**		
time	**q**	**c**	**time**	**q**	**c**
8.29.30	0.115	0.66300000	11.19.30	0.4995	1.6779000
8.30.00	0.4995	0.77410000	11.20.00	0.9712	1.8078000
8.30.30	0.5528	1.1310000	11.20.30	0.8421	2.0133000
8.31.00	0.5528	1.3247000	11.21.00	1.897	2.3204000
8.32.00	0.9712	1.3201000	11.22.00	1.897	2.1612000
8.34.00	0.9067	1.8998000	11.23.00	1.897	1.2210000
8.35.00	0.9712	1.2279000	11.24.00	1.897	1.8315000
8.36.00	0.8421	1.0938000	11.25.00	2.077	1.6952000
8.38.00	0.8421	1.0370000	11.27.00	1.897	1.5653000
8.40.00	0.9067	0.80720000	11.29.00	2.263	1.2864000
8.42.00	0.9712	0.93130000	11.31.00	2.077	1.0251000
8.45.00	0.8421	1.0469000	11.34.00	1.987	1.6714000
8.50.00	0.9712	0.76500000	11.39.00	1.481	0.83240000
8.55.00	0.9067	0.41720000	11.44.00	1.987	1.2600000
9.00.00	0.9067	0.83170000	11.49.00	2.456	2.2437000
9.05.00	0.8421	0.75910000	11.54.00	1.327	2.0437000
9.15.00	0.8421	1.0252000	11.59.00	1.327	0.59260000
9.20.00	0.7203	3.0830000	12.08.40	1.179	1.1522000
9.24.30	0.7203	2.4868000	12.09.10	0.8421	1.0299000
9.25.00		0.97720000	12.09.40	0.6061	0.68950000
9.25.30	0.4995	0.60290000	12.10.10	0.3724	0.84940000
9.25.30	0.2288	0.43540000	12.10.40	0.286	0.58740000
9.26.00	0.115	0.78680000	12.11.10	0.1716	0.51180000
9.26.30	0.0572	0.50470000	12.11.40	0.1144	0.45710000
9.27.00	0.0572	0.42380000	12.12.10	0.0858	0.21110000
9.27.30	0.0572	0.44330000	12.12.40	0.0286	0.55190000
9.28.00	0.0572	0.30500000	12.12.30		0.66322000
9.28.30	0.0572	0.09500000			

Caprock sites

Plot 1 Run 2			Plot 1 Run 3		
time	**q**	**c**	**time**	**q**	**c**
6.0	0.53	0.607	3.1		1.124
7.0	0.74	0.630	4.5	1.18	1.112
8.0	0.74	0.515	6.0	1.49	0.628
9.0	0.74	0.568	7.0	1.56	0.612
10.0	0.81	0.550	8.0	1.62	0.756
11.1	0.79	0.479	9.5	1.71	0.446
12.0	0.81	0.339	10.5	1.77	0.423
13.0	0.84	0.358	11.5	1.77	0.374
14.0	0.77	0.299	12.5	1.7	0.391
15.0	0.81	0.283	14.5	1.77	0.368
17.0	0.88	0.356	16.0	1.77	0.469
19.0	0.84	0.282	18.5	1.71	0.299
21.0	0.91	0.288	20.5	1.77	0.264
26.0	0.84	0.134	25.5	1.7	0.231
31.0	0.81	0.134	30.5	1.77	0.165
41.0	0.81	0.180	41.0	1.7	0.156
51.5	0.77	0.146	50.5	1.77	0.117
60.0	0.87	0.164	57.0	1.7	0.081
61.0	0.76	0.158	58.0	1.26	0.185
62.5	0.37	0.031	59.0	0.51	0.155
63.5	0.17	0.052	60.0	0.3	0.104
64.5	0.1	0.114	61.0	0.13	0.090
65.5	0.07	0.059	62.0	0.07	0.076
66.5	0.01	0.021			

Plot 1 Run 4			Plot 2 Run 2		
time	**q**	**c**	**time**	**q**	**c**
1.5	1.36	0.645	5.5		1.024
2.5	1.62	0.640	6.5	0.69	0.790
3.5	1.72	0.553	7.5	1.21	0.692
4.5	1.79	0.346	8.5	1.21	0.616
5.5	1.92	0.383	9.5	1.27	0.622
12.0	1.92	0.276	10.5	1.37	0.384
14.0	2.11	0.251	11.5	1.38	0.327
16.0	2.06	0.304	12.5	1.43	0.522
19.0	2.11	0.244	13.5	1.43	0.450
26.0	2.04	0.175	14.5	1.43	0.380
52.5	0.39	0.353	16.5	1.49	0.485

time	q	c	time	q	c
56.5	0.01	0.127	18.5	1.43	0.276
			20.5	1.55	0.680
			25.5	1.43	0.328
			30.5	1.21	0.271
			40.5	1.32	0.258
			51.0	1.27	0.097
			60.5	1.12	0.142
			60.5	1.12	0.183
			63.0	0.43	0.185
			64.0	0.28	0.109
			65.0	0.15	0.120
			66.0	0.11	0.062
			67.5	0.06	0.098

Plot 2 Run 3			**Plot 2 Run 4**		
time	**q**	**c**	**time**	**q**	**c**
2.8		2.263	6.0	2.28	0.469
4.0	1.25	1.345	9.0	2.22	0.430
5.0	1.92	1.144	11.0	2.25	0.418
6.5	2.05	0.992	13.5	2.3	0.379
7.5	2.04	0.651	15.0	2.07	0.368
9.0	2.11	0.844	17.0	2.23	0.464
10.0	2.18	0.793	20.0	2.15	0.429
11.0	2.04	0.724	23.5	2.3	0.450
12.0	2.04	0.639	28.0	2.16	0.210
14.0	2.11	0.475	38.0	2.07	0.208
15.5	2.05	0.616	50.5	1.73	0.351
18.0	2.11	0.493	52.0	0.83	0.442
20.0	2.06	0.066	53.0	0.44	0.405
25.0	2.12	0.343			
30.0	2.11	0.313			
40.5	2.06	0.310			
50.0	2.12	0.256			
57.5	1.77	0.300			
58.5	1.57	0.201			
59.5	0.81	0.117			
60.5	0.46	0.247			
61.5	0.34	0.209			
63.0	0.18	0.182			

The data below are the covered and uncovered sediment transport from the batter plots B1RF1QSS data (table 3.2) for 1 m^2 for determination of the rainsplash diffusion coefficients used in figure 3.6. Data are in units as above.

Plot 1 Run 1			**Plot 1 Run 2**			**Plot 1 Run 3**		
time	**q**	**c**	**time**	**q**	**c**	**time**	**q**	**c**
2.5	0.02	1.36	1	0.03	2.30	1	0.04	5.10
3.5	0.04	3.87	2	0.04	4.19	2	0.04	6.76
4.5	0.02	1.78	3	0.04	2.24	3	0.04	2.36
5.5	0.01	0.94	4	0.04	0.97	4	0.04	2.79
6.5	0.04	0.97	5	0.03	0.37	5	0.05	1.92
7.5	0.02	0.78	6	0.02	2.38	6	0.04	4.30
8.5	0.02	0.69	7	0.03	2.16	8	0.04	5.54
9.5	0.02	0.38	8	0.04	2.35	10	0.04	3.86
10.5	0.02	0.99	9	0.04	1.26	12	0.03	3.42
11.5	0.06	0.34	11	0.03	1.68	14	0.08	3.67
12.5	0.04	1.68	13	0.05	3.21	20	0.03	2.63
14.5	0.04	0.85	15	0.04	0.84	25	0.04	3.14
16.5	0.04	1.04	17	0.04	1.48	30	0.08	2.30
18.5	0.05	1.05	19	0.04	0.72	35	0.04	2.21
20	0.03	0.93	20.5	0.04	1.49	40	0.05	1.58
25	0.01	0.68	25.5	0.04	0.87	50	0.07	3.75
30	0.02	0.84	30.5	0.04	1.64	60	0.05	3.14
35	0.03	0.60	40.5	0.02	0.15	60.3	0.02	0.59
40	0.03	0.97				61.3	0.01	2.09
50	0.03	0.57				62.3	0.00	5.32
60	0.02	0.49						
61	0.01	0.85						
62	0.01	0.20						

Plot 1 Run 4			**Plot 1 Run 5**		
time	**q**	**c**	**time**	**q**	**c**
1	0.04	5.10	0.5	0.08	3.11
2	0.04	6.76	1	0.09	2.28
3	0.04	2.36	2	0.09	2.08
4	0.04	2.79	3	0.10	3.27
5	0.05	1.92	4	0.08	2.97
6	0.04	4.30	5	0.07	2.83
8	0.04	5.54	6	0.09	4.19
10	0.04	3.86	7	0.08	2.24
12	0.03	3.42	8	0.07	2.39

time	q	c	time	q	c
14	0.08	3.67	10	0.09	3.52
20	0.03	2.63	12	0.04	0.40
25	0.04	3.14	14	0.04	0.74
30	0.08	2.30	16	0.03	3.79
35	0.04	2.21	18	0.02	0.31
40	0.05	1.58	20	0.05	1.63
50	0.07	3.75	25	0.01	0.00
60	0.05	3.14	30	0.01	0.29
60.3	0.02	0.59	30.5	0.00	0.00
61.3	0.01	2.09	40	0.05	2.52
62.3	0.00	5.32	50	0.02	5.64
			60	0.07	1.61
			60.5	0.02	3.16
			61	0.01	0.00

Plot 2 Run 1			Plot 2 Run 2			Plot 2 Run 3		
time	q	c	time	q	c	time	q	c
7	0.01	3.76	4.5	0.02	0.75	1.5	0.04	0.40
8	0.01	0.25	5.5	0.04	0.42	2.5	0.04	0.24
9	0.01	0.20	6.5	0.03	0.25	3.5	0.04	0.03
10	0.01	0.26	7.5	0.02	0.33	4.5	0.04	0.08
11	0.01	0.35	8.5	0.02	0.25	5.5	0.04	0.22
12	0.01	0.58	9.5	0.02	0.35	6.5	0.04	0.09
15	0.01	0.05	10.5	0.03	0.23	8.5	0.04	0.00
17	0.01	0.12	11.5	0.02	0.29	10.5	0.04	0.31
19	0.01	0.01	12.5	0.04	0.25	12.5	0.05	0.02
20.5	0.01	0.57	14.5	0.03	0.24	14.5	0.05	0.21
25.5	0.02	0.32	16.5	0.03	0.22	20.5	0.06	0.00
30.5	0.02	0.05	18.5	0.05	0.26	25.5	0.05	0.06
35.5	0.02	0.36	25	0.03	0.15	30.5	0.05	0.00
40.5	0.02	0.06	30	0.02	0.09	35.5	0.08	0.00
50.5	0.005	0.34	40	0.01	0.61	40.5	0.06	0.00
62.5	0.003	0.02	43	0.01	0.37	50.5	0.04	0.00
63.5	0.001	0.50	44	0.00	0.10	60.5	0.03	0.00

Plot 2 Run 4			Plot 2 Run 5		
time	q	c	time	q	c
1.5	0.06	0.49	1	0.09	0.41
2.5	0.06	0.15	2	0.15	0.00
3.5	0.07	0.22	3	0.12	0.09
4.5	0.04	0.03	4	0.12	0.12
5.5	0.04	0.00	5	0.15	0.16
6.5	0.07	0.01	6	0.12	0.07
7.5	0.04	0.08	7	0.09	0.07
8.5	0.04	0.21	8	0.11	0.03
10.5	0.04	0.12	9	0.05	0.77
12.5	0.01	0.00	10	0.09	0.22
14.5	0.02	0.00	11	0.11	0.21
16.5	0.03	0.00	12.5	0.12	0.17
18.5	0.01	0.00	14.5	0.16	0.14
20.5	0.01	0.00	16.5	0.16	0.02
25.5	0.003	0.00	20.5	0.09	0.00
30.5	0.002	0.00	25.5	0.05	0.25
30.5	0.12	0.36			
35.5	0.07	0.33			
40.5	0.06	0.29			
50.5	0.04	0.07			
60.25	0.05	0.00			
60.75	0.03	0.11			
61.25	0.01	0.00			

References

Abrahams AD & Parsons AJ 1991. Resistance to overland flow on desert pavements and its implications for sediment transport modelling. *Water Resources Research* 27 (8), 1827−1836.

Andrews DJ & Bucknam RC 1987. Fitting degradation of shoreline scarps by a nonlinear diffusion model. *Journal of Geophysical Research* 92 (B12), 12857−12867.

Chow VT 1959. *Open-channel hydraulics*. McGraw-Hill, New York.

Culling WEH 1963. Soil creep and the development of hillside slopes. *Journal of Geology* 71 (2), 127−161.

Dunne T 1980. Formation and controls of channel networks. *Progress in Physical Geography* 4, 211−239.

Elliott JG 1988. Relations among drainage basin and hillslope morphology and channel stability of reclaimed surface coal mine, northwestern Colorado. *Transactions of the American Geophysical Union* 69 (44), 1224.

Field WG & Williams BJ 1987. A generalized kinematic catchment model. *Water Resources Research* 23 (8), 1693−1696.

Gilbert GK 1909. Convexity of hilltops. *Journal of Geology* 17, 344−350.

Henderson FM 1966. *Open channel flow.* MacMillan, New York.

Howard AD 1971. Simulation of stream networks by headward growth and branching. *Geographical Analysis* 3, 29−50.

Huang HQ & Willgoose GR 1992. *Numerical analyses of relations between basin hydrology, geomorphology and scale*. Research Report No 075.04.1992, Department of Civil Engineering and Surveying, University of Newcastle, Australia.

Huang HQ & Willgoose GR 1993. Flood frequency relationships dependent on catchment area: An investigation of causal relationships. *Towards the 21st Century*, Hydrology and Water Resources Symposium, Newcastle, 1993, The Institution of Engineers (Australia), 287–92.

Ijjasz-Vasquez EJ 1990. A channel network evolution model with subsurface saturation mechanism and analysis of the chaotic behaviour of the model. Master of Science Thesis, Massachusetts Institute of Technology, Boston, MA.

Intergovernmental Panel on Climate Change 1990. *Climate change: The IPCC scientific assessment.* Cambridge University Press, Cambridge.

Kirkby MJ 1971. Hillslope process-response models based on the continuity equation. In *Slopes: Form and process*, Institute of British Geographers Special Publications 3, London, 15−30.

Krawjewski WF, Rexroth DT & Kiriaki K 1991. *Optimal combining of ground-based sensors for the purpose of validating satellite-based rainfall estimates*. Final Report to National Aeronautics and Space Administration, University of Iowa.

Kuczera G 1983. Effect of sampling uncertainty and spatial correlation on an Empirical Bayes procedure for combining site and regional information. *Journal of Hydrology* 65, 373−398.

Leopold LB & Langbein WB 1962. *The concept of entropy in landscape evolution*. US Geological Survey Professional papers 500–A, USGS, Reston, Virginia.

Leopold LB, Wolman MG & Miller JP 1964. *Fluvial processes in geomorphology*. Freeman, London.

Loughran RJ 1977. Sediment transport from a rural catchment in New South Wales. *Journal of Hydrology* 34, 357–375.

Montgomery DR & Dietrich WE 1988. Where do channels begin? *Nature* 336, 232–234.

Moore ID & Burch GJ 1986. Sediment transport capacity of sheet and rill flow: Application of unit stream power theory. *Water Resources Research* 22 (8), 1350–1360.

Moore ID & Grayson RB 1991. Terrain-based catchment partitioning and runoff prediction using vector elevation data. *Water Resources Research* 27 (6), 177–1192.

Mosteller F & Tukey JW 1977. *Data analysis and regression*. Addision Wesley, Reading, MA.

Neave M 1991. Inter-rill erosion processes: A study of degradation of the Ranger Uranium Mine waste rock dump. Internal report 50, Supervising Scientist for the Alligator Rivers Region, Canberra. Unpublished paper.

Patton PC & Schumm SA 1975. Gully erosion, Northern Colorado, a threshold phenomena. *Geology* 3, 88–90.

Pilgrim DH 1987. Estimation of peak flows for small to medium sized rural catchments. In *Australian rainfall and runoff*, ed DH Pilgrim, The Institution of Engineers, Canberra, 93–116.

Richards B 1987. Settlement under rock dumps. CSIRO Division of Soils Focus Report No 1 to Ranger Uranium Mines Pty Ltd. Unpublished paper.

Riley SJ 1991. Analysis of pluviometer records, Darwin and Jabiru. Internal report 48, Supervising Scientist for the Alligator Rivers Region, Canberra. Unpublished paper.

Riley SJ 1992. Small scale studies of the erodibility of Ranger Waste Rock Dump. Internal report 64, Supervising Scientist for the Alligator Rivers Region, Canberra. Unpublished paper.

Riley SJ (in prep). Hydrogeomorphic modelling of rehabilitated landforms, Ranger Uranium Mine: Introduction and research strategy. Supervising Scientist for the Alligator Rivers Region, Research Report.

Smith TR & Bretherton FP 1972. Stability and the conservation of mass in drainage basin evolution. *Water Resources Research* 8 (6), 1506–1529.

Toy TJ & Hadley RF 1987. *Geomorphology and reclamation of disturbed lands*. Academic Press, Orlando.

Willgoose GR 1994. A physical explanation for an observed area-slope-elevation relationship for declining catchments. *Water Resources Research* 30 (2), 151–159.

Willgoose GR, Bras RL & Rodriguez-Iturbe I 1989. *A physically based channel network and catchment evolution model*. Technical Report 322, Ralph M Parsons Laboratory, Department of Civil Engineering, MIT, Boston, MA.

Willgoose GR, Bras RL & Rodriguez-Iturbe I 1990. A model of river basin evolution. *Transactions of American Geophysical Union* 71 (47), 1806–1807.

Willgoose GR, Bras RL & Rodriguez-Iturbe I 1991a. A physically based coupled network growth and hillslope evolution model: 1 Theory. *Water Resources Research* 27 (7), 1671−1684.

Willgoose GR, Bras RL & Rodriguez-Iturbe I 1991b. A physically based coupled network growth and hillslope evolution model: 2 Applications. *Water Resources Research* 27 (7), 1685−1696.

Willgoose GR, Bras RL & Rodriguez-Iturbe I 1991c. A physical explanation of an observed link area-slope relationship, *Water Resources Research* 27 (7), 1697−1702.

Willgoose GR, Bras RL & Rodriguez-Iturbe I 1991d. Results from a new model of river basin evolution, *Earth Surface Processes and Landforms* 16, 237−254.

Willgoose GR, Bras RL & Rodriguez-Iturbe I 1991e. The relationship between catchment and hillslope properties: The implications of a catchment evolution model, *Geomorphology* 5, 21−37.

Willgoose GR & Riley SJ 1993. Scale dependence of runoff and the hydrology of a proposed mine rehabilitation. In *Institution of Engineers Australia. Hydrology and Water Resources Symposium*. Newcastle, 30 June−2 July 1993, The Institution of Engineers (Australia), 159−164.

Williams DK & Riley SJ 1992. Some geomorphic thresholds related to gullying, Tin Camp Creek, Arnhem Land, Northern Territory, Australia. Internal report 59, Supervising Scientist for the Alligator Rivers Region, Canberra. Unpublished paper.

Williams GP 1989. Sediment concentration versus water discharge during single hydrologic events in rivers, *Journal of Hydrology* 111, 89−106.